UNIVERSITÀ DEGLI STUDI
DI MILANO

PhD degree in Systems Medicine (curriculum in Molecular Oncology)

European School of Molecular Medicine (SEMM)

Settore disciplinare: Med/04

Towards Patient-specific Models in High Grade Serous Ovarian Cancer (HGSOC): Linking Epigenetic Tracing of Cell of Origin with actionable Organoid Models

Raffaele Luongo

Istituto Europeo di Oncologia

Supervisor *Prof. Giuseppe Testa*

Co-Supervisor *Dr. Pietro Lo Riso*

Internal Advisor *Dr. Kristina Havas Cavalletti*

External Advisor *Prof. Riccardo Fodde*

PhD Coordinator*: Prof. Saverio Minucci*

ACCADEMIC YEAR 2019/2020

“Religion is a culture of faith;
science is a culture of doubt.”
Richard P. Feynman

TABLE OF CONTENTS

List of abbreviations

A1AT	Alpha 1-Antitrypsin
AdDF	Advanced DMEM/F12
AFG	Anterior Foregut
ALDH1	Aldehyde Dehydrogenase 1 family member
AMP	Adenosine monophosphate
AS	Ascites
ASCs	Adult Stem Cells
ATRA	All-Trans Retinoic Acid
BME	Basement Membrane Extract
BMPs	Bone Morphogenetic Proteins
BrdU	Bromodeoxyuridine
BSA	Bovina Serum Albumine
BTs	Borderline Tumors
CALB2	Calretinin Binding protein 2
cAMP	3',5'-cyclic AMP
CCL	Cancer Cell Lines
CCLE	Cancer Cell Line Encyclopedia
CCOC	Clear Cell Ovarian Carcinoma
CF	Cystic Fibrosis
CFTR	Cystic Fibrosis Transmembrane conductance Regulator
ChIP	Chromatin Immunoprecipitation
CICs	intra-ovarian Cortical Inclusion Cysts
CK	Cytokeratin
CRCs	Colorectal Cancers
CRISPR	Clustered Regularly Interspaced Short Palindromic Repeats
CSCs	Cancer Stem Cells
CUP	Cancers of Unknown Primary origin
DEA	Differentially Expression Analysis
DEGs	Differentially Expressed Genes
DHT	Dihydrotestosterone
DMS	Differentially Methylated Sites
DNA	Deoxyribonucleic Acid
ECM	Extracellular matrix

EDM	Epithelia Digestion Medium
EF1A	Elongation Factor 1 Alpha
EGF	Epidermal Growth Factor
EMT	Epithelial-mesenchymal transition
ENOC	Endometrioid Ovarian Cancer
EOC	Epithelial Ovarian Cancer
ESCs	Embryonic Stem Cells
FACS	Fluorescent Activated Cell Sorter
FAE	Fibered Autoencoder
FBS	Fetal Bovine Serum
FFPE	Formalin Fixed Paraffin Embedded
FGF	Fibroblast Growth Factor
FI	Fimbrial Epithelium
FIGO	Federation of Gynecology and Obstetrics
FRT	Female Reproductive Tract
FT	Fallopian tube
Fw	Forward
gDNA	Genomic DNA
GEM	Genetically Engineered Models
GEMs	Gel beads in Emulsion
GFP	Green Fluorescent Protein
GO	Gene Ontology
gRNA	guide RNA
GSK3	Glycogen Synthase Kinase 3
HCMI	Human Cancer Models Initiative
HEK	Human Embryonic Kidney
HER	Human EGF Receptor
HGF	Hepatocyte Growth Factor
HGSC	High-grade Serous Carcinoma
HGSOC	High Grade Serous Ovarian Cancer
HR	Homologous Recombination
HSCs	Hematopoietic Stem Cells
IEO	European Institute of Oncology
IF	Immunofluorescence

IL	Interleukin
IPA	Ingenuity Pathway Analysis
iPSCs	induced Pluripotent Stem Cells
iTOS	induced Tumorigenic Organoids
KEGG	Kyoto Encyclopedia of Genes and Genomes
LGSOC	Low-grade Serous Ovarian Cancer
LMP	Low Malignant Potential
LTR	Long Terminal Repeats
LV	Lentiviral Vector
MAPK	Mitogen-Activated Protein Kinase
MCCs	Multi-ciliated cells
MOC	Mucinous Ovarian Cancer
MSCs	Mesenchymal Stem Cells
NFDM	Non-fat dry milk
NIH	National Institute of Health
NTP	Nucleotide triphosphate
OC	Ovarian Cancer
OSE	Ovarian Surface Epithelium
PARP	Poly (ADP-Ribose) Polymerase
pBSO	Prophylactic bilateral salpingo-oophorectomy
PCA	Principal Component Analysis
PCR	Polymerase Chain Reaction
PDTXs	Patient-derived Tumor Xenografts
PGE2	Prostaglandin E2
PI3K	Phosphoinositide 3-kinase
PVDF	Polyvinylidene difluoride
RA	Retinoic Acid
RB	Retinoblastoma Protein
RNA	Ribonucleic Acid
RNAi	RNA interference
RRSO	risk-reducing salpingo-oophorectomy
RT	Room Temperature
Rv	Reverse
scRNAseq	Single-cell RNA sequencing

SDS-PAGE	Sodium Dodecyl Sulfate – Polyacylamide Gel Electrophoresis
shRNA	short hairpin RNA
STIC	Serous Tubal Intraepithelial Carcinomas
TA	Transit Amplifying cells
TCGA	The Cancer Genome Atlas
TGF-β	Transforming Growth Factor beta
UMAP	Uniform Manifold Approximation and Projection
UMI	Unique Molecular Identifiers
WHO	World Health Organization
WHV	Woodchuck Hepatitis Virus
WPRE	WHV Post-transcriptional Regulatory Element
ZIKV	ZIKA virus

Index of figures and tables

Figure Index

Table Index

ABSTRACT

ABSTRACT

Ovarian Cancer (OC) is a major cause of cancer-related mortality, due to the late-stage diagnosis and failure of surgery and chemotherapy to fully eradicate the disease, that is reflected in a high rate of tumor relapse after treatments. Patients with high-grade serous ovarian cancer (HGSOC), representing the largest majority of OC (~70%), have not experienced significant improvement in overall survival in last decades (*1*), pointing to the acute need to identify new predictive biomarkers and therapeutic targets for clinical settings.

This unresolved emergency derives from our poor understanding of HGSOC biology combined with the recognized lack of suitable clinically relevant models for this disease, as the available models fail to relate molecular aberrations to clinical histories (*2*). Moreover, one major challenge that sets HGSOC apart from all other solid tumors, that has witnessed significant progress in recent years, is the persistent uncertainty about its cell of origin and the consequent lack of molecular signatures for the unequivocal assignment of specific samples to either an ovarian surface epithelium (OSE) or a fallopian tube fimbrial epithelium (FI) origin, the two candidate tissues still debated in literature (*3*, *4*). Altogether, these aspects have hampered the dissection of pathogenic mechanisms and the identification of targets for improved clinical care of patients, driving us towards the embracement of new paradigms for effective advancements in the clinical setting.

To overcome these issues, in the past few years, in the lab, we have devoted our efforts to the identification of the cell of origin of the tumor and the development of a clinical model allowing the study of this disease. Our applications aimed at brought a valid boost towards those precision oncology approaches that promises to transform cancer care by delivering personalized treatments tailored to the genetic and epigenetic specificities of patients' tumors, whose remarkable heterogeneity characterizes even seemingly homogeneous histotypes.

This level of complexity urged the need to develop and validate patient-derived cancer models that recapitulate to a meaningful extent the features of primary or metastatic tumors, both for efficient drug development and for guiding therapeutic strategies. Among new technologies, patient-derived organoid cultures are emerging as powerful models able to recapitulate in a meaningful extent the features of primary tumors (*5*, *6*). Their value was proved both in guiding therapeutic decision for broadly curable tumors (*7*) and in gaining new insights for intractable tumors such as pancreatic adenocarcinoma (*8*). OC

studies have started to benefit from these advanced models only recently (*9–11*), and a huge part of this PhD work regards the generation of organoids models from both HGSOC and normal samples of FI and OSE, in order to encompass all kind of tissues useful for the study of the pathology. Indeed, while tumor organoids represent an *in vitro* proxy of OC at an advanced stage, normal organoids from healthy tissues can be used as control but also as an indefinitely expandable cellular model in which investigate tumor alterations in the context of a normal tissue. This is really significant also in light of our recent publications on the cell of origin of HGSOC (*12*), where we showed the establishment of a method that is able to stratify HGSOC tumors through an approach based on methylomics and transcriptomics that:

i) allows to distinguish OSE- from FI- derived tumors;
ii) allows to identify for each tumor subtype the specific transcriptomic alterations that could drive the tumorigenic process;
iii) reveals a prognostic value for the tissue of origin of this disease.

Taken together, these two sets of information could help in define the molecular mechanisms governing the disease at an unprecedented resolution, setting a paradigm for harnessing patient-specific cancer models in the complementary goal of dissecting pathogenic mechanisms and extracting their actionable features.

The extrapolation of information from organoids taking in consideration the cell of origin, through both the increase of our knowledge of the pathology and the identification of new markers and targets to be used as novel drug therapies, will prospectively pave the way to the improve the clinical care of patients with HGSOC.

INTRODUCTION

INTRODUCTION

1. OVARIAN CANCER

Ovarian Cancer (OC) is the eighth most commonly occurring cancer in women and the 18th most commonly occurring cancer overall. According with the American Cancer Society® it is also the fifth cause of death among female malignancy and the most lethal gynecological disease. Each year around 240.000 women worldwide are diagnosed with OC and 150.000 die for this pathology. These data are reflected in a risk of OC diagnosis in about 1/78 women, together with a risk of OC-caused death in 1/108 women. Taken together, these data highlight how OC is a significant source of morbidity and mortality in the global population.

This high rate of mortality is mainly due to the late-stage diagnosis, with this family of cancers that is asymptomatic in most of the cases and for most of the time, and diagnosed only when it has already metastasized, with a 5-year relative survival rate of only 29% in US (*13*). This is confirmed by the low percentage of cases (~15%) diagnosed with a localized tumor (stage 1), when the 5-year survival rate is 92% (*13*). The overall 5-year survival rate usually ranges around 40% across the globe, with negligible improvement in the last decades (*2*, *13*). This is really controversial when comparing OC with a lot other solid tumors such as breast, lung and colon ones, that show a relevant increase in the survival rate in last 50 years (*Fig. 1*) (*13*).

The failure of surgery and chemotherapy to fully eradicate the disease is another factor impacting improvements, that is reflected in a high rate of tumor relapse after treatments. Indeed, standard treatment procedures are still mainly based on extensive surgery and treatment with platinum derived compounds (cis- or carbo-platin), that were introduced in the clinical practice in the late 70s and co-adjuvated only recently with taxanes and, in few specific cases of patients with BRCA1 and BRCA2 (BRCA1/2) mutations (~10%), with poly (ADP-ribose) polymerase (PARP) inhibitors (*2*). Since then, no major advances in care of OC patients were achieved.

Despite its major health significance, the biology and etiology of OC is still poorly understood, pointing to the need to identify new predictive biomarkers and therapeutic targets for clinical settings.

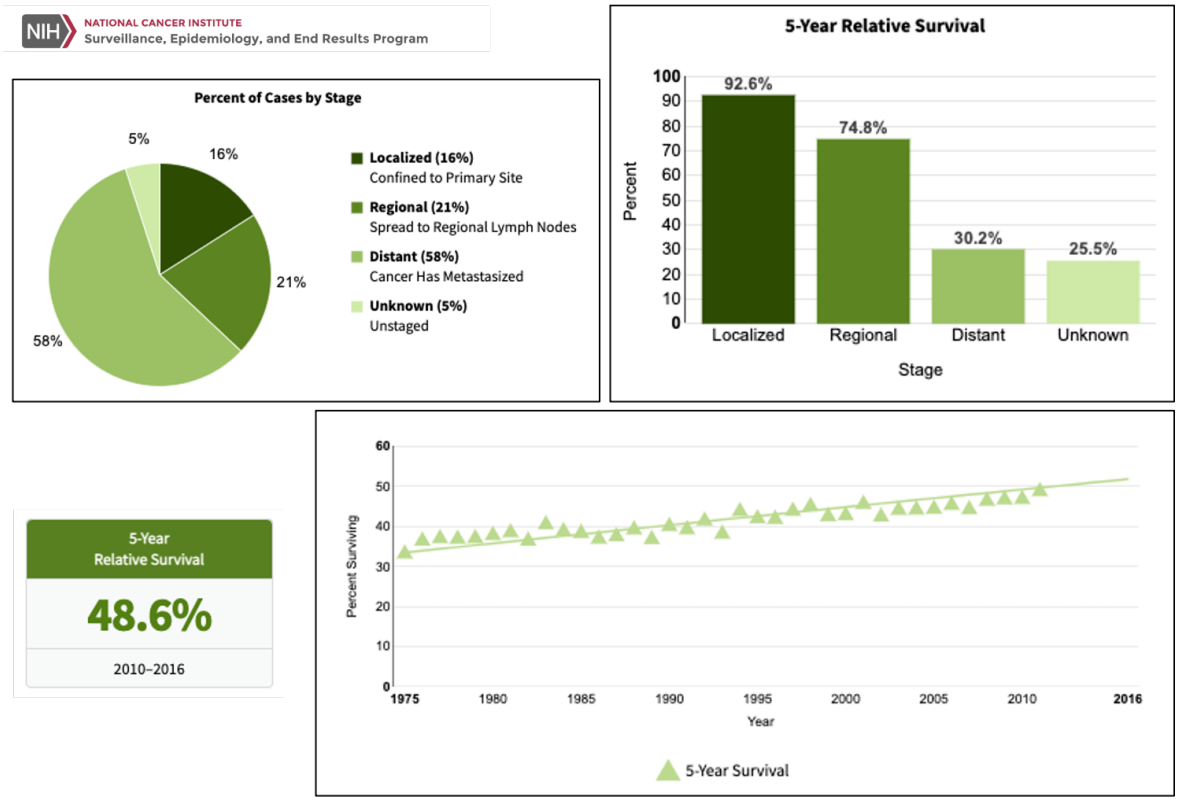

Figure 1. Ovarian cancer statistics from NIH.

The top left panel shows the percent of cases diagnosed at each stage. The top right panel show the 5-years survival rate relative to each stage. The lower panel shows the 5-year relative survival in the 2010-2016 timespan and the 5-year survival rate trend from the 1975 to 2012, projected to the 2016. Data available online: https://seer.cancer.gov.

Although the term "Ovarian Cancer" has been commonly associated to a single pathology, it encompasses a heterogenous group of diseases that share a common anatomical location. Indeed, nearly all benign and malignant ovarian tumors originate from one of three different cell types, specifically epithelial, stromal and germ cells, and on this basis can be collocated in three major categories, each one including numerous clinical subtypes (*14*). Moreover, tumors combining two or more subtypes are designated as mixed.

The most common type of ovarian tumors are the epithelial ones, that account approximately for the 60% of all tumors and for the 90% of malignant ones. The remaining 40% of non-epithelial origins usually don't progress to the malignant stage and account in the end for only 10% percent of malignancies, with a 5 - 6% of cases represented by sex cord-stromal tumors (e.g., granulosa cell tumors, thecomas, fibromas, etc.), and 2 - 3% of cases represented by germ cell tumors (e.g., teratomas, dysgerminomas, etc.) (*Fig. 2*).

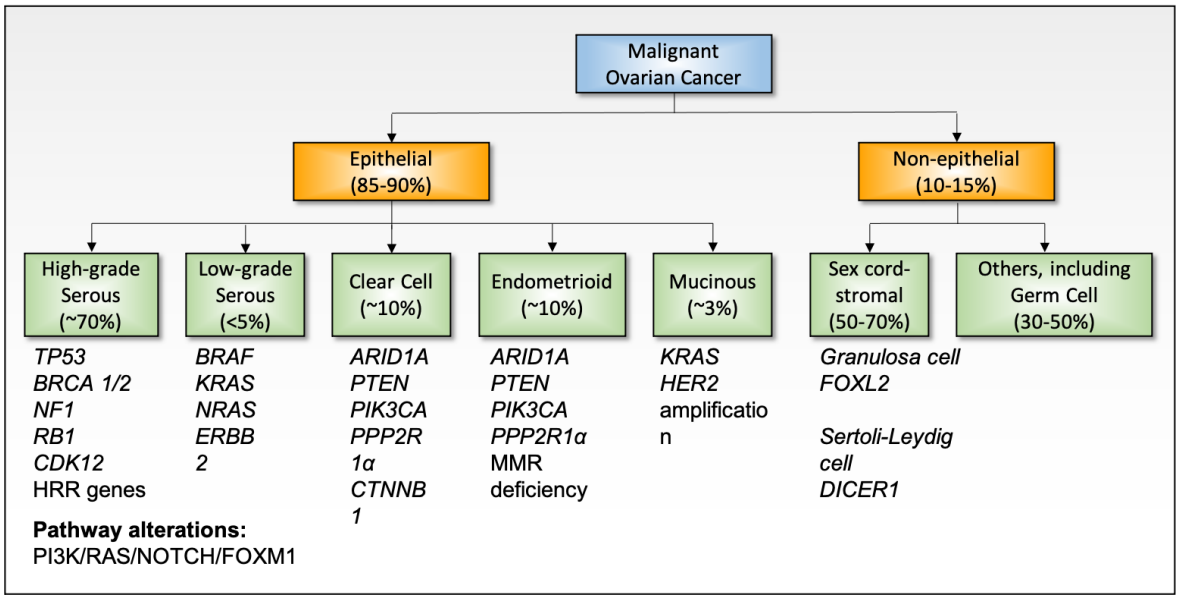

Figure 2. Malignant OC histotypes classification.

The several malignant OC histotypes are represented with the percentage of cases and the most common gene alterations.

Given their prevalence, most of researcher in the field focuses mainly on tumor derived from epithelial cells and so on the subcategory of ***Epithelial Ovarian Cancer*** (***EOC***).

1.1 Epithelial Ovarian Cancer (EOC)

Surface epithelial ovarian tumors occur primarily in women who are middle-aged or older and are rare in young adults, particularly before puberty (*15*). Epithelial OC reflects a heterogeneous disease with histologic subtypes (histotypes) that differ in their cellular origin, pathogenesis, molecular alterations, gene expression, and prognosis. According to WHO is possible to identify 7 different EOC subgroups, designated as follows: *serous, mucinous, endometrioid, clear cell, transitional cell (or Brenner type), mixed epithelial,* and *undifferentiated* (*16*). Each subtype could be further classified in:

i) *benign* if they lack of both exuberant cellular proliferation and invasive behavior;
ii) *borderline* (also known as atypically proliferating or of low malignant potential, LMP) if there is exuberant cellular proliferation but no invasive behavior;
iii) *malignant* if there is invasive behavior.

Another level of categorization was postulated by the International Federation of Gynecology and Obstetrics (FIGO) Committee, in order to provide standard terminology that allows comparison of patients between centers and to assign patients and their tumors to prognostic groups requiring specific treatments. In this classification, malignant diagnosed tumors are surgically and pathologically staged, to determine the level of the spreading of the tumor from the ovary (*1*). It is possible to identify 4 distinct stages (I – IV) with different severity of the disease:

I. Tumor confined to ovaries or fallopian tube(s);
II. Tumor involving one or both ovaries or fallopian tubes with extension from the pelvis or primary peritoneal cancer;
III. Tumor involving one or both ovaries or fallopian tubes, or primary peritoneal cancer, with cytologically or histologically confirmed spread to the peritoneum outside the pelvis and/or metastasis to the retroperitoneal lymph nodes;
IV. Distant metastasis excluding peritoneal metastases.

Moreover, on the basis of the apparent degree of cytological aberration, serous and endometrioid tumor subtype could be classified also as *low*- or *high-grade*. Thus, even if they share some similarities in histological appearance and terminology, high-grade and low-grade carcinomas are now considered to be two entirely different neoplasms, with distinct modes of carcinogenesis, molecular/genetic features and sites of origin (*16*).
The study of the pathology from the molecular and genetic points of view have led to a paradigm shift in the classification of this disease via the introduction of the dualistic model of ovarian carcinogenesis (*17*, *18*). This model segregates EOC subtypes into Type I and Type II categories:

I. Type I neoplasms usually evolve from pre-malignant or borderline LMP lesions, similarly to other epithelial cancers. From the genetic side, these tumors display frequent oncogenic alterations to many cellular signalling pathways such as RAS-MAPK and PI3K-AKT but are otherwise genomically stable and do not present mutation for the P53 gene (*18*). Clinically, these tumors typically are present as large, unilateral, cystic neoplasms that grow without relevant complication and when confined to the ovary show a positive prognosis (*18*). In this category are included low-grade tumors (serous, mucinous and transitional cell) and, although considered high-grade, clear cell tumors, and overall account for only 10% of the deaths from OC.

II. Conversely, Type II tumors are invariably high-grade, and comprises high-grade serous carcinoma (HGSC), carcinosarcoma, and undifferentiated carcinoma. These tumors are characterized by a high aggressiveness, rapid development and are usually present in an advanced stage (>75%). This result in a poor overall prognosis (*18*). From a genetic viewpoint, these Type II tumors are characterized by TP53 mutations and genomic instability due to defects in pathways contributing to DNA repair (*18*). The volume of tumor in the ovaries (with typically both ovaries involved) is less than that of the type I tumors, although the volume of extraovarian disease is generally much greater, often with massive disease in the omentum and mesentery, frequently accompanied by ascites (*18*). Type II neoplasms account for 90% of the deaths from ovarian cancer.

Among all malignant EOC, ***high-grade serous ovarian carcinoma*** (***HGSOC***) is by far the dominant subtype diagnosed clinically, accounting for the 70% of patients, with the remaining 30% shared among other 4 subtypes: endometrioid (ENOC; 10%), clear cell (CCOC; 10%), mucinous (MOC; 3%), and low-grade serous (LGSOC; <5%) (*15*). Moreover, is also the most lethal one, responsible for ~80% of deaths from all forms of ovarian cancer (*18*, *19*). HGSOC main characteristics are summarized in *Figure 3.*

1.2 High Grade Serous Ovarian Cancer (HGSOC)

HGSOC tumors are usually characterized by solid masses of cells with slit-like fenestrations or areas with papillary, glandular or cribriform architecture (*16*, *20*). The regions of solid growth are frequently accompanied by areas of extensive necrosis (*16*, *20*). From the cytological viewpoint, HGSOC is characterized by high-grade nuclear atypia with large, hyperchromatic, pleomorphic nuclei with the potential for multinucleation and with nucleoli that are usually prominent and might appear large and eosinophilic (*16*, *20*). The mitotic index is usually high, with abundant mitotic atypical figures. Areas of calcification typical of papillary tumors are also usually present as psammoma bodies (*16*, *20*) (*Fig.4*).

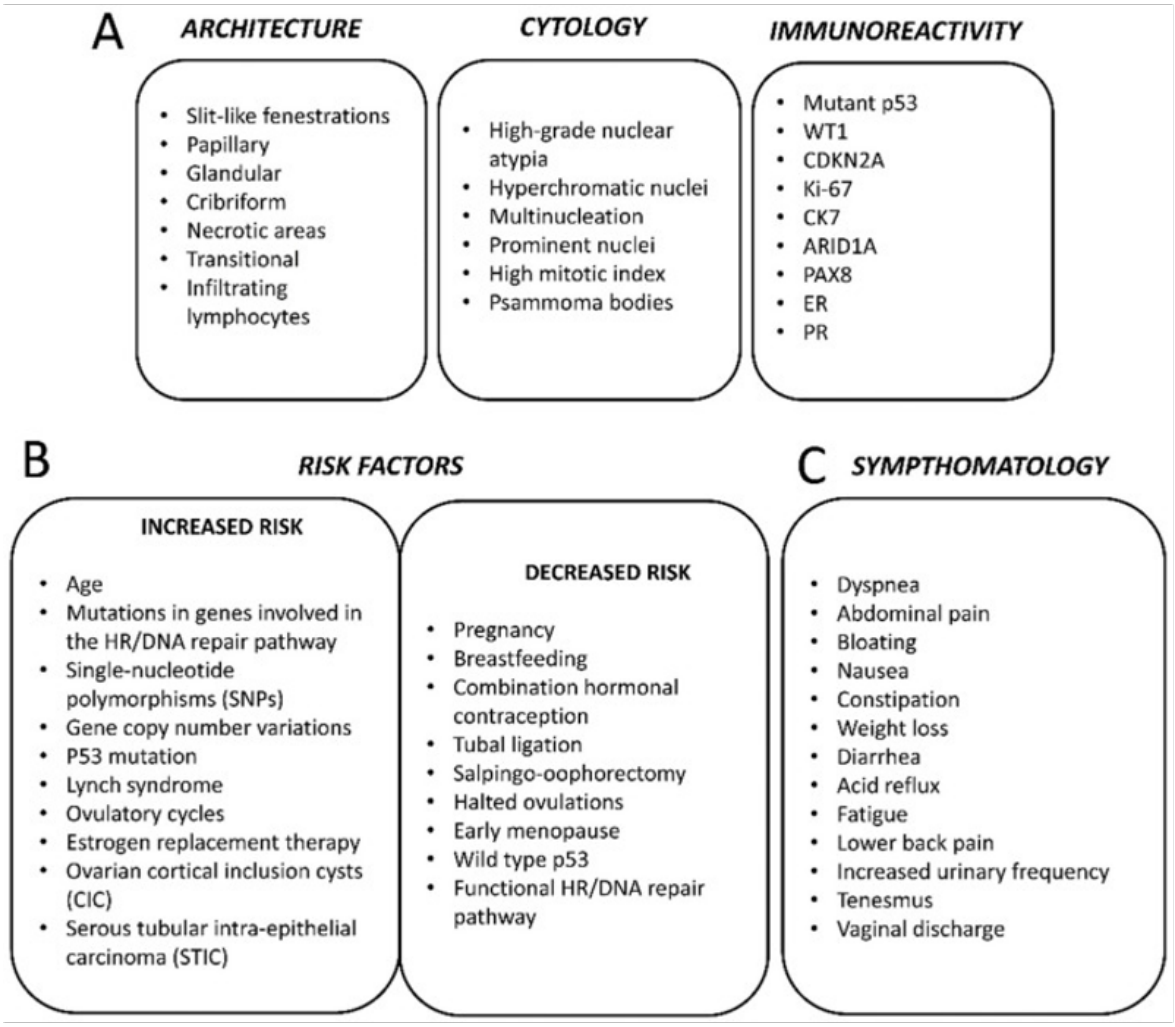

Figure 3. Histopathological features (A), risk factors (B) and symptoms (C) of HGSOC. *Picture from Lisio et al., 2019* (*20*).

From the genetic perspective, the vast majority of HGSOC (~90%) show a mutation in the TP53 gene, with mutations statistically recurrent in RB1, NF1, FAT3, CSMD3, GABRA6 and CDK12 genes (*21*). BRCA1/2 are germline mutated in around 20% of cases and are responsible for the majorities of familial cases and shows somatic mutations in a further 3% of cases (*21*). The combination of mutations, especially those regarding TP53 and BRCA1/2 genes, together with additional mutations in genes regulating the homologous recombination (HR) repair mechanism, are the main responsible for the high genomic instability of this carcinoma (*21*, *22*). Overall, these findings have suggested a model in which HR repair deficiency start a cascade of molecular events that define the evolution of HGSOC and direct its response to therapy (*22*).

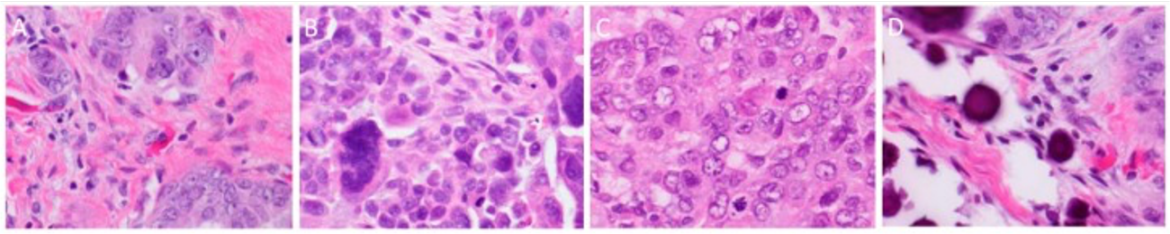

Figure 4. Cytological features of high-grade serous cancer.

A: *Multinucleated tumor giant cells;* ***B:*** *severe pleomorphism and prominent nucleoli;* ***C:*** *frequent mitotic figures;* ***D:*** *psammoma bodies. All original magnifications are x40. Pictures from Lisio et al., 2019* (*20*)*.*

However, although the increased understanding of the mutational profile of HGSOC, there is the still lack of fully validated, clinically relevant prognostic and predictive molecular markers. Identifying the underlying biology and molecular pathogenesis of the disease, shedding light on its heterogeneity and improving its understanding, is crucial for achieve a valid advance in treatment.

An interesting gene-based classification of HGSOC was introduced by Tothill and collaborators in 2008 (*23*), who transcriptionally profiled a large cohort of OC samples and identified 6 subtypes (C1 - C6), although only 4 were predominant in HGSOC. These subtypes represent specific categories: C1 (high stromal response), C2 (high immune signature), C4 (low stromal response), and C5 (low immune signature). Importantly, data show also that patients with C1-tumors displayed a significant trend toward early relapse and short overall survival. This trend is shared with the C5 subtype, and both clusters are characterized by a mesenchymal profile and a reduced presence of immune cells infiltrates (*23*). The identification of molecular subsets provides a context for additional genomic studies useful to understand the biology of the subtypes and of the pathology.

Despite the increased understanding of the mutational profile of HGSOC and its possible subclassification, providing also the basis for the formulation of hypothesis of the events for neoplasm initiation, the uncertainty about the cell of origin of the tumor has hampered the dissection of molecular mechanisms regulating the pathogenesis and the consequent improvement in the clinical care of patients. This aspect is nowadays still under debate and only recent research works are starting to shed light on this issue.

1.2.1 Cell of Origin of HGSOC

HGSOCs are usually diagnosed when they already have invaded the abdominal portion of patients, including the ovaries, leading to their attribution to an ovarian origin and the historical nomenclature of ovarian cancer. However, several evidences suggest that secretory epithelial cells of the distal portion of the fallopian tube, the fimbriae (and namely the fimbrial epithelium, FI), should be the precursors of at least a portion of HGSOCs.

Historically, the most common theory that lead to attribute the ovarian origin to this neoplasm was the so called "*incessant-ovulation hypothesis*" (*24*). This theory proposed that the repeated rupture and repair of the ovarian surface epithelium (OSE), due to the menstrual cycle, could led to an increased proliferation of cells generating an invagination and metaplasia of the OSE. This latter will lead to the generation of an intra-ovarian cortical inclusion cysts (CICs), which converges towards a Müllerian phenotype and is followed by the accumulation of deleterious mutations that results in the development of the neoplasm (*25*) (*Fig.5A)*.

However, the introduction of risk-reducing salpingo-oophorectomy (RRSO) in women with germline mutations in BRCA1 and BRCA2 lead to the identification of precursor lesions in the resected tubal tissue named serous tubal intraepithelial carcinomas (STIC) (*4*). This discovery started to challenge the long-held view that HGSOC should arise from the OSE and the intra-ovarian CICs, suggesting that the neoplasm could actually result anyway from CICs, however derived from the seeding of STIC-derived cells in the lumen of the ovary, favored by the ruptured stigmas of the surface epithelium during the menstrual cycle (*Fig.5B)*. In support of this hypothesis, studies with matched STIC and HGSOC revealed the presence of the same TP53 mutations in matched samples, suggesting that HGSOC could be clonally evolved from pre-neoplastic lesions in the fimbria (*26*) and the anatomical site of origin of many HGSCs. Recently, mutational analysis of associated STIC, primary HGSOC, and peritoneal metastasis from the same patient revealed the presence of a shared mutational spectrum, thus reinforcing the notion of a largely frequent, if not exclusive, fallopian origin (*27*).

Another arguable aspect is the understanding of why the precursor lesions of FI would find "fertile ground" in the ovary instead of developing directly in the fallopian tube (FT). However, evidence show that the FT environment is less prone than ovary to the growth and invasiveness of tumors, explaining also the high frequency of ovarian metastases originated from gastrointestinal, breast and lung cancers (*28*).

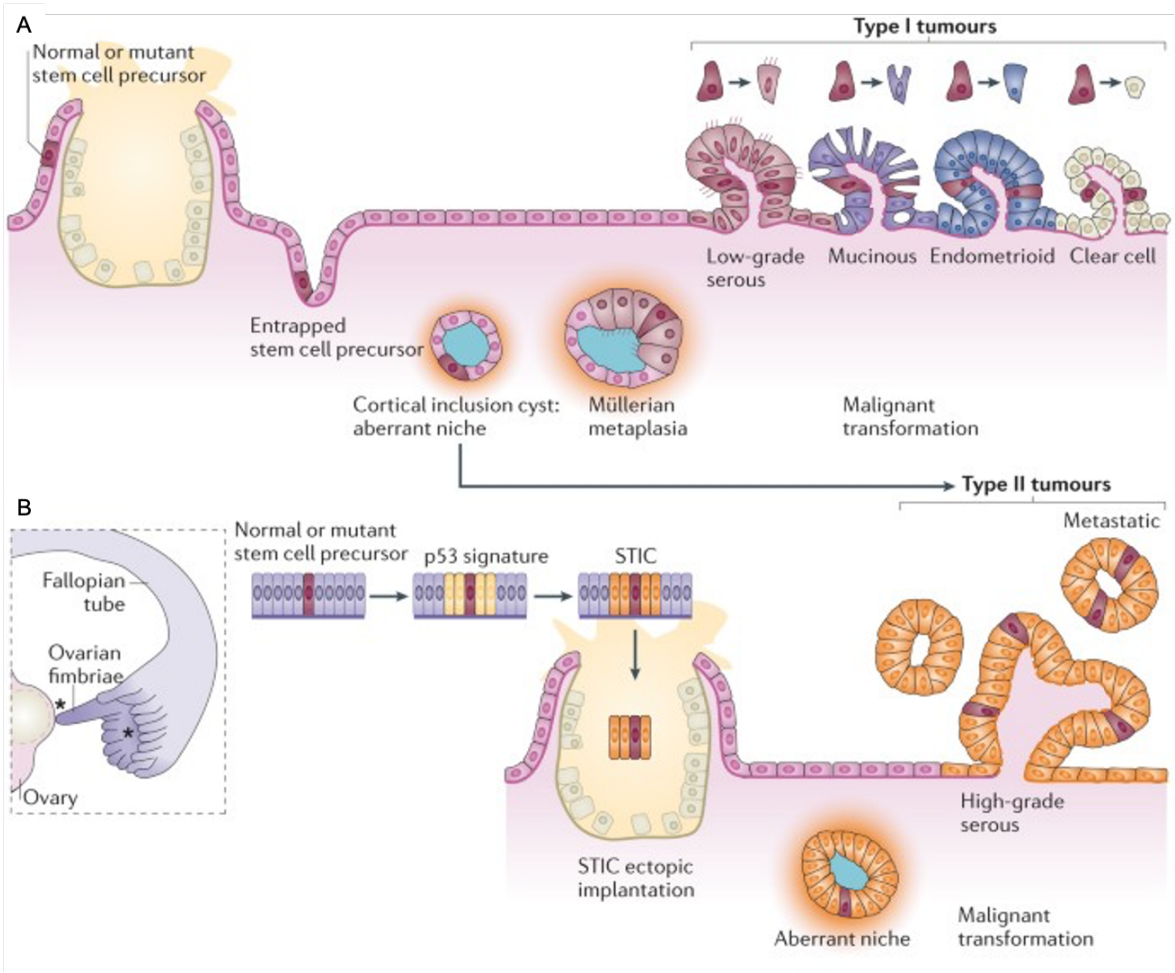

Figure 5. Tumorigenic models proposed for OC.

A: *Putative tumorigenic process of OSE derived OC. During incessant ovulation, an OSE stem cell becomes entrapped within the ovary cortex to form a cortical inclusion cyst (CICs) that, over the time, exposed to aberrant signals undergoes Müllerian metaplasia, followed by malignant transformation in type I EOC cell types. Alternatively, the OSE-derived CICs could arise type II tumors de novo.* ***B:*** *Putative tumorigenic process of fimbria derived OC. A putative fimbrial stem cell develops a p53 signature, followed by development of serous tubal intraepithelial carcinoma (STIC), that during ovulation could dislodges and becomes entrapped within the ovary cortex to form a cortical inclusion cyst and arise type II tumors. Picture from Ng and Barker, 2015* (*3*)

This aspect also influenced the incessant ovulation hypothesis, that was revisited posing emphasis on the possible role of the follicular fluid in creating a pro-inflammatory environment in the tuba during oocyte capture (*29*). Furthermore, the continuous break/repair cycle of the OSE could promote the implant of tumor cells shedding from the FI that in turn could further develop inside the ovary as primary inclusion cysts and, in a

second moment, as a complete HGSOC (*3*). Nevertheless, the exclusive attribution to the FI of the origin of HGSOC was still questionable since a significant proportion of HGSOC samples lack of STIC precursor lesion and, moreover, the reverse route of dissemination has been shown to be equally possible, with genomic studies supporting the possibility that at least a fraction of STIC, around the 25%, actually represent metastatic lesions of primarily ovarian lesions (*30*).

Given the supporting evidence to both theories, it was important to try to understand better if really both origins are plausible and, if it is true, if both give rise to a neoplasm with same clinical and molecular features and with the same prognostic value. The identification of signatures that allow to assign to each patient the correct origin would allow to improve the understanding of the HGSOC pathogenesis and identify critical pathways to be targeted clinically, in order to improve patient's care.

To overcome this problem, in the lab we recently published a work addressing this issue through a multi-omic approach, showing that both tissues can be considered as possible source of HGSOC, and that the origin of the tumor has a prognostic impact for the disease (*12*). Our findings support also the work of other groups that reach the same conclusion with a different set of experiments on mouse models (*31*).

In this work, we took advantage of the DNA methylation, one of the best characterized epigenetic mark, to stratify HGSOC in FI- and OSE- derived tumors. As known, DNA methylation acts through the addition of methyl group to the DNA molecule, influencing the transcriptional activity of a DNA segment without changing its sequence. One typical example is the deposition of DNA methylation at gene promoters that is associated to transcriptional repression of the downstream gene (reviewed in *32*). This important epigenetic process is also a relevant epigenetic tracer in the genomic imprinting, an inheritance process that causes genes to be expressed in a parent-of-origin-specific manner.

We decided to use DNA methylation as an epigenetic tracer for the cell of origin of HGSOC reasoning that, as in development, we expect tumor cells to retain a cell of origin-specific DNA methylation print, that we named OriPrint, which allow their stratification according to one of the two candidate tissues. A similar approach was also used to identify the origin to cancers of unknown primary (CUP) (*33*), offering for the first time a personalized treatment and improved care for patients.

To pursue our aim, we derived genome wide methylation profiles of FI and OSE samples and identified differentially methylated sites (DMSs) between the two tissues, and we then used those sites to stratify HGSOC solid tumors and metastatic Ascites (AS), both as

cultured cells from our cohort, and frozen tissues from a public cohort. We show that the cell of origin is the main responsible of the variability existing in DNA methylation between HGSOC samples, attributing, for the first time, a role for the cell of origin in determining the heterogeneity among different tumor samples. The possibility to epigenetically stratify tumors in FI-like and OSE-like prompted us to question whether the two subtypes have a different impact on patient's prognosis. To pursue this aim, we decided to interrogate a large retrospective cohort of formalin fixed paraffin embedded (FFPE) samples from our institute (European Institute of Oncology, IEO). However, since formalin fixation is known to compromise bisulfite-based DNA methylation, we translated our approach to the transcriptomics by RNAseq setting. To do so, we characterized the transcriptomic profile of our cultured samples and we then performed a differentially expression analysis (DEA) to identify differentially expressed genes (DEGs) between FI-like and OSE-like tumors, previously stratified by methylation. We then used the identified DEGs to stratify the RNAseq datasets derived from a macrodissected FFPE retrospective cohort and perform survival analysis. By this approach, we found that OSE-like tumors have a negative impact on patients' prognosis, and this was also confirmed when the approach is translated to two other published datasets, the TCGA and Tothill's ones (*21*, *23*).

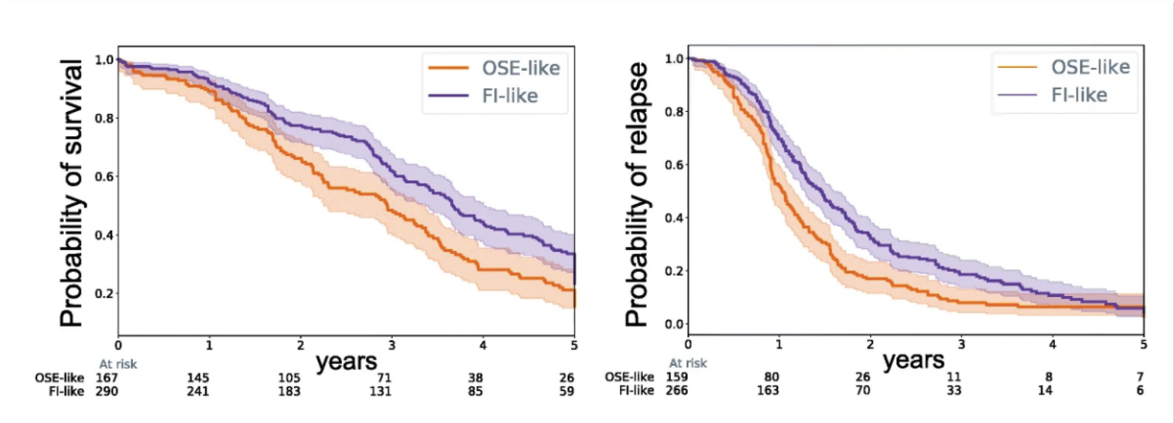

Figure 6. Cumulative overall (left) and disease-free (right) survival over 5 years of tumors arisen from the OSE or from the FI across different datasets.
From LoRiso et al., 2020 (*12*).

Interestingly, we also identified a specific enrichment in FI-like versus OSE-like tumors of previously described molecular subtypes of HGSOC (*23*). In particular, we found that the main subtype associated with OSE-like tumors is the C1 stromal category, which has been previously described as encompassing more aggressive and with poor outcome cases. This

evidence is in line with the survival status of patients in our cohort, with similar trends in TCGA and Tothill's cohort. Our results demonstrate that both fimbrial and ovarian surface epithelium can give rise to HGSOC in humans, supporting also the adoption of the more appropriate nomenclature high-grade serous tubo-ovarian carcinoma, and establish the feasibility of adopting the OriPrint-based classification for a rational stratification of patients (*12*).

All the recent advances in understanding the cell of origin and the genomic profiling of the disease were pursued by mainly using samples as frozen tissues, FFPE and biopsies from patients. Despite the current advances that those samples allowed to reach in the field, the recognized lack of clinically relevant models has strongly hampered the achievement of even more instrumental results.

1.2.2 Models used for study HGSOC

Conversely from other solid tumors, that could take advantage of several models to study the disease, HGSOC has started to benefit of more technological advancements only recently. The most common model used to study cancers were *cancer cell lines* (CCL). However, although several cell lines are available to model HGSOC, these are inadequately characterized in terms of histopathological features, genetic mutations, copy number alterations and gene expression patterns, being far from closely resemble the human disease (*19*, *34*) (*Fig.7*). Moreover, cell lines do not take into account the cell of origin of the tumor (*2*).

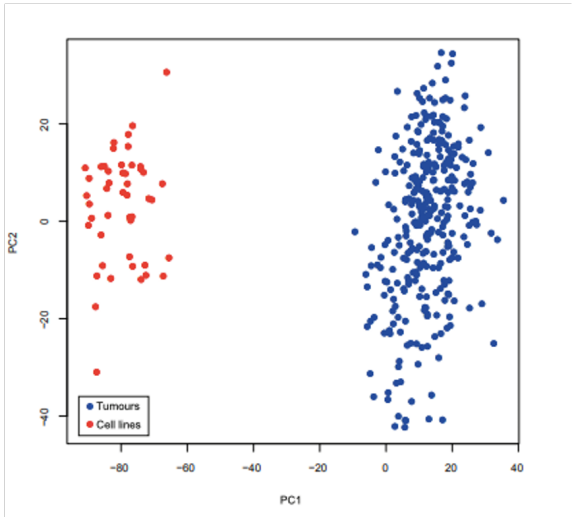

Figure 7. OC cell lines fairly recapitulates HGSOC in terms of gene expression.

Principal component analysis (PCA) comparing expression data from 47 OC cell lines (red) and 315 HGSOC tumor samples from TCGA (blue), using the 5000 most variable genes. Picture from Domcke et al, 2013 (*34*).

Interestingly, the analyses performed by Domcke and colleagues (*34*) showed that, at the publication date, the most frequently cells lines used to model HGSOC, specifically SKOV3 and A2780, were far from recapitulate an HGSOC but more closely relate to endometrioid cancers.

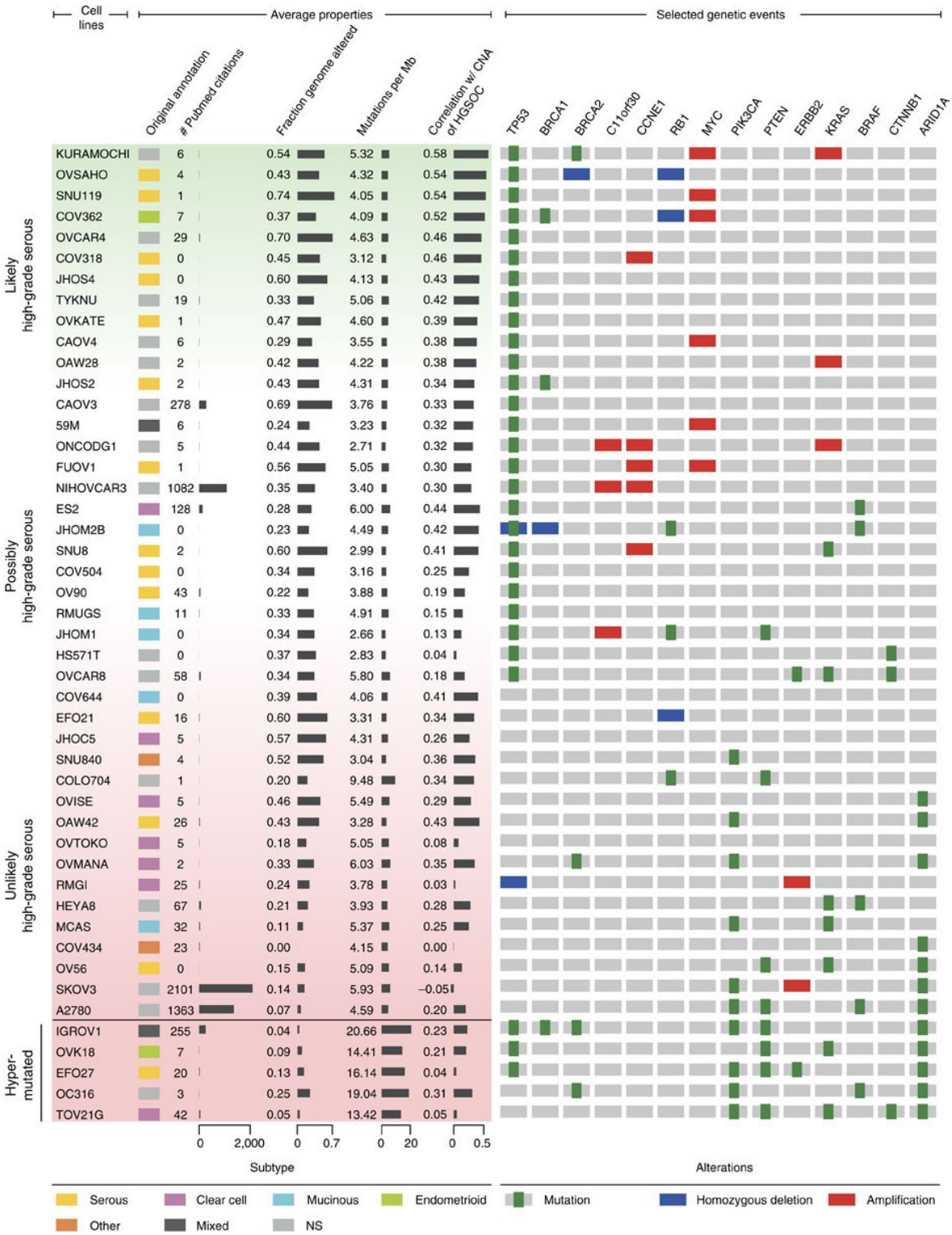

Figure 8. Ranking ovarian cancer cell lines by suitability as HGSOC models.

From Domcke et al. (*34*).

Contrariwise and surprisingly, some less used and undervalued cell lines seem recapitulate to a better extent the pathology from a mutational point of view and should be preferred to study HGSOC *(Fig.8)*.

The need to better understand the basis of HGSOC pathology pushed towards the establishment of other models that could allow a more in-depth sight on molecular mechanisms orchestrating the disease, and animal models were among most used models to study cancer, with a focus on murine models.

In recent years a lot of efforts were put in the development of mouse models of ovarian cancer, that can be divided in genetically engineered models (GEM) and Patient-derived Tumor Xenografts (PDTX).

Up to now, several GEM that histologically and molecularly resemble human HGSOC were developed, including models with mutant Tp53 and conditional inactivation of Pten and Brca1 or Brca2 (*19*, *35*). These mice develop HGSOC from a precursor STIC, recapitulating the tumor evolution pattern typical of fallopian tube carcinogenesis. Similarly, Kim and colleagues, in 2015, developed a GEM with a triple knock-out of P53, Dicer and Pten that grow HGSC both from fallopian tube and the ovary (*36*). Although GEM could be useful to study specific mutations, they are not perfectly able to recapitulate the whole neoplasm complexity and, given its great heterogeneity, additional GEM of other driving mutations should be needed to explore other tumor subset and obtain a wider viewpoint of the pathology. Moreover, if driving mutations are unknown, it is not possible to generate GEM.

PDTX are generated implanting the tissue or cells of a patient's tumor into an immunodeficient mouse, in order to create an environment that allows the natural growth of the tumor, its monitoring and the evaluations of treatment' response for the original patient (*37*). These models have been extensively used to propagate *in vivo* primary tumor cells, that usually undergo senescence upon culturing, and to investigate the patients' response to treatment and the eventual onset of resistance mechanisms. However, the use of immunocompromised mice clearly reduces the effect of the tumor immune microenvironment on tumor growth, and they're routinely use in research settings is not technically easy, requiring also a significant economic effort to be pursued.

Despite the available models listed above, there is a strong consensus that clinically relevant *in vitro models* should be established to improve the investigation of this pathology.

Patient-derived primary cell cultures could provide a more effective and accessible model system. Differently from cell lines, primary cells, being derived directly from patients, closely resemble the genetic and epigenetic background of cells *in vivo*, mimicking their physiological state and, although for a short period of time, are expected to maintain their *in vivo* functions. Despite their advantages and conversely from cell lines, primary cells are extremely sensitive in cell culture experiments and are usually differentiated and post-mitotic cells, which is reflected in a finite lifespan and limited expansion capacity. This means that these cells are no longer able to divide, and their proliferation potential is low. The restricted lifespan is the major limitation of primary cells, preventing their use for several applications, such as genetic engineering. Moreover, the establishment of primary cells culture and the identification of ideal culture conditions able to guarantee their optimal growth without altering considerably their transcription and epigenetic profile is difficult to achieve. Despite of difficulties, several groups were able to generate a protocol to derive primary cell cultures from ovarian cancer patients (*38–40*), providing useful and more precise tools to study the pathology.

However, the low success in culture establishment and limits described above drove the scientific community towards the embracement of new paradigms and models that could bring effective advancements in the clinical setting. These models should be able to phenotypically and genotypically interrogate the real human malignancy, discovering new principles underlying the disease and highlighting the differences from normal tissues.

Among technological advances, ***organoids*** are emerging as a powerful system to investigate tissues. Organoids can be derived both from healthy and diseased tissue of each individual, propagated *in vitro*, and preserved as frozen stocks. Moreover, tumor-organoids capture the essential uniqueness of each individual tumor, integrating its genetic, epigenetic and cellular heterogeneity and making it experimentally tractable in a manner that has been so far impossible to attain.

2. ORGANOIDS

Organoids represent miniature self-organizing, three-dimensional structure that recapitulate the architecture and growth pattern of the tissue from which they originate.

The self-organizing capacity of vertebrate cells was demonstrated half a century ago, showing that also after the complete dissociation, cells can reaggregate and reconstruct the original architecture of an organ (*41*, *42*). Given the fact that this organotypic cultures self-organize during cell sorting and reaggregation experiments, developmental biologists coined the term "organoids", although it was initially used in oncology as a synonym of teratoma and dermoid cysts and was firstly reported in 1946 (*43*).

Interestingly, if we look at the popularity of the term organoids on Pubmed (*Fig. 9*), a first trend of popularity was showed exactly during years 1965 - 1985, precisely for its use in those developmental biology studies regarding the dissociation and reaggregation of tissues (reviewed in *41*). Thereafter, there was a sharp decline and a period of flat calm for about 20 years, followed by a robust rise after 2009, when new work on a conceptually different organoids system were emerging as a 3D culture reconstruction of tissues.

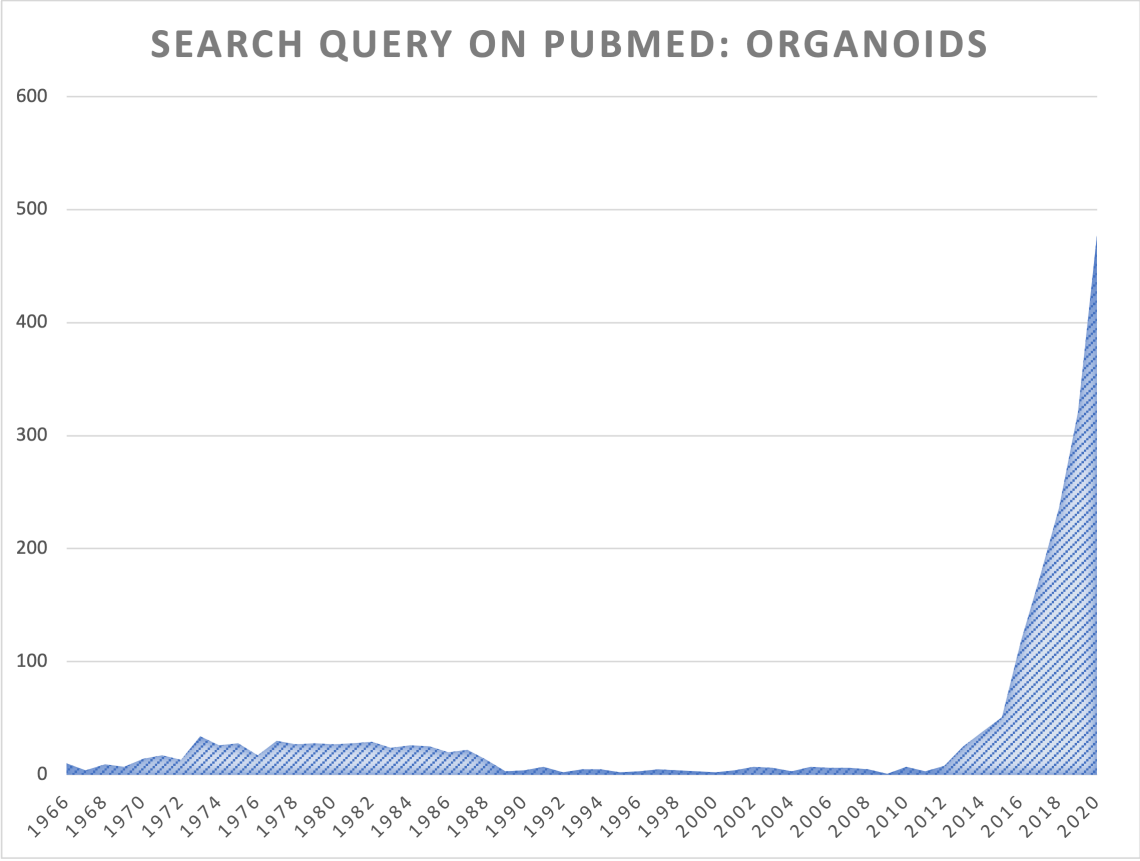

Figure 9. Citations by year for the term "organoids" on Pubmed.

Data from 1966 to 2020.

Despite the term “organoid” was not used, the first reconstitution of a 3D tissue structure was performed by Rheinwald and Green in 1975 (*44*), where they described the first long-term culture of normal human cells, combining freshly isolated keratinocytes with irradiated mouse 3T3 fibroblasts. They observe that, as in stratified skin, cell division was confined to the basal layer with superficial layers consisting of terminally differentiating keratinocytes that gradually developed a cornified cell envelope. Their work paved the way for first treatments using autologous cells culture with subsequent reimplantation in patient of keratinocyte (*45*) and, later, of cornea (*46*). This was the first use, albeit unaware, of cultured stem cells, the kind of cells responsible of the successfully evolution of organoids.
As showed by Fig. 9, nowadays the use of organoids and tridimensional culture is really on an exponential growth, and this was also made possible by the intensely increased understanding of stem cells biology, the cells at the foundation of organoids technology.

2.1 Stem Cells (SCs)

Cellular differentiation is an essential process for development, growth, reproduction and survival of every multicellular organism. For this reason, its regulation was heavily investigated in last decades. At the apex of differentiation processes there are the so named stem cells, undifferentiated (or partially differentiated) cells able to self-renew and, upon specific stimuli, to undergo asymmetric divisions and start a differentiation program.
The self-renewal and differentiation abilities of stem cells is strictly regulated by dynamic interaction between genetics, epigenetics and extrinsic signalling.
On the basis of the self-renewal and differentiation capabilities, stem cells were classified in several subtypes *(Fig. 10)*:

- ***Totipotent*** are those stem cells able to differentiate in every kind of cells of the organism including embryonal annex tissues like amnios and chorion. The iconic totipotent stem cell is the ***zygote***. However, are totipotent stem cells also first blastomeres of the mammal embryonic development, up to the moment of embryo compaction, necessary for the formation of the blastocele, which occurs at the 8-cell stage.
- ***Pluripotent*** are the stem cells that are able to originate all the tissues of the body, making exception for embryonic annex. During the morula compaction, the transition from toti- to pluripotency is marked. Indeed, at this stage we can observe the formation of two different cellular population, one that will give rise to the trophectoderm, from which the extraembryonic tissues will arise, and the other one,

the inner cell mass (ICM) that will give rise to all tissues of the embryo. The prototype of pluripotent stem cells is ***Embryonic Stem Cells*** (***ESCs***), accompanied by the more recently introduced (and nowadays more used) ***induced Pluripotent Stem Cells*** (***iPSCs***), that are pluripotent cells experimentally generated from somatic cells, through a reprogramming process

- ***Multipotent*** stem cells include those cells with a restricted differentiation power, able to differentiate only in few cell types. A classic example of multipotent stem cells is ***Adult Stem Cells*** (***ASCs***), which are found in body tissues and are usually able to derive only cells of tissues in which they are resident.
- ***Unipotent*** stem cells, finally, are stem cells able to differentiate only in one type of cell. Those cells lost most of their stem cell properties and it is currently unclear if true unipotent stem cells exist. They are often associated to precursor cells, known as the intermediate cells existing before terminal differentiation.

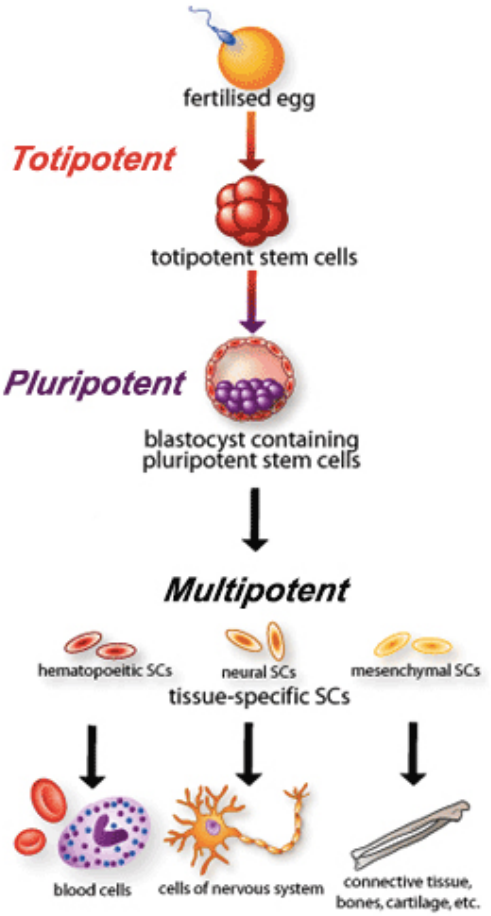

Figure 10. Representation of the in vivo stem cells potency.

Given their relevant properties, the interest in stem cells use in therapy has soared, especially for regenerative medicine. In this field, ASCs and iPSCs have aroused a significant heed, since their use should avoid the phenomenon of tissue rejection typically encountered in transplantation therapies. Indeed, being directly derived from patients, these cells should be recognized as *self-autologous* from the immune system avoiding the rejection reaction. Moreover, specific SCs populations where discovered also in cancer, the so defined Cancer Stem Cells (CSCs), whose involvement in specific features of the pathology became continuously more important, increasing the interest in the field for understanding their precise role and functions.

2.1.1 Induced Pluripotent Stem Cells (iPSCs)

As suggested by the name, induced pluripotent stem cells are terminally differentiated somatic cells that, upon the induction through specific stimuli, are brought back to their naïve state allowing them to acquire pluripotency and to act as pluripotent cells. The process through which they are reset is called ***cellular reprogramming***.

Like ESCs, iPSCs can be indefinitely propagated *in vitro* in an undifferentiated status and, upon specific *in vitro* stimulation, could be differentiated in different cellular types. Moreover, even after an extensive *in vitro* proliferation when implanted in an early embryo they are able to participate to the normal embryo development.

Conversely from somatic cells, which are characterized by a small nucleus, a few evident nucleolus and abundant cytoplasm, iPSCs (like ESCs) shows very big nuclei and nucleoli surrounded by a poor cytoplasm.

The generation of iPSCs was a breakthrough in the stem cell field and in their prospective use in a wide variety of fields, ranging from regenerative medicine to drug screening and *in vitro* disease modelling. The work of Takahashi and Yamanaka, in 2006, was one of the most impacting publication ever (*47*). In their work, they showed that, through the use of only 4 specific genes, identified as reprogramming factors, they were able to reprogram embryonic and adult murine fibroblasts. The following year the same approach was applied to human fibroblasts, achieving the same result (*48*).

The generation of iPSCs initially foresee the use of lentiviruses to deliver the reprogramming factors, but new technological advancements showed that it was possible to reprogram somatic cells also through integration-free methods, ranging from RNAs to small chemicals, increasing their clinical safety. Furthermore, the ability to induce the

differentiation of these cells in always more different kinds of somatic cells is increased during years, making their clinical use more effective.

The possibility to derive iPSCs from virtually any differentiated cell allow also the possibility to model genetic disorders *in vitro*. This is of particular relevance for neurological disorders, given the frequent inaccessibility to brain patient tissues. Indeed, once obtained a cell from a patient with a specific genetic disorder, the possibility to reprogram that cell in an iPSCs provide an unlimited source of cells to use for multiple purposes, ranging from the study of the evolution of the pathology, when iPSCs are differentiated in the somatic cells of interest, to their use in drug screening.

2.1.2 Adult Stem Cells (ASCs)

In our body, stem cells are present during the entire lifespan of an individual, from early development to the adult life. Stem Cells isolated from adult tissues are named ***Adult Stem Cells*** (***ASCs***). Similar to other stem cells, ASCs are able to self-renew and differentiate in several lineages, although with a limited differentiative capability, usually restricted to cells of tissues in which ASCs reside.

The main aim of ASCs is to guarantee the normal tissues homeostasis, enabling the turnover of cells that are lost during aging or for some kind of tissue damage, in a process called tissue turnover. To allow this process, ASCs, conversely from ESCs that replicate fast, are mainly found in a quiescent low metabolic state (*49*, *50*). This is possible because the differentiation is considered a hierarchical process, where, upstream, a stem cell give rise to an intermediate population of cells with reduced self-renewal and differentiation ability called committed progenitors or Transit Amplifying cells (TA). These cells, characterized by a high proliferation potential, replicate fast increasing their numbers and simultaneously reducing the amount of division performed by the original stem cell, in order to preserve the stem cells pool.

The different kind of signals that could “activate” a quiescent adult stem cell are several, like, for example, tissue damage. Indeed, the ASCs activity is strongly influenced by the micro-environment of the specific tissue in which they reside, the so named ***niche***. The niche could be defined as a specific anatomic site whose composition and features regulates the way in which ASCs participate to generation, maintenance and repair of the tissue (*51*). The niche protects stem cells from a putative depletion but, in the meantime, also protects the organism from an unwanted potential aberrant proliferation of those cells.

In other words, to guarantee the long-term homeostasis of tissues, the number of ASCs of each tissue should be constant to avoid hyperplasia or tissue degeneration phenomena, highlighting the need of a perfect balance between proliferation and differentiation of ASCs. The main mechanisms through which the ASCs pool is retained while ensuring the generation of a differentiated progeny are the ***asymmetric cell division*** and the ***population asymmetry*** *(Fig.11)*. In the first case, the stem cell gives rise to two daughter cells, one of which, identical to the mother, will retain stem capacity. The other cell, conversely, will undergo differentiation, becoming a progenitor. In the second case, instead, the asymmetry concerns the entire population rather than single cell and is achieved through different symmetrical divisions of the stem cell. These symmetrical division occur with equal frequency and give rise to two stem cells or two progenitor cells respectively (*52*).

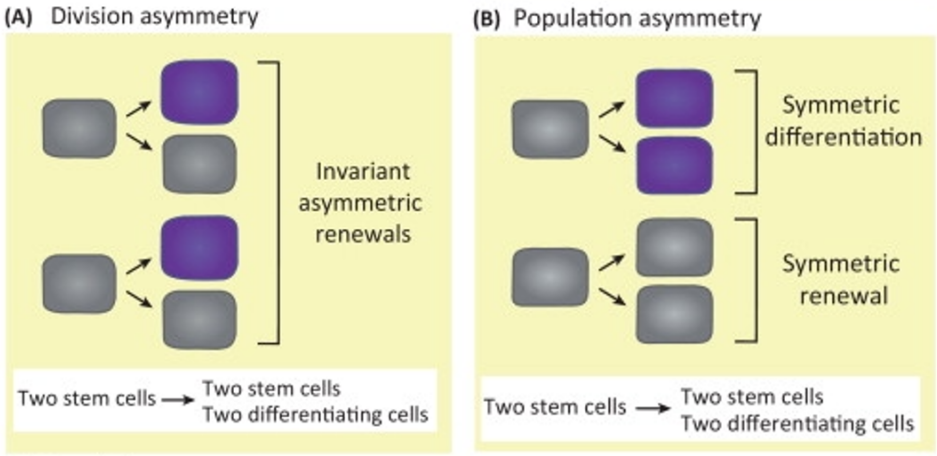

Figure. 11. Division and population asymmetry. *Adapted from Stine and Matunis* (*53*).

Interestingly, although first models assumed the existence of a single quiescent stem cell population residing within the specific tissue niche, some doubts arose regarding the ability of these long-term quiescent ASCs to support the normal homeostasis of rapidly regenerating tissues, such as blood and intestine. Indeed, the normal model in which ASCs generate TA, which in turn differentiate in somatic cells, was not satisfactory, given the short lifespan and restricted self-renewal ability of progenitors. Further study, therefore, identified different active and quiescent population of stem cells in several tissues, located in separate albeit adjacent sites (*54*). The most studied ASCs, the Hematopoietic Stem Cells (HSCs), provided most of the information regarding ASCs and it was among these cells that, indeed, two different stem subpopulations were firstly identified. These ASC assure the daily and long term production of blood cells (*55*).

2.1.3 Cancer Stem Cells (CSCs)

Cancer stem cells (CSCs) are cancer cells possessing features associated with normal stem cells and able to give rise to all cell types found in a particular cancer sample. The CSCs concept was proposed decades ago, claiming that CSCs may sustain tumor growth, similarly to the renewal of healthy tissues, through the stem cells processes of self-renewal and differentiation, and it has gradually become clearer that many tumors harbor CSCs in dedicated niches. CSCs play a role in not only the creation of cancer but also its evolution, metastasis and recurrence (reviewed in *56*). Indeed, such cells are hypothesized to persist in tumors as a distinct population and cause relapse and metastasis by giving rise to new tumors. Therefore, development of specific therapies specifically targeting CSCs holds hope for improvement of survival and quality of life of cancer patients, especially of those with metastatic diseases.

CSCs have been identified in many common cancer types, including leukemia, breast, colorectal and brain cancers and, of relevance for this thesis, also OC (reviewed in *57*).

The accumulation of knowledge on healthy and diseased stem cells, acquired during decades of studies, have brought to the increased number of applications available for this kind of cells. Among all the available applications, the possibility to use these cells to generate tridimensional structure *in vitro* has allowed the generation of the tridimensional culture technology called organoids that nowadays really represent a breakthrough in the modelling of tissues and diseases.

2.2 Rise of the organoids

Austin Smith, one of the most recognized experts in the stem cell-field and director of the Stem Cell Institute at the University of Cambridge, UK, identified organoids as the probably most significant development in the stem-cell filed of the last decade. Nowadays, organoids have become an independent research field and a precise definition of the term organoid became increasingly important. An organoid, simply defined as resembling an organ, must be followed by several features that are characteristics of organs. Organoids must be composed of different cell type of the organ it models, it should exhibit some function specific of that organ and cells in the organoid should be organized similarly to the originating organ itself. Madeline Lancaster and Juergen A. Knoblich in an important reviews defined an organoid as “a structure containing several cell types that develop from stem cells or organ progenitors and self-organize through cell sorting and spatially restricted lineage commitment, similar to the process in vivo” (*41*) *(Fig.12)*.

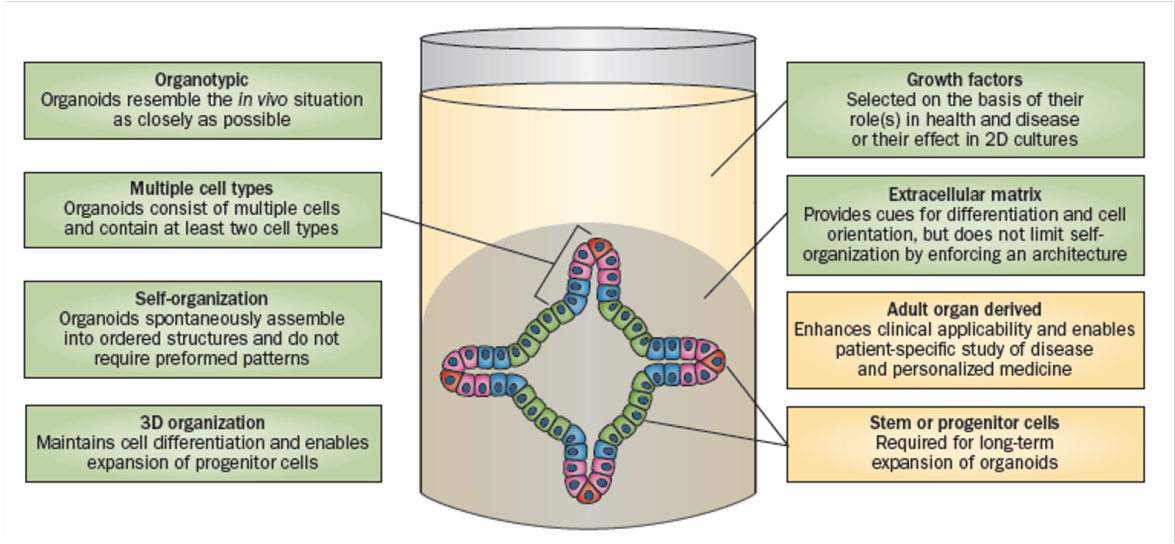

Figure 12. Representation of organoids culture system and its main features.
From Rookmaaker et al, 2015 (*58*).

The first report of generation from a stem cell of a structure resembling an organ was in 2008, when researchers in Japan generated layered spheres reminiscent of a cerebral cortex from murine and human ESCs (*59*). The year after Sasai announcement, Hans Clevers at the Utrecht University, in Netherlands, reported the creation of a mini gut and so the first real generation of an organoid (*60*). This result was achieved thanks to the discovery, in the same lab, of a population of ASCs with an unlimited capacity to divide and replenish the intestinal lining in mice in 2007 (*61*). This discovery prompted Clevers' lab in the task of culturing these SCs, a result reached the following year by Toshiro Sato (*60*), who, rather than culture those cells in a normal culture of flat cells, decided to embed ASCs in Matrigel, an artificial extracellular matrix, and surround them with several nutrients, growth factor and small molecule.

The growing of a mini gut was based on the assumptions obtained combining previously defined insights in the growth requirements of intestinal epithelium. First of all, were identified three factors related to the proliferation of crypts and the expansion of crypt numbers: the Wnt signalling and the Wnt agonist R-spondin1, the epidermal growth factor (EGF) and Noggin, an inhibitor of several bone morphogenetic proteins (BMPs). Then was decided to explore the use of laminin-rich Matrigel since laminin-α1 and -α2 are strongly enriched at the crypt base. After several trials, their discoveries confirmed that crypts growth required EGF and R-spondin1 and their passaging revealed a requirement for Noggin (*60*). Interestingly, was observed that cells divided and differentiated into multiple types, forming hollow spheres with protrusions enriched of structures that resembled the

intestine's nutrient-absorbing villi and crypts. They observed also that the crypt region underwent continuous budding events, reminiscent of crypt fission, and Paneth cells were always present at the bud site. Very surprisingly, these organoids could be propagated *in vitro* and were cultured for more than 8 months without losing the described features. The work went even further, with the derivation of organoids also from isolated single $Lgr5^+$ sorted cells, plated at single cell resolution. Moreover, organoids derived from single stem cells were indistinguishable in appearance from those derived from whole crypts (*60*).

These organoids represent a really important resource for disease modeling and for drug testing and, indeed, they were soon used to model and study cystic fibrosis, and, in perspective, they could be used to model several other pathologies (*62*).

Since Clevers' lab achievement in 2009, efforts to grow stem cells into rudimentary organs have taken off and researchers around the world have worked to produced three-dimensional structures from a wide variety of tissues. Of particular relevance was also the work by Madaline Lancaster and colleagues in 2013 (*63*) with the derivation of structures resembling embryonic brain obtained from culture of ESCs induced to differentiate in neural rosettes, clusters of cells that can differentiate in several types of neuron. Interestingly, cultured cells refused to stick to the bottom of the culture plate, floating and forming strange spheres in which were recognized the presence of the dark cells of the developing retina, an outgrowth of the developing brain. Moreover, when sliced, these spheres showed a variety of neurons, confirming the development of a rudimental brain in a dish. They named this pluripotent stem cell-derived three-dimensional structure as cerebral organoids, showing that they were constituted of various discrete, although interdependent, brain regions, including a cerebral cortex containing progenitor populations that organize and produce mature cortical neuron subtypes. Furthermore, they showed that cerebral organoids recapitulate features of human cortical development, namely characteristic progenitor zone organization with abundant outer radial glial stem cells (*63*). Moreover, using RNA interference (RNAi) and patient-specific iPSCs they were able to model some aspect of the microcephaly, a disorder that has been difficult to recapitulate in mice. They demonstrated that patient organoids show a premature neuronal differentiation, a defect that could help to explain the disease phenotype. These discoveries redeem the need of an in vitro model of human brain development that allow to recapitulate the complexity of the human brain and study many brain disorders.

The two pioneering studies show how, starting from two different kind of stem cells, it is possible to recapitulate *in vitro* tridimensional structure resembling those of the organs

from which they derive. Organoids can be expanded, cryopreserved as biobanks and easily manipulated using molecular biology techniques available today. Organoids represent an important bridge between traditional 2D cultures and *in vivo* mouse/human models, as they are more physiologically relevant than monolayer culture models and are far more amenable to manipulation of niche components, signalling pathways and genome editing than *in vivo* models (*64*). The features of organoids made them a significant technological advance and paved the way to the development of the number of different organoid culture systems available today.

2.3 Organoid culture systems

Organoids, being stem cell-derived and self-organizing 3D cultures, can be classified on the base of the kind of stem cells from which they derive, namely pluripotent stem cells (PSCs), that includes ESCs and iPSCs, and organ restricted ASCs. Both approaches exploit the proliferation potential of stem cells in culture and, despite for PSCs this potential has been an essential prerequisite for their discovery, ASCs were long believed to be incapable of significant expansion outside of the body. Moreover, new insights in organs stem cell niches have allowed the development of growth factor cocktails that mimic them, supporting the maintenance of stem cell outside the body and showcasing the ability of these cells, when pushed to differentiate in culture, to self-organize into structures reflecting features of the tissues to which they are fated. Nowadays, organoids from a wide variety of body tissues, derived both from PSCs and ASCs, are available and used to study tissues, model diseases and correct gene-based pathology through personalized medicine approaches (*Fig. 13)*. The more relevant organoid systems, divided on the basis of the stem cell from which are derived, are briefly discussed below.

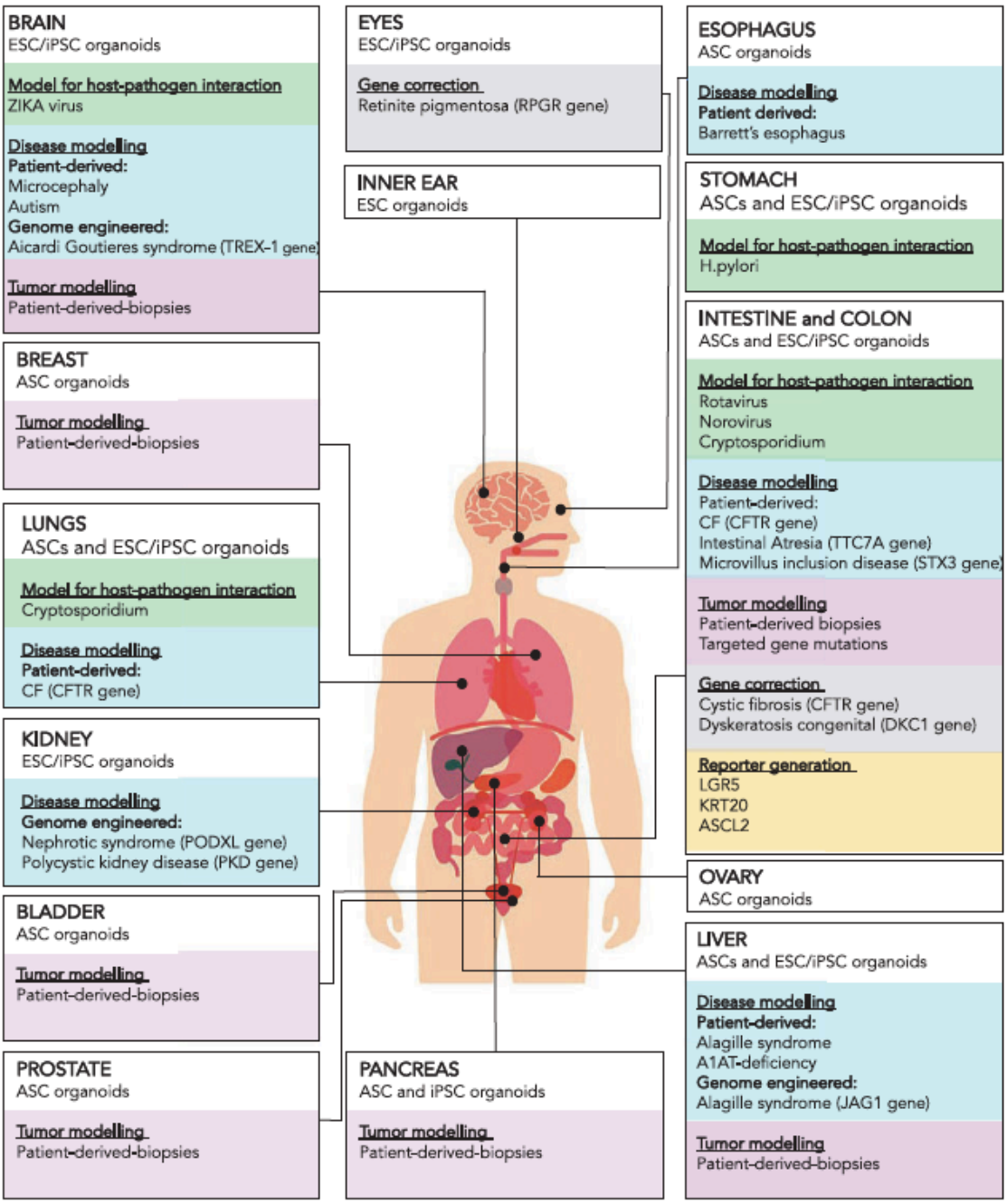

Figure 13. List of tissues from which organoids have been derived and their relative applications. *From Artegiani and Clevers, 2018 (65).*

2.3.1 Pluripotent stem cells (PSCs) organoids

The possibility to differentiate PSCs in terminally differentiated cells was of strong interest from the discovery of these special cells. Sasai and colleagues were the first to bring the differentiation concept to a higher level, comprehensively of also spatial patterning and morphogenesis. In few years of work, they were able to develop methods to generate brain structures, retina, and pituitary gland *in vitro* (*59*, *66*, *67*), and then they were followed by many other groups interested in differentiating PSCs in other tissues.

Nervous systems organoids

In the absence of any inhibitors of neural differentiation, such as BMPs, Wnts or Nodal, ESCs cultured tends to spontaneously proceed towards neural differentiation, showing a neural-default state for ESCs. On the basis of this notion, Sasai and colleagues designed a serum-free floating culture of embryoid body-like aggregates, plating PSCs derived from growth factor-free 2D cultures in non-adherent culture plates and, after 7 days, replating them in adhesion plates (*59*). When replated, cells differentiate and polarize to form a continuous neurectoderm-like epithelium that further generates stratified cortical tissues containing cortical progenitors, deep and superficial cortical-layer neurons and so called Cajal-Retzius cells. Basically, they observed that in the absence of growth factors, the generated cortical tissue spontaneously adopts a rostral hypothalamic fate (*59*).

Few years later, Lancaster and Knoblich, in Wien, took this approach to a further level generating brain organoids (or mini-brains), neural structure composed of several different brain regions (*63*). Similar to Sasai method, they started with floating embryoid bodies but, instead of replating them in adhesion culture, the aggregates were embedded in the artificial laminin-rich extracellular matrix called Matrigel, allowing the outgrowth of large neuroepithelial buds which spontaneously developed into various brain regions.

The next step was performed by using selectively identified growth factor in order to guide the differentiation towards specific region of the brain. In this way was possible to provide regional identity to brain structure such as *dorsal cortex*, *ventral forebrain*, *cerebellum*, *adenohypophysis*, *hippocampus* and *retina* (reviewed in *6*).

Gastric organoids

Stomach and intestine are derived from the definitive endoderm, that can be generated from PSCs by a treatment with Activin-A. The subsequent supplementing of BMP inhibitors and of FGF and Wnt activators could drive the cells towards a foregut fate, that is further pushed towards a posterior foregut fate, the precursor of the stomach, by the application of retinoic acid (RA). Finally, high levels of EGF converted these precursor into human gastric organoids, characterized by primitive gastric gland and pit-like domains, proliferative zones with Lgr5+ stem cells and mucous cells (*68*).

Alternatively, the addition of FGF4 and WNT3a to activin treated PSCs lead the differentiation towards the mid-/hindgut fates and the addition of the pro-intestinal growth factor cocktail identified by the Clevers lab (*60*) and featured by the presence of R-Spo1, EGF and Noggin allow the derivation of small intestinal organoids also from PSCs (*69*).

Liver organoids

Liver is another organ derived from the endoderm and specifically from the foregut endoderm, where progenitor cells delaminate and form the liver bud. The differentiation in hepatic endoderm is a complex procedure, that entails the cross-signaling between endodermal, epithelial, mesenchymal, and endothelial progenitors. Taniguchi and collaborators were able to derive hepatic endodermal PSCs in adherent culture by the use of activin, bFGF and BMP4. Then, this hepatic induced PSCs were mixed with mesenchymal stem cells (MSCs) and endothelial cells, plated at high density on a layer of Matrigel, and what they obtain were spontaneously formed 3D aggregates, reminiscent of an adult liver (*70*). Moreover, these liver organoids contain blood vessels and present liver-specific functions such as protein production and human-specific drug metabolism.

Few years later, another group was able to differentiate PSCs into cholangiocyte-like cells and using 3D culture conditions based on the addition of EGF and other common factors they promote the maturation of bile duct cells driving their polarization into cystic organoids exhibiting a morphology and functionality reminiscent of primary bile duct (*71*).

Lung organoids

Lung derive from the ventral foregut endoderm progenitor population of cells named Nkx2-1^{+}. A first protocol to differentiate PSCs in primordial lung progenitors foresees the activin-induced definitive endoderm derivation followed by a first treatment with TGFb /BMP inhibitors and later by a BMP/FGF stimulation. Later on, Rossant and colleagues reported the generation of lung organoids from iPSCs involving an air-liquid interphase culture (*72*). A couple of years later, Snoeck and colleagues designed an improved four-stage, 50-day protocol in which activin treated PSCs were treated with BMP, TGF-b, and Wnt inhibitor, inducing anterior foregut endoderm. Then, these cells were ventralized using Wnt, BMP, FGF, and RA to obtain lung and airway progenitors. Finally, through the use of Wnt, FGF, c-AMP, and glucocorticoids they were able to obtain different epithelial cell types such as basal, goblet, Clara, ciliated, type I and type II alveolar cells (*73*).

Generation of lung organoids was further refined the following year by Spence and collaborators, following a slightly different protocol in terms of molecules used. They started again from activin induced PSCs, but they then combine the inhibition of TGFb and BMP with the activation of FGF4 and Wnt to obtain an anterior foregut fate, that was then venrally specified towards a lung fate by the activation of the hedgehog pathway. Then, upon embedding in Matrigel and prolonged exposure to Fgf10, they were able to obtain mature lung organoids, that could be propagated for several months and resembled proximal airways, containing basal cells, ciliated cells, and Clara cells, with alveolar cells

present in early culture but lost later on (*74*). However, a more refined generation of 3D lung organoids was achieved only recently in a follow-up study of Spence group where they showed the ability to differentiate foregut spheroids into two distinct types of organoids, human lung organoids and bud tip progenitor organoids. The first were obtained culturing foregut spheroids with high level of FGF10 and low concentration of FBS, the latter are cultured in a serum-free environment with FGF7, CHIR-99021, and all-trans retinoic acid (ATRA) (*75*).

Kidney organoids

With more than 20 specialized type of cells, from the architectural viewpoint the kidney is the most complex organ of the body. Conversely from tissues described until now, the adult (or metanephric) kidney derives from the mesoderm, precisely from the posterior end of the intermediate mesoderm, which gives rise to the two kidney progenitor populations, the ureteric epithelium and the metanephric mesenchyme, that in turn form the collecting ducts and nephrons. Despite the complex spatial and temporal regulation of kidney organogenesis, protocols for the derivation of mini-kidneys from PSCs were established relatively quickly (reviewed in *6*).

The first described kidney organoids were introduced only in 2015 by Little and colleagues. They showed that culturing PSCs in adherence conditions in the presence of Wnt for 4 days, followed by and exposure to Fgf9 for 3 days started the differentiation process. After this, cells were detached and cultured as 3D organoids for up to 3 weeks, with an increase in nephrons numbers upon a brief exposure (1hr) to a Wnt agonist in the early phase of organoid culture, leading to a complex multicellular kidney organoid containing fully segmented nephrons and surrounded by endothelia and renal interstitium. These kidney organoids may contain more than 500 nephrons with defined glomeruli that occasionally show evidence of endothelial invasion and comprise a Bowman's capsule with podocytes and connected to proximal tubules (*76*).

2.3.2 Adult Stem Cells (ASCs) organoids

Conversely from PSCs-derived organoids, that are established following developmental processes, organoids derived from ASCs follow a different path. Indeed, in order to commit ASCs towards the formation of an organoid, it is important to reproduce specifically the stem cell niche environment during tissue turnover or damage repairing.

An important factor shown to be relevant for all epithelial ASCs is the Wnt pathway, that seems to act as a major driver of the behavior of these cells (*77*). Moreover, it was found

that Lgr5, a receptor for R-spondins (a Wnt-amplifying secreted proteins family encoded by a Wnt target gene), marks active ASCs in many epithelia (*77*). On this basis it is clear that the Wnt pathway play a pivotal role in the generation of ASCs-derived organoids and Wnt activator molecules are key components of most ASCs culture protocols.

Interestingly, it is possible to start organoid cultures from small fragment of primary tissue, avoiding the need of purified ASCs. This is possibly due to the fact that culture conditions could mimic a damage situation, starting a response which in many tissues could lead to the re-acquirement of a stem cell fate to already committed cells (*78*).

Gastrointestinal tract derived organoids

As already stated previously, organoids of the gastrointestinal tract were the first to be generated, with the breakthrough work of the Clevers' lab in 2009 on small intestine. To achieve the result, Clevers and collaborators started from a deep understanding of the intestinal stem cell compartment. Beginning from the knowledge that small intestinal epithelium displays an extremely short turnover time of ~5 days, they identified actively proliferating Lgr5+ intestinal stem cells at the crypt base, with their proliferative TA daughter cells to occupy the remainder of the crypts structure and, upon differentiation, move onto the flanks of the villi to eventually die at the villus tips (*6*, *61*). Crypt stem cells are tightly regulated by the interconnection of four signaling pathways (reviewed in *79*):

i) ***Wnt*** constitutes the key pathway to maintain stem cell fate and drive proliferation of stem and TA cells.
ii) ***Notch*** helps to maintain the undifferentiated state of proliferative stem and TA cells. When this signaling is blocked, the cells differentiate into goblet cells.
iii) ***EGF*** fulfill a strong mitogenic effect on stem and TA cells.
iv) ***BMP*** signals are active in the villus compartment and their inhibition is crucial to create a crypt-permissive environment.

With this wealth of knowledge and encouraged by the observation that Lgr5 crypt stem cells can go through thousands of cell divisions *in vivo*, they established the first culture of 3D epithelial organoids from Lgr5 stem cells of mouse (*60*). These organoids recapitulate the *in vivo* counterpart and consist of a simple highly polarized epithelium, encasing a central lumen, with crypt-like structures projected outwards and the basal side of cells directed towards the surrounding extracellular artificial matrix. Moreover, enterocyte brush borders form the luminal surface and the secretion by Paneth and goblet cells occurs towards the lumen.

All these results were achieved resuspending in Matrigel whole crypts or single cells in Matrigel and adding a serum-free medium supplemented with R-Spondin1, EGF and Noggin. Further works refined the protocol and allowed to derive organoids also from other gastrointestinal tract tissues and, above all, from human tissues.

First of all, they observed that the addition of Wnt3A to the combination of growth factors allowed the growth of mouse colon organoids. The requirement for Wnt3a is probably due to the fact that the colon epithelium itself makes little, if any, Wnt (*80*). To obtain organoids from human tissues they needed to add other molecules to the cocktail of growth factor. The addition of nicotinamide together with molecules inhibiting the TGF-β receptor type I Alk and p38 were required for long-term culture of human small intestine and colon organoids, showing also that these organoids are stable, both from the genetic and phenotypic viewpoint (*80*).

The identification of rapidly proliferating Lgr5 stem cells at the base of pyloric glands of the adult mouse stomach has allowed, one year after the development of intestinal organoids, the generation of organoids also from the mouse stomach (*81*). The protocol was similar to the one previously discussed but showed a strictly requirement for a Wnt3a conditioned medium and the addition of FGF10. Several years later, the long-term culturing of organoids was achieved also for the human stomach, through the addition in the culture medium of gastrin, an hormone responsible for gastric acid secretion aiding also the gastric motility (*82*).

Pancreas organoids

The several cell types of adult pancreas present a slow turn-over rate. Moreover, in physiological condition the Wnt signaling is inactive and Lgr5 is not expressed, although this situation is reverted upon injury of the tissue. Despite of this, single isolated duct cells could be cultured long-term as pancreatic progenitor organoids when exposed to cell culture conditions similar to the one of mouse stomach organoids, with R-spo1, EGF, Noggin, FGF10 and Nicotinamide to be needful for the long-term propagation of pancreatic organoids (*83*). Similar results were achieved few years later by the same group also on human pancreatic tissues, through the use of a gastric organoids culture medium supplemented with an inhibitor of TGF-β receptors and the Prostaglandin E2 (PGE2) (*84*).

Liver Organoids

The progenitor liver cells are in a close kinship with those of pancreas. Indeed, like for the pancreas, the two cell types of the adult liver, hepatocytes and bile duct cells, turn over at a very slow rate and, again, Lgr5 is not expressed at appreciable levels in the healthy adult

mouse liver, but appear following toxic damage close to bile ducts, together with a strong Wnt pathway activation. It was shown that these damage-induced Lgr5+ cells generated hepatocytes and bile ducts in vivo and, when cultured in 3D conditions, could be clonally expanded as organoids mainly composed of progenitor cells expressing early bile duct and hepatocyte markers. However, the removal of mitotic stimuli simultaneously with the inhibition of Notch led to hepatocyte lineage differentiation and, moreover, when transplanted in mice into functional hepatocytes. For these kind of organoids, the starting media was the one of human gastric organoids but the key factors were the addition of the Hepatocyte Growth Factor (HGF) and the removal of Noggin and Wnt3a after 4 days of culture (*85*). A couple of years later, in a follow-up study of the same group the conditions for the growth of liver organoids derived also from human tissues were defined. In this case, the protocol was similar to the one of mouse liver organoids, but Noggin and Wnt3a conditioned medium were removed after 3 days and we find the addition of Forskolin, a cell-permeable activator of adenylyl cyclase, to the cocktail of molecules (*86*). Interestingly, the paper shows also that the majority of mature bile duct cells could initiate the growth of clonal liver organoid characterized by a high genomic stability at the structural level and ability to maturate in hepatocytes when transplanted in mice.

Esophagus organoids

Differently from other epithelial tissues, esophagus is characterized by a keratinizing stratified epithelium. In mouse, basal cells of esophagus epithelium represent a heterogeneous population of proliferative cells which, when grown in 3D conditions, are able to arise organoids that were morphologically similar to normal esophageal tissue, with small basal-like cells in contact with the extracellular matrix, large flat suprabasal-like cells in the interior, and hardened keratinized material in the center. This result was achieved by Lagasse and collaborator using again a medium based on the gastric organoids one, using gastrin, p38 MAPK and TGF-β inhibitors and replacing R-spo1 with the other member of the family, R-spo2 (*87*).

Lung Organoids

The development of organoids from primary lung tissues encountered several difficulties compared to the advancement achieved with PSCs derived lung organoids. To understand factors required for the growing of organoids, Tadakoro and colleagues, in 2014, taking advantage of a so called “tracheospheres assays”, developed years before by Hogan and Colleagues, identified Interleukin-6 (IL-6) as a key factor for the formation of multiciliated

cells at the expense of secretory and basal cells, the only two kind of cells that were differentiated till that moment (reviewed in *79*).

The development of distal airways (‘‘alveolospheres’’) organoids was achieved more recently, thanks to the identification of a rare self-renewing surfactant-secreting type II cell acts that act as stem cell to regenerate the alveolar epithelium, comprising also gas-exchanging type I cells. Despite of this, cells could be cultured only for a short-period and culture conditions are still not fully defined, requiring co-culture with non-epithelial cells (*88*, *89*).

Prostate Organoids

The prostate consists of a pseudostratified epithelium composed of basal and luminal cells. In 2014, two independent groups developed protocols to derive long-term propagable mouse and human prostate organoids, composed of fully differentiated basal and luminal cells. Clevers’ group based their work on previously developed organoids system, although they noticed that this time the stimulation with R-spondin/Wnt signal was not essential for continued growth of the organoids but it improved the induction towards luminal cells and the consequent prostate-like pseudostratified structure of the organoids. The key factor was the addition of dihydrotestosterone (DHT) both for murine and human tissues, despite the latter required more factors, including FGF10, FGF2, PGE2 and a p38 MAPK inhibitor. Moreover, they observed that both single human luminal and basal cells were able to give rise to organoids, though luminal-cell-derived organoids resemble in a closer way the prostate glands (*90*).

Conversely, Shen and colleagues based their culture on a Matrigel/EGF-based system, using an hepatocyte culture medium supplemented with the charcoal-stripped FBS and DHT (*91*).

Mammary gland organoids

The mammary gland consists of a bilayered pseudostratified epithelium composed of cells grouped in two categories, on the basis of their location: luminal and basal cells. Luminal cells are present on the inner surface of the epithelium and are responsible of the secretion of milk, while basal cells are on the contractile outer layer of myoepithelium and are in charge of ejecting milk.

The generation of long-term organoids was accomplished only last year (2020) by Brugge and collaborators, basing on the observation that a subset of cells expressing basal surface markers (CD49+EpCAM−) is able to generate both basal and luminal cells, displaying properties of tissue-specific adult progenitor cells, and taking advantage of a protocol

published by Clevers lab for breast cancer organoids. They reported the generation of organoid cultures of epithelial cells derived from histologically normal breast tissue, that are composed of three well-characterized human epithelial cell populations, specifically basal/stem cells, luminal progenitors, and mature luminal cells (*92*). The key factor for the development of these organoids was the human EGF receptor (HER) tyrosine kinases -3 and -4 named Neuregulin 1 (or Heregulin-β) (*93*).

Female reproductive tract organoids

Given their relevance for this thesis, organoids derived from fallopian tube, ovaries and uterus are treated as a separate paragraph *(Fig. 14)*.

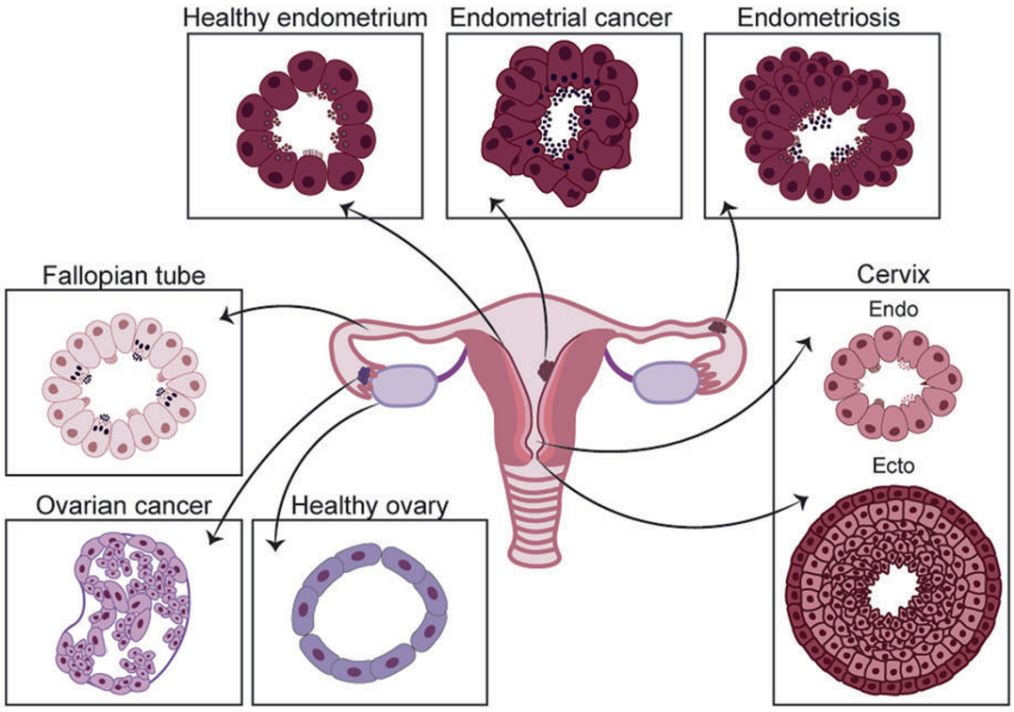

Figure 14. Representation of FRT tissues and organoids derived from them.
Adapted from Alzamil, Nikolakopoulou and Turco, 2020 (*94*).

2.4 Female reproductive tract organoids (FRT)

In amphigonic organisms, the female reproductive tract (FRT) is the whole set of organs and structures that allow reproduction and mating. It consists of the external vulva and internal vagina, uterus with its cervix, fallopian tube and ovaries, although only the last three will be treated here since are the most relevant for reproduction and their involvement in diseases.

FRT develops during fetal and early postnatal life and derive principally from the Müllerian ducts (or paramesonephric ducts) that in turn develop from the intermediate mesoderm of the urogenital ridge. Müllerian ducts are initially present in both sexes, but the secretion of anti-Müllerian hormone results in regression of the Müllerian ducts in males. Conversely, in females this structure differentiates into upper vagina, cervix, uterus and fallopian tube. The ovaries, instead, are derived from the genital ridge which forms on the medial side of the urogenital ridge.

Since the epithelium of these tissues are cyclically exposed to hormonal changes, the tissue turnover and self-renewal mechanisms are critical for their integrity and to guarantee the correct execution of tissues functions. This observation underscores the presence of stem cells in these tissues and, although the existence of stem cell pools has been described, their precise identity, biology and location is still unclear and under debate (reviewed in *3*).

2.4.1 Organoids of Ovarian Surface Epithelium

The two ovaries are main responsible for the cyclical maturation and release of oocytes into the fallopian tubes to allow fertilization. However, they also act as endocrine glands, secreting estrogen and progesterone hormones, that act together to coordinate the cyclical changes in the endometrium of the uterus and allow embryo implantation.

The adult mammalian ovary is composed of germ cells (oocytes or oogonia) and somatic cells such as granulosa, theca and OSE cells, supported by stroma.

Despite no proper stem cell activity has been detected and showed for germline, granulosa and theca cells, some studies support the possibility that some stem-like cells are present in these tissues, opening questions and interesting research areas (reviewed in *3*). The situation is quite different for the OSE, which should undergo monthly readjustment after the release of the follicle, a process that should be supported by stem cells.

The OSE is a single-layered epithelium in which cells transition between a squamous and a cuboidal shape, depending on positional and oestrus cues. Human OSE expresses several classical stem cell markers, including NANOG, CD44 and aldehyde dehydrogenase 1 family member A1 (ALDH1A). The stem activity is supported also by a study that demonstrate the presence of quiescent OSE cells retaining bromodeoxyuridine (BrdU) and showing enhanced *in vitro* colony formation, two important stem cells features, and other *in vivo* fate mapping studies that provide direct evidence for the existence and locations of self-renewing epithelial stem cells in the adult mouse ovary (reviewed in *3*). Moreover, both mouse and human ovaries present cells that express Lgr5 (reviewed in *3*).

Together, this evidence supports the idea that OSE cells could originate organoids when cultured in suitable conditions. However, no long-term cultures of the healthy ovarian epithelium were obtained in previous years, while being shown only recently by a huge work on OC organoids by Clevers and collaborators (*10*). In this work they obtained ovaries from women undergoing prophylactic bilateral salpingo-oophorectomy (pBSO) and after a mechanic treatment and an enzymatical digestion they resuspended cells in a Basement Membrane Extract (BME) similar to Matrigel, adding an appropriate serum-free medium conditioned with Wnt3a, R-Spo1 and Noggin media and with several supplements and growth factor like EGF, FGF, Neuregulin, Forskolin, Nicotinamide, an inhibitor of TGF-β receptor kinases, and the β-estradiol hormone. With this combination of factors they were able to generate OSE organoids with an organized epithelium in a cystic phenotype, with some epithelium folds and invaginations appearing upon organoid maturation (*10*). The epithelial composition of organoids was demonstrated by the presence of the epithelial marker cytokeratin 8 (KRT8). Despite these data, OSE organoids show a slow growth rate compared to other normal tissue organoids and, up to now, no other protocols or papers were published on OSE organoids.

2.4.2 Fallopian Tube Organoids

Fallopian tubes are bilateral ducts that connect the uterus to the ovaries and is possible to identify four segments: the fimbriated ends bordering the ovaries (infundibulum), the ampulla, the ampulla–isthmus junction, and the isthmus. The single layer simple columnar epithelium of the FT is composed mainly of secretory cells that produce tubular fluid that enhance the zygote/oocyte motility and ciliated cells that capture the oocyte when it is released at ovulation and guide it down into the ampullary–isthmus junction for fertilization. The highest number of ciliated cells is located in the fimbriae (up to 80%) and decrease towards the isthmus (~30%). Moreover, basal cells intercalated among ciliated and secretory ones were identified and, likely ciliated ones, are mainly based at the distal end of the FT, the fimbria (*95*).

The continuous exposition to ovarian follicular fluid able to damage the fimbrial epithelium should provide an evidence for the presence of stem cells in this tissue. Despite this, fate-mapping studies that formally document the presence of stem cells in the adult fimbria are currently lacking. However, several studies have described stem-like epithelial cells concentrated at the fimbriated end of the fallopian tube (or oviduct) in humans and mice (reviewed in *3*). Interestingly, LGR5 is not expressed in mouse fimbriae but it is in

the human one. Moreover, cells lacking markers for ciliated (β-tubulin +, TUBB4^{+}) or secretory (paired box 8 +, PAX8^{+}) cells were founded in humans and identified as fimbrial stem-like cells. These basally located cells express the CD44 marker (CD44^{+}) and were capable of generating *in vitro* spheres that contained differentiated ciliated, secretory and basal cells (*95*).

Albeit the lack of information on the stem cell compartment, the first FRT organoids were derived from the fallopian tube, in a 2015 paper published by Meyer and colleagues (*96*). In this breakthrough work for the field, epithelial cells isolated from the FT by an enzymatic treatment followed by a scalpel scraping were firstly grown as monolayers, probably to improve the isolation of epithelial cells, and then embedded into Matrigel and exposed to a cocktail of factors very similar in composition to the one of mini gut organoids. The serum free culture media was conditioned with Wnt3a and R-spondin1 media and completed by the presence of EGF, Noggin, FGF10, Nicotinamide and an inhibitor of TGF-β receptor kinases. With this protocol they were able to generate cystic organoids resembling an epithelium surrounding a cavity (recapitulating the native tissue architecture) and showing a robust growth and long-term maintenance in culture (*96*). Organoids were characterized by the presence of both ciliated and secretory cells and, moreover, they recapitulate also the *in vivo* phenotype functionally, as demonstrated by their ability to respond to female hormones, i.e. estrogen and progesterone (*96*). This work indirectly demonstrates also the existence of ASCs in the human FT epithelium, that are regulated by the Wnt and Notch signalling.

More recently, Clevers and collaborators, in the same paper where was demonstrated the generation of OSE organoids, show the derivation of organoids also from the fallopian tube, with a slightly different protocol that avoid the 2D culture of cells (*10*). The organoids they obtained were really similar to the ones generated by Kessler, both in term of recapitulating the *in vivo* tissue and propagability. Moreover, they showed also the possibility to genetically modify these organoids through the use of CRISPR/Cas9 and lentivirus technology in order to induce a tumor phenotype and observe the early stage of development of OC (*10*).

2.4.3 Endometrial organoids

The endometrium, with its mucous membrane, is the inner epithelial layer of the uterus and is essential for the mammalian reproduction. It consists of a single columnar epithelium and in human is organized into a functional layer and the underlying basal layer of support.

The functional layer is composed by a luminal epithelium that eventually invaginates into the stroma, reaching as far as the basal layer, in order to give rise to the glandular epithelium. Whilst the luminal epithelium provides the site of implantation for the embryo, the glandular secretions support the development of the conceptus during the early weeks of pregnancy (*94*).

Given the involvement of endometrium during menstruation, where ovarian hormones control and drive the shedding of the functional layer and its regeneration and differentiation, the presence of stem cells that allow constant regeneration cycles is clearly supported and so also the possibility to generate organoids from this tissue.

Although initial approaches to generate endometrium 3D models failed, in the last years long-term culture of mouse and human endometrial organoids were established (*97*, *98*). Following the mini-gut culture system, these organoids were obtained through an enzymatic digestion of the tissue, that allow the release of glandular fragments, followed by the embedding in Matrigel and culturing with a cocktail medium rich of Wnt pathway activators such as RSPO1, WNT3A, CHIR99021 (an extremely potent inhibitor of glycogen synthase kinase 3, GSK3) and growth factors as EGF, HGF, and FGF10 to promote proliferation, inhibitors of TGF-β and BMP (Noggin), to prevent differentiation and nicotinamide to allow long-term culture. Generated organoids show a spheroid epithelial morphology with a central lumen surrounded by a single epithelial layer and recapitulate also in vivo functions, by responding to estrogen and progesterone. Indeed, treatment with estrogen increases the number of $Ki67^+$ proliferative cells and stimulates the generation of ciliated cells (*99*). Moreover, the clonogenic ability of endometrial organoids allows the exploration of putative markers of human endometrial stem cells and lead to the identification of candidate $CDH2^+$ cells characterized by higher clonogenic and proliferative capacities (reviewed in *94*).

3. ORGANOIDS FOR DISEASE MODELING

Nowadays, organoids culture system has been developed for a number of different tissues and given its incredible features and ability in recapitulate primary tissues and their development and maintenance, this technology has the potential to revolutionize the biomedical research. Indeed, organoids, as well as being a tool for studying development and homeostasis of tissues, when derived from patients with specific disorders, represent a precious instrument to investigate the related underlying mechanisms, holding great promise for translational research *(Fig. 14)*.

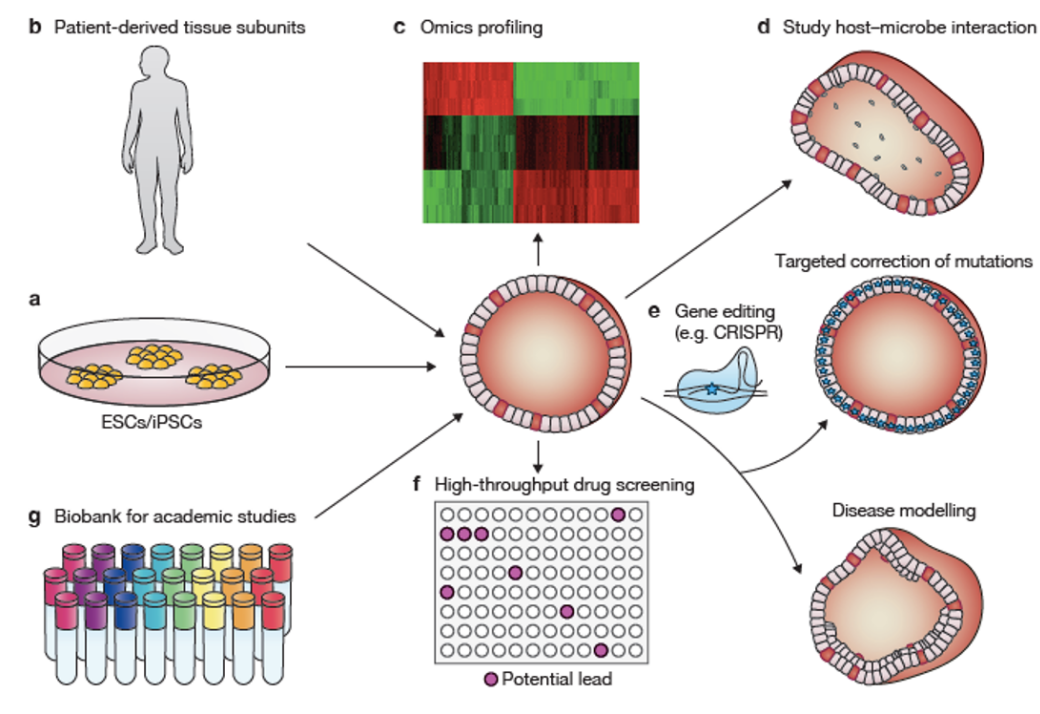

Figure 14. Applications of organoid technology for studying development, homeostasis and diseases.

Organoids derived from (a) pluripotent stem cells or (b) ASCs from tissues could contribute to the study of development and homeostasis. Moreover, the (c) high-throughput multi-layered profiling of organoids could enable the delineation of the contribution of various signalling pathways in development and their dysregulation in disease. Organoids allow also to study (d) the host-microbe interaction and can be used to (e) model genetic disorder using patient derived tissues or through the targeted introduction of mutations. In the meantime, the correction of targeted mutations could be used for personalized medicine approaches. Finally, (f) organoids represent a physiological model that can be used in high-throughput drug screens and (g) could be collected as living biobank.

From Fatehullah, Tan and Barker, 2016 (*64*).

The more relevant usage of the organoid culture system to study and model diseases regards *infectious disease*, *genetic and hereditary disorders* and *cancer*.

Infectious disease

Conversely from animal models, human-derived organoids are not hampered by interspecies differences when used for disease modelling. Moreover, being composed of multiple different cell types present in the tissue of origin and given the possibility to modulate the media composition in order to skew the differentiation towards specific cell lineages, organoids represent a more complete system to study infectious diseases and ***host–pathogen interaction***. Probably the best example is represented by studies on the ZIKA virus (ZIKV). The ZIKV act through a strong teratogenic effect, with infection of pregnant women being associated with microcephaly in newborns (*100*). In 2016 the WHO declared the ZIKV outbreak in Central and South America as a public health emergency of international concern. However, to study ZIKV infection and pathogenesis was required a valid model system, that was identified in brain organoids. Indeed, PSCs derived brain organoids recapitulate many features of cortical development, including the formation of a distinct human-specific outer radial glia cell layer. Several groups independently decided to infect brain organoids with ZIKV and the obtained results show the preferential infection of neural progenitors, resulting in cell death, decreased proliferation, and a reduced neuronal cell-layer volume, providing a good model for ZIKV-associated microcephaly (*101*, *102*). Moreover, other works have also exploited brain organoids in drug development to prevent or treat ZIKV infection (*103*, *104*).

Another important organoid system used to study pathogen-host interaction was intestinal organoids, which have found various applications. Indeed, these organoids were used to model human enteric virus infection, such as ones of *Rotavirus* and *Norovirus*, common causes of diarrhea and acute gastroenteritis respectively (reviewed in *105*). Moreover, intestinal organoids were also used to study bacterial pathogens like *Clostridium difficile*, *Shigella flexneri*, and *Salmonella enterica* (reviewed in *105*) responsible of acute gastrointestinal diseases and diarrhea, but also chronic infection that can cause gastric ulcer and cancer. This is the case of the *Helicobacter Pylori*, that was injected directly into the lumen of gastric organoids in order to model the natural pathogen-host interaction that happens at the apical side of the stomach epithelium. The experimental model showed that the primary response was the induction of NF-kB target gene and that the gastric gland lineage shows the highest inflammatory response to the infection, representing, at least in this model, a mechanistic link to gastric cancer (*82*).

Taken together, these discoveries underline the usefulness of organoid models to mimic the interaction of pathogens as well as commensal microbiota (reviewed in *105*) with human tissues and paved the way for further studies aimed at understanding additional pathogen infection mechanisms.

Genetic and Hereditary disorders

In addition to providing a natural environment to promote and study microorganism infection, the use of organoids to model human genetic diseases is increasing constantly. Generally, it is possible to recognize two different kind of approaches at the problem (*65*):

i. organoids derived from patient biopsies
ii. wild-type organoids engineered with specific genetic mutations

The possibility to explore genetic disease was initially exploited with PSCs derived organoids, in particular brain organoids. The 2013 work of Lancaster and Knoblich (*63*) laid the foundations for such approaches, showing the possibility to reproduce the phenotype of microcephaly *in vitro*. Further work showed the possibility to study other neurological disorder like autism (*106*), and the possibility to generate iPSCs from patient with variegate genetic disorders and the possibility to differentiate iPSCs in specific cell lineages expanded consistently the use of patient iPSCs derived organoids.

The potential of organoids derived from patient primary tissues was demonstrated, for example, by the establishment of ductal cell-liver organoids derived from patient with Alagille syndrome and Alpha 1-Antitrypsin (A1AT) deficiency, which reproduced the defects observed *in vivo* (*86*), but also from the use of intestinal organoids derived from patient carrying variegated genetic diseases (reviewed in *65*). Among them we could find also the probably best example of organoids model derived from patient biopsies, i.e. cystic fibrosis (CF) case.

CF is caused by a spectrum of mutations in the cystic fibrosis transmembrane conductance regulator (CFTR) gene, which encodes a chloride channel normally expressed in epithelial cells of many organs. To investigate the effect of such mutations, human intestinal organoids were derived from CF patients carrying the common *CFTR ΔF508* mutation and the CTFR functionality was assessed comparing the wild-type and CF derived organoids response to Forskolin (*107*), which normally induce the activation of the channel. They observe that while healthy organoids responded to the treatment, CF patients derived organoids do not. Moreover, they tested the response to different drugs (CFTR correctors or potentiator) of CF organoids isolated from patients harboring different mutations, including rare variants, and noticed that the response to forskolin was restored by each

drug but was largely variable between individual organoids of different donors (*107*). This observation paved the way to the development of living biobank of CF organoids harboring specific mutations, that allow high-throughput studies to identify specific drugs for each specific mutation, highlighting the utility of organoids for personalized medicine.

The potential of patient derived organoids in personalized and regenerative medicine is underlined from their possible combination with genome-editing technologies. The advent of clustered regularly interspaced short palindromic repeats (CRISPR)/CRISPR associated protein 9 (Cas9) technology incredibly facilitated the targeting of any genomic locus that can be recognized by a specific RNA guide (reviewed in *108*). The combination of organoids and CRISPR technologies (*109*), together with its utility in personalized medicine represents a convenient approach to study the effect of specific mutations in a wild type tissue, allowing also to study those specific mutations that are lethal during development or in early life and for which obtaining patient-derived biopsies is essentially impossible.

Several studies have introduced genetic mutations in PSCs derived organoids, recapitulating features of diseases in different tissues. For example, the CRISPR driven loss-of-function mutations in PODXL (*110*) and PKD (*111*) genes in iPSCs-derived kidney organoids induced defects that mimic respectively the nephrotic syndrome and polycystic kidney disease, helping in understanding the pathogenesis context. Similarly, engineered iPSCs-derived liver organoids elucidated the effect of different mutations in the JAG1 gene on the bile ducts formation and development of Alagille syndrome (*112*). Again, engineering brain organoids with specific mutations in the TREX-1 gene, Muotri and collaborators showed that deficiency in this gene increases neural death and results in reduced organoid size, reproducing the Aicardi Goutiere`s syndrome, an autoimmune disease associated with, among others, intellectual problems (*113*).

Despite its utility in reproducing genetic disorders, the combination CRISPR and organoid technology found its maximum expression in the possibility to correct specific genetic lesions in patient-derived organoids. Again, the proof-of-concept study was performed on CF organoids, where a *ΔF508* mutation was corrected by homologous recombination using the CRISPR/Cas9 system (*62*). The corrected organoids showed restoration of CFTR function and, more importantly, this approach could be clinically relevant when combined with organoid engraftment in the appropriate site.

Cancer organoids

Given the relevance of the topic for this thesis, it will be treated as a separate subchapter.

3.1 Cancer organoids

Over the past decades, our knowledge on cancer has increased immensely and substantial progresses in the treatment of certain types of tumors were achieved. Despite this, cancer remains a major worldwide health problem. One of the major hurdles for the development of novel therapeutic strategies dwell in the translation of scientific knowledge to the clinic, which is mainly due to the poor capability of many cancer models to recapitulate patient's tumors complexity and, as a consequence, the failing in clinical trial of many drugs that, instead, perform well in cancer models (*5*). Since their development, the possibility to use organoids to study cancer was really tempting. Indeed, the features of the technology and the possibility to derive organoids from each specific patient allow to study in depth individual tumors and explore inter- and intra-patient heterogeneity. Moreover, it is possible to derive healthy organoids from the same patient to be used as control, both for molecular analyses and drug screening *(Fig. 15)*.

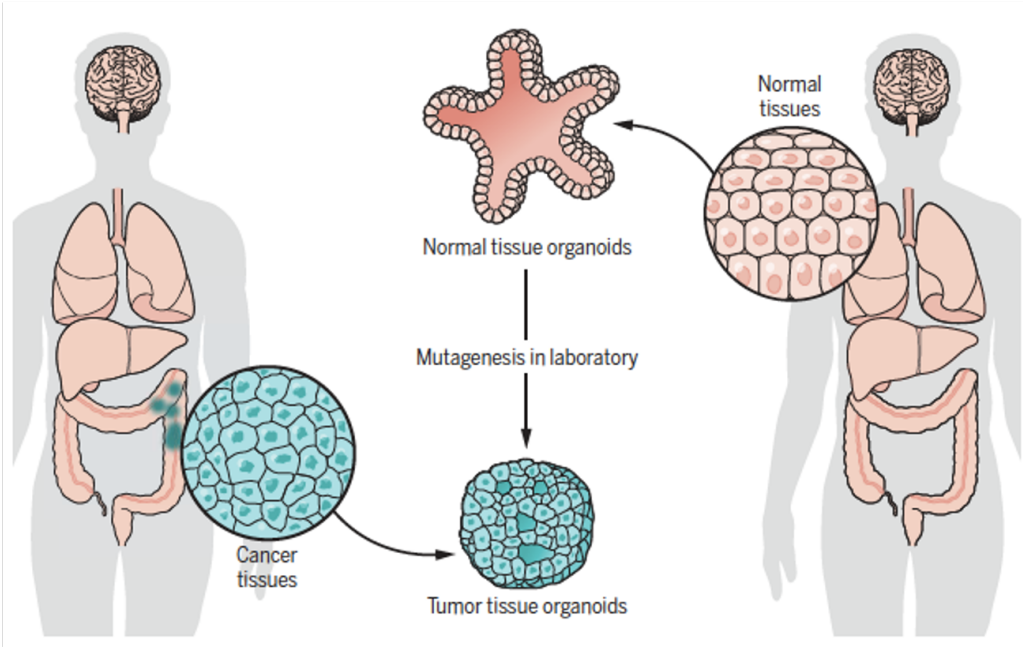

Figure 15. Generation of human cancer organoids.

Human cancer organoids can be generated directly from neoplastic tissues (left) or by genetic modification of organoids developed from normal tissues (right).

Picture from Tuveson and Clevers, 2019 (*114*).

Until organoids development, cancer cell lines (CCLs) and PDTXs were commonly used models to study cancer. Despite their contribution to the understanding of dynamics underlying the pathology, these models present several drawbacks (reviewed in *5*).

For CCLs these limitations are:

- the development from primary patient material is very inefficient and involves extensive adaptation and selection to *in vitro* 2D culture conditions
- as only few clones are able to be expanded and maintained over many passages, the derived CCLs may have undergone substantial genetic changes and no longer recapitulate the genetic heterogeneity of the original tumors
- absence of normal tissue derived control cell lines.

PDTXs have the advantage of mimicking the biological features of the human tumor much better than *in vitro* culture models but have limitations like:

- the use of animals
- limited engraftment efficiencies for subsets of patient tumors
- the approach is expensive and time and resource consuming
- may undergo mouse- specific tumor evolution

Patient-derived 3D cultures of cells isolated from tumor biopsies were named ***tumoroids*** and could represent a bridge between CCLs and animal models.

On the basis of mini gut system, R-spondin-based culture conditions to propagate several human carcinomas has been established and, nowadays, cancer organoids are available for colorectal (*80*, *115*), pancreatic (*84*), prostate (*116*), liver (both hepatocellular carcinoma and cholangiocarcinoma) (*117*), gastric (*118*, *119*), breast (*93*), bladder (*120*), kidney (*121*), esophagus (*122*), lung (*123*), and ovarian cancers (*9*, *10*), often from both primary tumors and metastasis.

Albeit it is counterintuitive, tumor organoids do not grow faster per se than their matching normal organoid counterparts and, in many cases, they even grow at slower rates, possibly due to higher rates of mitotic failures and subsequent cell death (*5*). However, the possibility to both indefinitely propagate *in vitro* tumoroids and cryopreserve them has prompted the establishment of "***living biobank"***, large collection of a series of tumoroid lines (and matching healthy organoids when possible) that represent the full histopathological diversity of the disease and that can be expanded over time. These living biobanks represent a precious resource available for the community, that can be shared and used to study specific tumors (or subtypes of that tumor) and tested to determine whether organoids have predictive value for drug responses for individual patients. A lot of effort was put on generating large collection of tumoroids of different cancers and nowadays

there were several biobanks available (reviewed in *5*) and currently, a combined effort of several institutes which is known as the Human Cancer Models Initiative (HCMI) is ongoing to generate a large, globally accessible bank of new cancer cell culture models, especially organoids, available for the research community.

Biobanks allowed to show that tumor-derived organoids preserve the histopathological and genetic features of the tumor they were derived from and remain genetically and phenotypically stable also after prolonged culture. Indeed, genomic analyses comparing tumoroid lines and the matching tumors, both at early and late passages, have consistently revealed a well-maintained mutational profile. This highly conserved genomic landscape is particularly crucial, as it makes tumoroids a trustworthy and expandable source of material recapitulating the features of the parental tumor to perform genotype–phenotype correlation analysis, functional tests and assess drug response (*65*). The maintenance of tumor heterogeneity in culture is a factor that is often underestimated in genotype-phenotype relationships and a really strong point of tumoroids compared to other cancer models (reviewed in *124*).

Although the inter-tumor heterogeneity is well retained in organoid culture, it is less clear if it is true also for the intra-tumor heterogeneity. Indeed, cancer is caused by the gradual accumulation of mutations in "driving" genes, and, therefore, individual tumor cells within the same tumor contain different sets of genetic alterations. Despite the relevant role believed to be played by this intra-tumor heterogeneity in cancer progression and therapy resistance, knowledge of how it arises and contributes to disease progression is still limited. A very interesting study published by Roerink and colleagues exploited organoid technology to study intra-tumor heterogeneity of colorectal cancers (CRCs) in great detail, allowing molecular and functional analyses at the single-cell level previously not possible (*125*). Using tumoroids generated from single cells, they perform an in-depth analysis of the genetic, epigenetic and transcriptomic profiles of different regions of the same tumor, revealing that CRCs cells exhibit extensive mutational diversification, with a striking increase in the mutation rate derived mainly from *de novo* mutational processes (*125*). Moreover, they observe that anticancer drug responses are noticeably different between even closely related cells of the same tumor, suggesting that pharmacological heterogeneity likely reflects epigenetic changes that alter gene expression among single cells in a tumor, showing a different drug sensitivity of different tumor subclones (*125*).

This work was a first proof of the ability of tumoroids to capture intra-tumor as well as inter-tumor heterogeneity, and that both should be considered when performing drug

screenings. On this aspect, the poor recapitulation of native tumors by CCLs may have contributed to the high failure rate of newly discovered drugs in clinical trials, mainly performed on that cancer model. For this reason, patient- derived tumor organoids, better recapitulating primary tumors features, should represent improved models for the identification and testing of new anticancer drugs.

Currently, the development of high-throughput screening on tumoroids is ongoing, but drug screenings of medium scale have been reported in most of the recent generated biobank, yielding promising results (reviewed in *5*) and underscoring the potential of tumoroids as a preclinical model and predictive tool for treatment efficacy. These studies showed that the sensitivity to treatment could be correlated with a defined mutational profile and, importantly, that drug resistance *in vitro* mirrors the patient treatment response. Moreover, another important advantage of using organoids for drug development and testing is the availability of both healthy and tumor tissues derived organoids, which allow to compare the response between the two and selecting drugs that target specifically tumoroids, resulting in a reduced toxicity on patients. And even more, the possibility to establish hepatic organoid cultures could provide a relevant model for preclinical testing of the hepatotoxicity of experimental compounds, avoiding the drug- induced liver failure, that caused several clinical trials to fail.

Another important advantage of the use of organoids is the possibility to study cancer initiation and progression in normal healthy organoids, going to induce the carcinogenesis in a controlled way.

An example of this powerful tool could be the use of organoids to explore the link between infectious agents and cancer development, as shown by the gastric cancer induction by the *H. pilori* already discussed above (*82*). It is estimated that at least one on five cancer are linked to infectious agent, although in many cases it is not known how a particular pathogen contributes to malignant transformation. For this reason, co-culture systems of organoids with different types of pathogens or the voluntary infection of organoids with specific infectious agents could potentially be used to study these processes.

Furthermore, the recent advent of the CRISPR/Cas9 genome editing technology allowed to introduce combinations of common driver mutations to generate cancer progression models (*126*, *127*). Using these models, it was shown that the introduction of driver mutations could lead to the onset of the tumoral phenotype in the normal context and, in some tissues, that the growth become independent of culture media factors such as EGF,

WNT, R-spondin 1 and Noggin. Moreover, it was shown that the loss of specific genes could drive the chromosome instability and aneuploidy (*114*, reviewed in *124*).

Despite their powerful applications, also organoids as model show some limitations. Among them, one of the intrinsic limitations of organoid culture is the lack of stroma, blood vessels and immune cells, that hamper the dissection of the interaction of tumor cells with the environment. This limitation could be addressed by the developing of co-culture with additional cellular (and microbial) elements. Another limit is the requirement for mouse-derived extracellular matrix (ECM) substitutes, like Matrigel, and, in some organoid cultures, for fetal calf serum (FCS), required, as example, for the production of the WNT-conditioned medium used in growth media, that lead to the incorporation of undefined extrinsic factors that may influence the outcome of experiments. Recently synthetic artificial matrices that support the growth of mouse and human intestinal organoids were developed and could possibly replace mouse-derived ECM substitutes. However, these matrices still need further steps of optimization in order to increase the efficiency and to sustain the growth of organoids derived from other organs as well (*128*).

Another possible limitation could derive from the higher growth rate of organoids raised from normal epithelia compared to the one of organoids derived from advanced cancer. This could possibly result in an overgrowth of normal organoid-derived cells contaminating the tumoroid culture.

Finally, up to now tumoroids were grown only from carcinomas, namely tumors of epithelial origin and it is currently unclear whether the organoid approach can be adapted for organoid culture systems from nonepithelial tumors. However, the recent advances in growing organoids from primary glioblastoma tissues may set the stage for growing non-epithelial tumors (*129*).

Despite these limitations, organoids have powerfully emerged as a physiologically relevant *in vitro* model to study cancer, bridging the gap between current cancer models and paving the way to new interesting and useful applications, providing plausible positive impact for basic cancer research and personalized medicine.

3.1.1 Organoid models of Ovarian Cancer

Over the past decades, it has become increasingly clear that OC is a heterogeneous disease consisting of a wide spectrum of distinct molecular and clinical entities, pointing to the need to develop novel models that recapitulate the features of the tumors to a better extent than CCLs and PDTXs. In the last couple of years, organoid culture of EOC have been established to study and address clinical challenges still affecting this pathology.

The starting point was the development of a protocol for the generation of FT organoids (*96*), which was then adapted and optimized to derive also organoids from cancerous tissues.

The potential of an organoid platform for studying OC was firstly illustrated by D'Andrea and collaborators in a work showing short-term cultured HGSOC organoids (7-10 d) characterized at the genomic level and then used in various assays to study DNA repair inhibitor response (*9*). The authors demonstrate that organoids match the tumors from which they are derived, both genetically and functionally, and detected multiple examples of tumor heterogeneity in the same patient and, moreover, showed that organoids could be used to accurately test predict clinical response of HGSOC patients to DNA repair inhibitors. Taken together, results achieved from D'Andrea and colleagues provide promising expectation on the organoid system to study OC.

The efficient derivation and long-term expansion of OC organoids to exploit the full potential of organoids to study OC was achieved by Clevers' lab in 2019 (*10*). To improve organoid derivation rate, Kopper and colleagues decided to start testing the addition of specific compounds to the growth medium. They followed two main guiding criteria:

i) compounds previously reported to be highly expressed in ovarian tumors and therefore hypothesized to support OC growth
ii) factors used to support OC cell growth and other types of tumor organoids.

They noticed that the addition of hydrocortisone, forskolin and heregulin-β to the medium elaborated by Kessler for FT organoids improved the efficiency of OC organoid derivation. Moreover, they discovered that Wnt-conditioned medium, an essential component of the FT medium, was not essential for all tumor organoid lines and conversely it had a negative effect on some of the lines, presumably due to the presence of serum in the conditioned medium and not to Wnt itself. With these modifications they were able to generate organoids from non-malignant BTs, as well as MOC, CCOC, ENOC, LGS and HGS carcinomas, showing the possibility to propagate organoids for long-term (>30 passages) as well as to cryopreserve and recover them with a high efficiency (~85%). They then

showed that organoids recapitulate primary tumors at the histopathological level maintaining also the correspondent genomic landscape. Moreover, through the use of a novel single-cell DNA sequencing analysis they confirmed that organoids reliably capture the tumor heterogeneity in culture, even after prolonged passaging. In the same work, they derived also normal healthy FT and OSE organoids and show that FT organoids could be genetically modified by introducing knockouts of TP53 and RB1 genes, providing a model to study tumorigenesis *in vitro*. Finally, they also performed drug screening assays, comparing organoid lines derived from primary chemosensitive and recurrent chemoresistant tumors of a single patient, confirming that the organoid line derived from the recurrent tumor shows an increased resistance to platinum-based therapy. Finally, to validate whether *in vitro* drug sensitivity is recapitulated *in vivo* they also tried to orthotopically or subcutaneously transplant OC organoid into immunodeficient mice, endorsing the findings by testing the same drugs *in vivo* and achieving the same result.

The publication by Kopper and colleagues, together with the living OC organoid biobank generated, paved the way to several other studies that exploit the potential of organoids to study OC (*130–133*). All those papers corroborate the ability of organoids to recapitulate histo-pathologically and genetically the corresponding primary tumors and confirm the drug sensitivity of the system, validating the inter- and intra- patient sensitivity (*132*). The retention of tumor heterogeneity in culture was also supported by a promising preprinted paper by our lab, in which we show the development of a single-cell monoclonal organoid platform that was analyzed through the use of the recently developed single-cell sequencing technology (*134*).

An interesting work by Kessler and colleagues show the generation of HGSOC organoids applying a different protocol from the one provided by Clevers' lab, delivering interesting insights (*11*). They observe that Wnt pathway activation impair the growth of cancer organoids, which, instead, require active BMP signaling to be generated. Conversely, healthy FT organoids depend on BMP suppression by Noggin. This was also confirmed when they performed a triple stable shRNA knockdown of p53, Pten and retinoblastoma protein (RB) in FT organoids, inducing a tumoral phenotype. Indeed, when tumorigenic organoids were cultivated in the normal fallopian tube organoid medium, a growth arrest was triggered and a low Wnt environment was required for ensure a long-term growth. Transcriptomic analyses of normal vs. tumorigenic induced organoids confirmed that the depletion of tumor suppressors triggers changes in the regulation of stemness and differentiation but are likely not sufficient to drive transformation of healthy epithelium

until the presence of a Wnt signal, whose lack of activation is indeed a requirement for maintaining stemness and preventing differentiation in HGSOC.

Overall, these studies provide important insight into fundamental biological processes of HGSOC development, and the achieved results highlight the potential of OC organoids to guide precision medicine, particularly in predicting patient-specific responses in preclinical drug screening.

MATERIALS AND METHODS

MATERIALS AND METHODS

1. Primary samples processing

Both normal and tumor primary samples used in the project were provided by the European Institute of Oncology (IEO) biobank. Non-tumor fallopian tubes or ovaries from biopsies of patients that underwent preventive hystero-salpingo-oophorectomy for non-ovarian gynecological pathologies are respectively sources of FI ad OSE. Tumor samples, instead, comprise both primary solid HGSOC and metastasis in the form of the ascitic fluid (AS). The diagnosis of HGSOC was confirmed by the IEO pathology unit, according to the 2014 World Health Organization (WHO) standard classification (*16*). Tumor and normal samples are processed with different procedures.

Upon arrival, ***solid tumors*** were cut into small pieces using a scalpel and then minced with scissors. The subsequent enzymatic digestion was performed with two different protocol for the 2D and 3D cultures. For adherent culture, samples were digested for 1 to 4hr with an Epithelia Digestion Medium (EDM) composed of Ham's F12 (Gibco, #31765035) and DMEM (Sigma, #D6429) 1:1, supplemented with 1% penicillin/streptomycin (Gibco, #15070063), 1 µg/ml insulin (Sigma, #I0516), 0.2 µg/ml hydrocortisone (Sigma, #H0888), 10 ng/ml EGF (Peprotech, #100-15), 200 U/ml collagenase (Sigma, #C2674), and 100 U/ml hyaluronydase (Sigma, #H3884). During the digestion, the tissue suspension was pipetted each 30 minutes, with pipette of different size, till it passes through a P1000 tip. Then, the digested tissue suspensions were passed through a 40-µm cell strainer and centrifuged at 500g for 3 min. Given the nature of the samples, the presence of red blood cells is expected, and, in case the cell pellet was visibly red, it was resuspended in an erythrocyte lysis buffer (ACK buffer, Gibco, #A1049201) and leaved at room temperature for 3 min, after which it was centrifuged at 500g for 3 min. Up to 3 (and maximum 3) steps of ACK buffer could be required to totally remove red blood cells. Then, cells were washed in PBS and centrifuged at 500g for 3 min and plated on Collagen I-coated flasks or plate (BD Biosciences). The processing of primary tumors for 3D culture was initially performed using the same protocol described above. However, once available, it was substituted with the protocol showed by Kopper and colleague for the generation of OC organoids (*10*). More in detail, after tumor tissues were minced, they were washed with 10ml of Advanced DMEM/F12 (ThermoFisher, #12634010) containing 1x Glutamax (Gibco, #35050061), 10 mM HEPES (Gibco, #15630080) and 1% penicillin/streptomycin,

henceforth named AdDF+++, and big tissue pieces were dropped to the tube bottom by gravity (for 2-5 min). Then, the supernatant was collected and centrifuged at 1,000 r.p.m. for 5 min. Remaining big tissue pieces were digested in 5–10 ml AdDF+++ supplemented with 5 µM RHO/ROCK pathway inhibitor (Clinisciences, A3008-10MG) containing 0.5-1.0 mg/ml collagenase (Sigma, C9407) on an orbital shaker at 37 °C for 0.5-1.0 hr. The digested tissue suspension was then sheared using 5 ml plastic pipettes and strained over a 100µm filter. Eventually, still present large tissue pieces entered a subsequent digestion and shearing step. The suspensions from various steps were them merged and the final suspension was centrifuged at 1,000 r.p.m. and the pellet was resuspended in 10 ml AdDF+++ and centrifuged again at 1,000 r.p.m. Again, in case of a visible red pellet, erythrocytes were lysed with ACK buffer for 5 min at room temperature, followed by an additional wash with 10 ml AdDF+++ and a final centrifugation at 1,000 r.p.m.

Conversely, ascitic fluid were directly centrifuged for at 500g for 5 minutes and the cell pellet was resuspended in ACK buffer as described before. Following erythrocytes lysis, the cell pellet was washed with 10 ml of an epithelial-specific culture medium, for adherent culture, or AdDF+++, for 3D culture, and centrifuged at 500g for 5 minutes. Finally, as for solid tumors, cells were resuspended in an appropriate culture media for 2D culture or in Matrigel for organoids generation.

On the other hand, normal primary samples were both treated in the same way. Biopsies of fimbriae and ovaries were washed in PBS and treated with Dispase 1 mg/mL for 30 min at 37°C. Then, epithelial cells from the distal portion of the fimbria and the surface of the ovary were scraped with a scalpel and pelleted at 500g for 3 minutes. Eventually present red blood cells were lysed by ACK solution as described above and isolated epithelial cells were cultured in 2D or 3D with different protocols.

1.1 Primary cells culture

For adherent culture, cells derived from all tissues were plated in collagenated flasks or plates and maintained with the same epithelial-specific culture medium that we named Epi-medium. This basal medium is composed of a 1:1 mixture of DMEM/F12 supplemented with 1% FBS NA (ThermoFisher, #26140), 1% Pen-Strep, 0.2% respectively of gentamycin (Lonza, #17-519L) and amphotericin (Roche, #15290026), 10mM HEPES, 10 µg/ml human transferrin (Sigma, #T8158), 1 µg/ml insulin, 1 µg/ml hydrocortisone, 50 µM L-ascorbic acid (Sigma, #A4544), 15 nM sodium selenite (Sigma, #S5261), 0.1mM ethanolamine (Sigma, #E9508) and 50 ng/ml cholera toxin (Sigma, # C8052). When used,

the basal medium was completed with 10 ng/ml EGF, 35 µg/ml BPE (Gibco, 13028014), 10 nM T3 (Sigma, #T5516), and 10 nM β-estradiol (Sigma, #E2758), and stored for 2 days maximum.

Compounds	***Producer***
R-spondin1	Peprotech #120-38
Wnt3a	Peprotech #315-20
Noggin	Peprotech #120-10C
FGF10	Peprotech #100-26
EGF	Peprotech #AF-100-15
Heregulin-β	Peprotech #100-03
B27	Gibco #17504001
N2	Gibco #17502048
Primocin	Aurogene SRL #ant-pm-1
PGE2	Bio-Techne SRL #2296/10
A83-01 (TGF-β R Kinase Inhibitor IV)	MedChem Express #HY-10432
SB202190 (p38 MAP kinase inhibitor)	MedChem Express #HY-10295
ROCK inhibitor (Y-27632)	Cliniscience #A3008
Forskolin (10mM)	Sigma #F3917
Nicotinamide	Sigma #N0636
N-Acetylcysteine	Sigma #A9165
Hydrocortisone	Sigma #H0888
Cholera Toxin	Sigma #C8052
BPE	Sigma #P-1476
B-Estradiol	Sigma #E2758
T3	Sigma #T6397
Progesterone	Sigma #P8783

Table 1. List of compounds tested for organoids culture.

1.2 Organoids culture

To generate organoids, cell pellets from the four different sources were resuspended in cold growth factor reduced Matrigel (Corning, # 354230) or Cultrex growth factor reduced BME type 2 (Trevigen, 3533-005-02) and a 50 µl drops of cell/matrix suspension were plated and in the middle of the well of a pre-warmed 24-well plate (Nunc Cell-Culture

Treated 24 well, ThermoFisher, 142475) and allowed to solidify for 30 min at 37°C. Initially, following the protocols provided by Kessler and collaborators (*96*), cells were firstly plated in adherence conditions, until a 70% confluence was reached, and then were trypsinized and resuspended in Matrigel as described above. I was then able to avoid the 2D culture step and this was also confirmed by the Clevers' lab (*10*), whose protocols allows to resuspend cells directly in the extracellular matrix. Once the ECM was stabilized, an appropriate organoid growth medium specific for each tissue was added, and plates were transferred to humidified 37°C/5% CO_2 incubators. During years, several different media were tried, and all different components tested are showed in Table 1. Each component was tested at different concentration, alone or in combination with others, at least on 3 different samples.

The final media used for the different tissues were the ones showed by Kopper and colleagues (*10*). The composition of these culture media is reported in Table 2.

Medium was changed every 3-4 days and organoids were passaged every 1-4 weeks. The organoid splitting was tried with mechanical or enzymatical dissociation. Initially, for the mechanical treatment the Matrigel was dissolved cold AdDF and the organoids were vigorously pipetted with a fire polished glass Pasteur pipette, in a 15 ml Falcon tube. Then, organoids were centrifuged and resuspended in Matrigel at the desired density. To avoid the use of Pasteur pipette and stress organoids too much, the splitting protocol was moved towards enzymatic treatment. After the removal of the culture medium, the Matrigel was at first dissolved pipetting with cold AdDF and once liquid, the suspension was centrifuged, the supernatant removed and organoids resuspended in TrypLE Express (Gibco, #12604013) for 5 min. Then the suspension was centrifuged at 300g for 5 min and organoids were resuspended in Matrigel at the desired density to be replated. In substitution of TrypLE, were tested also Accutase (Sigma, #A6964) and Trypsine/EDTA (Gibco, #R001100). The last enzymatic protocol used avoid the dissolving step with cold medium and foresee the removal of organoid culture medium and the addition of TrypLE or Accutase directly to the Matrigel drop for 5 min at 37°C, and the subsequent disaggregation of organoids trough the mechanical pipetting with a P200 tip.

The protocol showed by Kopper and colleagues was the last used and foresee the mechanical shearing through the vigorous pipetting with a P1000 pipet tip connected to P200 pipet tip without a filter. Dense organoids that were not easily sheared mechanically were digested with the last enzymatic splitting protocol described and through the use of Accutase.

Compound	**OC**	**OCwnt**	**FI**	**OSE**
WNT (CM)	-	20%	40%	50%
R-spo1 (CM)	10%	10%	10%	10%
B27 (50x)	1x	1x	1x	1x
N-Acetylcysteine (500mM)	1.25mM	1.25mM	1.25mM	1.25mM
Primocin	1x	1x	1x	1x
Nicotinamide (1M)	10mm	10mm	10mm	10mm
A83-01 (5mM)	0.5uM	0.5uM	0.5uM	0.5uM
Fgf10 (100µg/ml)	10ng/ml	10ng/ml	-	-
Heregulinβ-1 (75µg/ml)	37,5ng/ml	37,5ng/ml	-	37,5ng/ml
Noggin (100µg/ml)	100ng/ml	100ng/ml	100ng/ml	100ng/ml
Y27632 (100mM)	5uM	5uM	5uM	5uM
EGF (500µg/ml)	5 ng/ml	5 ng/ml	12,5 ng/ml	12,5 ng/ml
Forskolin (10mM)	10 uM	10 uM	-	10 uM
Hydrocortisone (250µg/ml)	0,5 ug/mL	0,5 ug/mL	-	0,5 ug/mL
β-Estradiol (100µM)	100nM	100nM	-	100nM

Table 2. Composition of organoids growth media for tumors (OC and OCwnt) and normal FI and OSE organoids.

1.3 Cell lines culture

Ovarian Cancer cell lines used were Kuramochi, NIH-OVCAR3, OVSAHO and OV-90. These cell lines were cultured normally in adherence plate and cultured with specific culture media. Kuramochi and OVSAHO were cultured in 1:1 DMEM/F12, 10% FBS, 1% P/S, 0,5% Glutamine (2mM). NIH-OVCAR3 were cultured in 1:1 DMEM/F12, 10% FBS, 1% P/S, 0,5% Glutamine (2mM). OV-90 growth in a 1:1 mixture of MCDB 105 and Medium 199, 15% FBS, 1% P/S.

All cell lines have been propagated through trypsin incubation and replated at 1:4-8 ratio.

2. Preparation of conditioned media for organoids culture

For achieve the organoids growth, in addition of using recombinant protein, the effect of using conditioned media were tested, since their use in several organoid culture systems was described. Conditioned media of R-Spondin1 and Wnt3a were generated using commercially available cell lines and following manufacturer's protocols.

R-spondin1 conditioned medium was prepared from *R-spondin1 Cells* (Cultrex, # 3710-001), a 293T cell line stably transfected to express murine Rspo1 with an N-terminal HA epitope tag and fused to a C-terminal murine IgG2a Fc fragment to allow also the protein purification. The protocol foresees the culture of these cells in presence of a selection growth media (DMEM with 10%FBS, 1%P/S 1x Glutaax and 300µg/ml of Zeocing) for 5 days, followed by the removing of the selection. When at 80% of confluency, the medium is replaced with Advanced DMEM/F12 containing GlutaMAX, and the culture is continued for 7-10 day, after which the supernatant is collected and centrifuged at 3,000 x g for 15 minutes at 4°C to remove cells and debris. The supernatant is then filtered to 0.22µm and stored for the further utilization.

Wnt3a conditioned medium is generated through the L Wnt-3A cell line provided by the ATCC® with #CRL-2647. These C3H/An cells were transfected with a Wnt-3A expression vector that allow the selection of stable clones in DMEM-10% FBS medium containing 0.4 mg/ml of G418 (Roche, 472787800). To generate the conditioned medium, cells were splitted 1:10 and cultured in a growth medium without G418 for 4 days. Then the medium is removed and stored, since it represents the first batch of conditioned medium. Fresh growth medium is added, and cells were allowed to grow for other 3 days, after which the second batch of conditioned medium is taken and mixed to the first batch 1:1. Finally, the conditioned medium is 0.22µm filtered and stored for later use.

3. Immunohistochemistry

To perform immunophenotypic analyses, organoids were fixed with 4% paraformaldehyde (ChemCruz, sc-281692) for 30 min at RT and then the Matrigel drop was washed in PBS. Organoids were then released from Matrigel through vigorous pipetting in cold PBS and centrifuged at 300g for 5 min. The cell pellet was then resuspended in 2% low melt agarose and the suspension was put in a disposable mold and allowed to solidify at -20°C for 30 min. When solid, the drop of agarose was removed from the mold and placed in an embedding cassette which underwent dehydration and paraffin embedding. Finally, organoids were cut in 5µm sections and stained.

The staining was performed following classical immunohistochemistry procedures. In brief, sections were deparaffinized, rehydrated, treated with the right pH6 epitope retrieval solution (Leica Microsystems, # AR9961). Then, endogenous peroxidases were quenched with 3% H_2O_2 for 5 min and sections were firstly blocked for 30 min in TBS-Tween-20 0,05% (TBS-T) with 2% Serum, 2% BSA and then incubated with primary antibodies in

blocking solution for 1.5h, rinsed and incubated with secondary antibodies in TBS-T with 2% BSA for 1h. Finally, sections were rinsed, treated with DAPI to stain nuclei, rinsed again and the slide were mounted with Mowiol (Sigma, #81381). The list of used antibodies is provided in Table 3.
Images were acquired on a Leica SP8 AOBS confocal microscopy.

Antibodies	**Producer**	**Catalog #**
Anti Foxj1 1:100	Sigma Aldrich S.r.l.	HPA005714
Anti-detyrosinated α-Tubulin 1:1000	Abcam	ab48389
Anti-Pax8 (M) 1:100	BioCare Medical	438
Anti-CK7 1:10000	Abcam	ab68459
Anti-Ki67 1:100	Abcam	ab15580

Table 3. List of antibodies used for immuno- characterization of organoids.

4. Imaging

For time-lapse imaging, organoids were plated in Matrigel in glass-bottom 24-well plates (MatTek, P24G-0-13-F) and mounted on an inverted confocal laser scanning microscope (Leica SP8), which was equipped with a culture chamber held at 37°C. Organoids were shot for 7 days, without changing medium. Mineral oil was added over the medium to avoid its evaporation.

5. Protein extraction

The protein extraction from ovarian cancer cell lines was performed using the RIPA buffer for cell lysis. The RIPA buffer stock solution is composed of TrisHCl 50mM, NaCl 150mM, EDTA 1mM, SDS 1%, DOC (DeOxyCholic Acid) 0,5% in H_20 and is stored at 4°C. The working solution was prepared at use and foresee the addition of 1% Igepal CA-630 (Sigma, #I8896), 1x of Halt Protease Inhibitor Cocktail (ThermoFisher, #78430) and 1mM of PMSF (Phenyl Methyl Sulfonyl Fluoride).
Frozen cell pellets were resuspended in an adequate volume of lysis buffer (50-70 µl for $1x10^6$ cells), pipetted vigorously and incubated in ice for 30 min, after which the lysate is sonicated with the Branson 450 Digital Sonifier (Marshall Scientific). Then, the sonicated lysate is centrifuged at 13200 rpm for 10 min at 4°C and the supernatant containing the protein extract is recovered and stored at -80°C.

The protein concentration was evaluated using the Pierce™ BCA Protein Assay Kit (Thermo, #23225) following manufacturer protocol. The kit allows to measure the total protein concentration developing a colorimetric reaction and comparing the absorbance at λ562nm (A 562nm) of proteins extract with the one of a calibration line generated calculating the A 562nm of several known concentrations of Bovina Serum Albumine (BSA).

6. Western Blot

Once quantified, 25-30 µg of protein homogenate were mixed with the Loading Buffer (Laemmli buffer, 0.25 M Tris-HCl pH 6.8, 100 mM DTT, 10% SDS, 50% Glycerol, 0.05% bromphenol blue) and incubated at 95°C for 10 minutes to allow protein denaturation needed to achieve a correct electrophoretic separation. Hence, the protein extract underwent SDS-PAGE (Sodium Dodecyl Sulfate – Polyacylamide Gel Electrophoresis), where denaturated peptides are negatively charged and move towards the positive electrode and are separated on the basis of their molecular weight. Smaller proteins migrate faster, and the concentration of Acrylamide determine the gel resolution: the more is higher the concentration of Acrylamide, better is the concentration of smaller proteins. The 10x running buffer used for the gel run was prepared with 3,03g/L di Tris Base, 14,41g/L di Glicina e 1g di SDS. Once partitioned, proteins were transferred on Trans-Blot Turbo PVDF (polyvinylidene difluoride) membrane (Bio-Rad, #1704156) using the Trans-Blot Turbo Transfer System (Bio-Rad, #1704150).

The transfer of proteins on the membrane was evaluated using the Ponceau S (0.5% (w/v) Ponceau S in 1% acetic acid) and non-specific bounds between antibodies and membrane are avoided incubating the membrane in blocking solution constitute of 5% non-fat dry milk (NFDM) in TBS-T (20mM Tris-HCl pH 7.5, 150mM NaCl, 0.1% Tween 20), for 1 hour at RT. Then, the membrane is incubated with primary antibodies for 1.5 hours at RT followed by 3 washing of 15 min with TBS-T at RT and a final incubation of 1 hour at RT with secondary antibodies. At this point, another 3 washes of 15 minutes in TBS-T are performed and the membrane was used for the detection.

Primary antibodies used were the Anti-Pax8 (BioCare Medical, #438) at 1:100 and the Anti-beta Actin (Abcam, #ab8227) at 1:10000

The immunoreactive band were revealed using the Chemidoc XRS+ (Bio-Rad, #1708265) and the pixel intensity was quantified using Image J.

7. Single-cell isolation for 10x Genomics

For single cell RNA seq experiments both fresh tissues and organoids were dissociated for generating single-cell gene-expression libraries.

Fresh primary tissues were processed as for cell culture, but the digestion is pushed until the tissues is dissociated at the single cell level. Then, cells are centrifuged at 300g for 5 min and washed in l 1X PBS with 0.04% BSA. After the following resuspension, to avoid the presence of clumps, cells are forced through a Flowmi™ 40 microns Cell Strainer (Bel-Art™, #H13680-0040) and counted with a TC-20 automated cell counter, checking cells viability. Only samples with a viability higher than 60% were used. If necessary, the volume is adjusted to obtain the target cell concentration.

Similarly, organoids were released from Matrigel using the Corning® Cell Recovery Solution (Corning, 354253) and disaggregated at single cell mechanically and enzymatically using Accutase for 10 min at 37°C. Once dissociated, cells are centrifuged and treated as described above.

8. Library preparation and single-cell sequencing

Single cells were processed through the 10X Chromium 3' Single Cell Platform using the Chromium Single Cell 3' Library V2 kit (10X Genomics, Pleasanton, CA), following the manufacturer's protocol. Briefly, ~5000 cells were loaded into each channel of the 10x Genomics microfluidic system chip to be partitioned into gel beads in emulsion (GEMs) in the Chromium instrument. The gel beads used are coated with unique primers bearing 10× cell barcodes, unique molecular identifiers (UMI) and poly(dT) sequences and the partitioning is followed by cell lysis and barcoded reverse transcription of RNA in the droplets. Breaking of the emulsion is then succeeded by amplification, fragmentation and addition of adapters and sample indices compatible with Illumina sequencing. Final libraries were then pooled together, quantified by real-time quantitative PCR (the calibration was performed using an in-house control sequencing library) and their size profiles were examined by an Agilent Bioanalyzer 2100 using a High Sensitivity DNA chip (Agilent, # 5067-4626). Libraries were sequenced on Illumina NOVAseq 6000 platform using the v2 Kit (Illumina, San Diego, CA) with a customized paired end, dual indexing (26/8/0/98-bp) format according to the manufacturer's protocol. A total coverage of 250M reads per samples was used in order to achieve a coverage of ~50.000 reads per cell.

9. Bioinformatic analyses of scRNAseq data

The bioinformatic analyses of single cells sequencing data were performed by the bioinformatic unit of the laboratory.

Single cell sequenced libraries were aligned with CellRanger pipeline, using Hg38 for the index of reference transcripts. Resulting data were imported in python as anndata object and scanpy vs 1.3.1 and pandas were used for downstream analyses in python. Normalization of data was performed following the Seurat pipeline (*135*).

For visualization purposes, neighbors were showed as UMAP (*136*) or diffusion map (*137*), on CellXgene VIP (*138*).

The integration of data was performed using a deep-learning approach based on neural network and named Fibered Autencoder (FAE) (*139*) that allow to identify differences between data and correct the confounding factors (batch effects) which in this experimental setting correspond to the different processing of sample types (fresh tissue vs organoids).

The identification of clusters was performed applying the Leiden algorithm (*140*) and the subpopulation assignment was performed manually through the detection of markers and differentially expressed genes (DEGs).

10. Lentiviral vector design

The lentiviral vector (LV) design was thought to achieve the simultaneous tag of cell's nuclei, for imaging purposes, and to induce the expression of specific shRNA, together with another fluorescent marker to follow the induction, for knockdown experiments *(Fig. 16)*.

The vector contains both an inducible and a constitutive part, everything included between two long terminal repeats (LTR).

The constitutive part consists of a H2B-mRuby3 cassette, to mark cell's nuclei in red, fused through a T2A (derived from *Thosea Asigna virus 2A*) self-cleaving peptide with a Tet3G cassette, to allow a Tet-on system activation. Everything is merged in turn with a Puro Resistance cassette through another self-cleaving peptide, the P2A (derived from *Porcine Teschovirus-1 2A*). Finally, we found a Woodchuck Hepatitis Virus (WHV) Post-transcriptional Regulatory Element (WPRE). The expression of the constitutive part is under the control of an Elongation Factor 1 Alpha (EF1A) promoter.

The inducible part, instead, consists of a farnesylated mNeongreen followed by a miRE cassette and everything is regulated by a tet-on Pol II promoter. The addition of the tetra-

or doxycycline induce the expression of the mNeongreen and the miRE cassette in which is possible to clone shRNA of interest. The farnesylation added to the mNeongreen allow to mark in green the membrane of cells in which is induced the expression of the shRNA. The vector was synthesized by VectorBuilder and named *VB1021msk*.

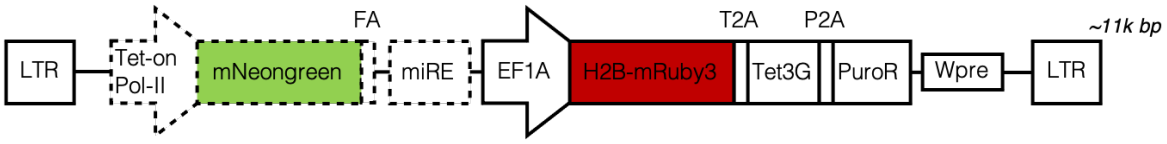

Figure 16. Schematic representation of VB1021msk.

11. Lentiviral vector production

The preparation of vector stocks was performed in human embryonic kidney (HEK) 293T (HEK293T) cell line using the calcium phosphate transfection followed by ultracentrifugation for virus concentration. The choose of 293T was due to optimal DNA recipients' capability of these cells in transfection procedures.

For transfection, $9x10^6$ 293T cells were seeded in 15 cm dishes 24 hours before transfection and incubated in IMDM 10% FBS, 1% Pen/Strepto. One hour before transfection the medium was replaced. To produce lentiviruses, for each dish of 293T a plasmid DNA mix was prepared with 9 µg of pMD2-VSV-G, 12.5 µg of pMDLg/pRRE, 6.25 µg of pILVV01, 15µg of pAdvantage and 37 µg of transfer vector VB1021msk.

The plasmid solution was made up to a final volume of 1125 µL with 0.1X TE/dH2O (2:1) in a 15 mL polypropylene tube and finally 125 µl of 2.5 M CaCl2 were added and the solution was mixed. DNA precipitate was formed by dropwise addition of 1300 µl 2X HBS solution (281 mM NaCl, 100mM HEPES, 1.5 mM Na2HPO4, pH 7.12, 0.22 µM filtered) to the 1300 µl of DNA-TE-CaCl2 mixture while vortexing at full speed and immediately added to 293T cells supernatant. After transfection, cells were incubated with the CaPi-precipitated plasmid DNA at 37°C for other 12-14 hours and after which medium was replaced with 16 mL of fresh medium. 30 hours after medium changing the supernatant was collected, filtered through 0.22 µm pore nitrocellulose filter and ultracentrifuged at 20.000 rpm for 2 hours in an Optima XE-90 Ultracentrifuge (Beckman coulter) at RT. Pellets containing the vector were resuspended in a volume of sterile PBS representing 1/500 of the starting medium volume (usually 150 µL for 250-fold concentration), pooled and rotate on a wheel at RT for 1 hour. The concentrated vector preparation was then divided into small aliquots (15 µl) and stored at -80°C.

12. Lentiviral infection of HEK293T and FI organoids

For the lentiviral infection, different protocols were used for adherent culture and 3D organoids.

The 293T infection was performed using a classical infection protocol. Briefly, cells were plated in a 6-well tissue culture plate in normal growth medium that was replaced the day of transfection with 1ml of fresh medium containing an aliquot of the virus. The medium was mixed gently through the plate to allow the spread on all cells. After 48 hours of exposition, the medium is replaced with fresh growth medium and the subsequent day the cells were selected in puromycin.

For the infection of organoids two different protocol were tested. The first protocol foresees the addition of the virus to the growth medium of organoids for 48 hours, changing then the medium with fresh one. Conversely, in the other protocol the Matrigel was dissolved using fresh cold medium and organoids from 2 drops were centrifuged at 300g for 5 min. Then, organoids were resuspended in 250µl of AdDF and two aliquots of virus was added to the suspension. Organoids and virus are then incubated on a rotator at 37°C for 6 hours, after which organoids were pelleted and resuspended in Matrigel for the culture.

13. CRISPR/Cas9 experiment design

The genetic engineering with CRISPR/Cas9 of ovarian cancer cell lines was designed to use a synthetic Cas9 protein purified by the Cogentech Biochemistry Facility of the IFOM (Istituto Firc di Oncologia Molecolare), Milan. The protein was solubilized in a Transduction Buffer (*141*) (5x Transduction Buffer: 500mM NaCl, 25mM NaH2PO4, 250mMNDSB-201, 150mM glycerol, 75mM glycine, 1.25mM MgCl2, 1mM 2-mercaptoethanol pH8.0). This Cas9 is characterized by the addition of a nuclear localization signal (NLS) that drive the protein directly in the nucleus upon the electroporation.

The donor plasmid was designed using Benchling and the HaloTag sequence was recovered online from SnapGene. The Pax8 sequence was derived from the UCSC Genome Browser and ~1Kb homology arms (HA) were designed on the 5'-UTR and the 1st exon of the gene. The donor plasmid presents a hygromycin resistance cassette without stop codon and fused through a T2A self-cleaving peptide to the HaloTag sequence,

everything included between the two HA *(Fig.17)*. The vector was produced by VectorBuilder.

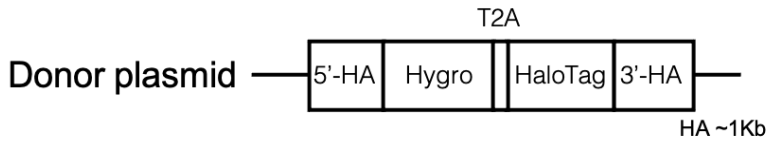

Figure 17. Schematic representation of the donor plasmid for the CRISPR/Cas9 set-up.

The gRNA was designed using the "CRISPR/Cas9 guides design and analyze" tool of Benchling, selecting the guide with the highest score of fold change. The gRNA sequence is showed in table 4. The last 3 bp of the sequence represent the PAM (Protospacer Adjacent Motif) recognized by the Cas9 for the cut. The gRNA map on the 3'-HA and mismatch on the 3'-HA of the plasmid was designed to avoid cuts by the Cas9 upon its integration. The gRNA was produced by an *in vitro* synthesis.

Sequence	***Nucleotides***
gRNA	CATCAGATCTGGTAAGAACGCCG
gRNA oligo Fw	5'-TAATACGACTCACTATAGCATCAGATCTGGTAAGAACG-3'
gRNA oligo Rv	5'-TTCTAGCTCTAAAACCGTTCTTACCAGATCTGATG-3'

Table 4. Nucleotides sequences of gRNA and Fw and Rv oligos for its synthesis.

14. gRNA in vitro synthesis

The gRNA *in vitro* synthesis was performed using the GeneArt Precision gRNA Synthesis Kit (Invitrogen, #A29377), following manufacturer protocol. Briefly, gRNA oligos (Sigma, sequence showed in Table 5) were assembled performing a PCR reaction using Phusion High-Fidelity DNA pol (ThermoScientific, #F-530) with following parameters:

Cycle step	***Temperature***	***Time***	***Cycles***
Initial Denaturation	98°C	10 seconds	1X
Denaturation	98°C	5 seconds	32X
Annealing	55°C	15 seconds	
Final extension	72°C	1 minute	1X
Hold	4°C	Hold	1X

Table 5. PCR steps for gRNA DNA template assembly.

Then, to perform the RNA *in vitro* transcription reaction, the gRNA DNA template from the PCR assembly was incubated with nucleotide triphosphate (NTP) mix and both TranscriptAid Enzyme and buffer for 4 hours at 37°C, followed by the degradation of eventual DNA contaminant by the DNase I (included in the kit) for 15 min at 37°C.
At this point, the transcribed gRNA quality was checked by gel electrophoresis, evaluating the presence of 100bps bands and the gRNA was purified mixing it with a Binding buffer and ethanol and loading it in a GeneJET™ RNA Purification Micro Column. The column then underwent subsequent cycles of rinse with Wash buffers and finally the gRNA was eluted in nuclease-free water. The eluted gRNA was used immediately or stored at -80°C.

15. Transfection of Ovarian Cancer Cell Lines

The insertion of the HaloTag sequence in the Pax8 gene was performed on three OC cell lines expressing Pax8 and, accordingly to Domcke and colleagues (*34*), most-likely recapitulating HGSOC: Kuramochi, OVSAHO and NIH-OVACAR3. The transfection was performed using the Neon Transfection System (Invitrogen, MPK5000) following the manufacturer protocol, and the best electroporation conditions were determined with a prior transfection of cells with a Green Fluorescent Protein (GFP) expressing plasmid (pCAG-GFP, Addgene #11150).
Briefly, cells were trypsinized and counted using an automatic cell counter. Then, $2.4x10^6$ cells were centrifuged and resuspended in a resuspension buffer (Buffer T). Before the electroporation, 10µg of Cas 9 and 5µg of gRNA are incubated at 37°C for 10 min. Then, the Cas9/gRNA complex and the plasmid are added to the cell suspension and aliquot of $4x10^5$ cells underwent electroporation.
The electroporation conditions used for each cell line are showed in Table 6.

Cell Line	**Voltage**	**Time**	**Pulse n.**
Kuramochi	1200 V	20 ms	3
OVSAHO	1200 V	30 ms	3
NIH-OVCAR3	1000 V	30 ms	3

Table 6. Electroporation conditions for OC cell lines.

After electroporation, transfected cells were selected through hygromycin resistance or by FACS/sorting. Kuramochi and OVSAHO were selected for 14 days with 400ug/ml and 800ug/ml Hygromycin respectively. NIH-OVCAR3, conversely, were hypersensitive to

Hygromycin despite the introduction of the resistance cassette in the genome and were selected using FACS/Sorter.

After their isolation, positive cells were manually plated as single cells in 96 wells plate and allowed to grow for weeks until sufficient numbers of cells to allow further analyses were achieved.

The identification of homo- and heterozygous clones was performed by PCR.

16. Staining with TMR ligand

The Halo-Tag is an engineered, catalytically inactive derivative of a hydrolase with a modified active site which has an increased rate of specific ligand binding. Under physiological conditions, this covalent bond form rapidly and is highly specific and essentially irreversible, allowing the staining of positive live cells expressing the Halo-Tag. The stain with a Halo-Tag ligand allow to both validate the transfection and sort cells. To stain positive cells, we used the Halo-Tag TMR ligand (Promega, G8251) following the manufacturer protocol. Briefly, the TMR ligand stock solution was diluted 1:200 in warm culture medium and added to cells, replacing it with one-fifth of cells growth medium. Cells were incubated with the TMR ligand for 15 min at 37°C, after which three complete rinses with fresh warm growth medium were performed. Then, cells were incubated for 30 min at 37°C to wash unbound ligand and finally the medium was replaced with fresh warm culture medium and analyzed under the microscope for the validation of the transfection and harvested as for normal passaging for the FACS/Sorting.

17. FACS/Sorting of NIH-OVCAR3 cells

The TMR ligand present a wavelength with an Ex=555nm and an Em=585nm. For this reason, NIH-OVCAR3 were sorted on a BD FACSJazz™ Cell Sorter exciting cells with a 561nm laser. Positive sorted cells were then reanalyzed through FACS to observe the percentage of positive cells sorted.

18. Genomic DNA extraction from cells in culture

Cell lines were harvested by trypsin and pelleted at 500g for 3 min and then washed in DPBS. Dry cell pellets were stored at -80°C until the extraction, that was performed using the Qiagen DNeasy® blood and tissue kit, according to manufacturer protocol. Briefly, cell pellets were lysed in proteinase K and the RNA was depleted through the use of RNAse

(Qiagen). Then, the lysate was loaded onto the DNA binding column, in order to remove contaminants and enzyme inhibitors through two subsequent wash. Finally, gDNA was eluted in ddH2O and stored at 4°C until use.

19. PCR for validating the integration of the HaloTag

For validating the allelic status of the HaloTag integration was designed a four primers PCR screen. Primers used are showed in Table 7.

Primer	***Sequence***
Locus Fw	TTAGTGTGGACATTCTTCGTG
Locus Rv	GGCTAAATAGAGATCTCAGCC
Hygro Rw	TTCGATCAGAAACTTCTCGAC
HaloTag Fw	TGAATCTGCTGCAAGAAGAC

Table 7. List of primers used for the PCR screening of Kuramochi colonies

The PCR screen was designed in this way:

- A signal coming only from the two Locus primer means that there was no integration in the gene locus.
- A signal from the Locus Fw and Hygro Rw primers indicate the 5' integration.
- A signal from the HaloTag Fw and Locus Rw primers indicate the 3' integration.
- A signal from both the Locus primers and the 5' and 3' integration primers indicate a heterozygous (monoallelic) integration.
- A signal from the 5' and the 3' integration couple of primers but not from the Locus primers indicate a homozygous (biallelic) integration.
- Signal coning only from the 5' or 3' position suggests some genetic rearrangement.

20. Halo-ChIP (*Chromatin ImmunoPrecipitation)*

To identify DNA binding sites of Pax8 we performed a ChIP taking advantage of the HaloCHIP™ System (Promega, G9410), which allows to covalently capture crosslinked protein:DNA complexes using a resin-based ligand, the HaloLink™ Resin, and avoiding the need for antibodies. The HaloChIP was performed following the manufacturer protocol. Briefly, Kuramochi transfected cells were plated in 15 cm dishes and fixed through the addition of 37% formaldehyde to a final concentration of 1% for 10 min at RT.

Then, formaldehyde crosslinking is quenched by 125mM of Glycine for 5 min at RT after which fixed cells are rinsed three times by ice cold PBS. Cells are then collected using a cell scraper and pelleted at 2000g for 5 min at 4°C. Cell pellet was lysed using first a cytoplasm lysis buffer, to isolate nuclei, and then with a mammalian lysis buffer, everything followed also by a mechanical disruption passing the lysate through a 25-gauge needle. In order to obtain fragments of 500-1500 bp, the cell lysate underwent a sonication step, performed with the Covaris S220 Sonicator and using 100 W of Peak Incidendce Power, 4% of Duty Factor, 200 cycles per burst and treat the DNA for 240 seconds. Sonicated samples are centrifuged at 14000g for 5 min at 4°C and then the supernatant is mixed with the HaloLink™ Resin and the mixture is incubated for 3 hours at RT in constant mixing using a tube rotator. After incubation, the mixture is centrifuged at 800g for 2 min at RT and the supernatant is stored as input material. Conversely, the resin is exposed to the mammalian lysis buffer and mixed vigorously, before underwent to several washes step with nuclease-free water, washing buffer and LiCl buffer. To release the DNA, the resin is then incubated overnight at 65°C with a Reversal buffer, centrifuged and the supernatant containing the released DNA is stored for subsequent analyses.

RESULTS

RESULTS

The current status of knowledge on ovarian cancer underlines the need to improve the understanding of the biology of the disease. The dearth of validate clinically-significant models and the uncertainty about the tissue of origin were the main aspects explored in the lab in which this PhD project was carried out. On one hand, we were able to shed light on the problem of the cell of origin of HGSOC, identifying also genes, like PAX8, that could be of relevance in the origin-specific tumorigenesis (*12*). On the other side, the definition of clinically-relevant models has been the focus of this PhD project.

1. Derivation of organoids

Over the last decades, the lack of suitable clinical models to study Ovarian Cancer has hampered the development of new therapies and, consequently, the improvement of patients' clinical care. Indeed, common cancer cell lines and PDTX used to model the pathology have contributed to cancer research but presents a number of drawbacks that does not allow to recapitulate the human pathology to a meaningful extent. For these reasons, the possibility to exploit organoids potential to model the disease and gain insight into molecular mechanisms driving its pathogenesis was enticing.

To investigate the disease, its onset and its progression, in the lab we were interested in developing a platform comprising organoids derived from both healthy and tumor tissues. Given the dual origin of OC (*12*), we aimed at deriving organoids from both normal fimbria and ovarian surface epithelium. Indeed, the possibility to study normal healthy tissues could help in shedding light on origin-specific molecular mechanisms driving the disease. From the other perspective, the derivation of organoids directly from patients' tumors will provide a tool to study the pathology in a patient-specific manner, allowing to investigate the presence of mechanisms that are shared or not between different patients and derive tumor subtypes with same features that could take advantage from a specific drug treatment. Moreover, the possibility to derive organoids from both primary solid tumors and metastasis in the form of ascites have the potential to gain insight also in molecular mechanisms driving the metastasization process. For these reasons, we thought that the generation of tumor organoids should encompass both solid tumor and metastatic ascites. Among all OC, given its clinical relevance we focused only on the HGSOC histotypes.

The methodological starting point for this project was the paper published in 2015 from Thomas F. Meyer and colleagues (*96*) that showed the possibility to culture organoids from the fallopian tube using a specific cocktail of growth factor. Despite of this, the possibility to generate organoids from OSE and tumors was unaddressed.

1.1 Derivation of fimbrial epithelium organoids

To generate organoids from the fallopian tube fimbrial epithelium, I started trying to replicate the protocol showed by Kessler and colleagues adapting it in order to isolate only fimbrial cells (and not the entire fallopian tube). For this reason, primary samples were processed, and epithelial cells obtained were seeded in adherence condition, following the protocol used in the lab to culture primary FI cells. Then, follows their transfer to Matrigel matrix and plating in three-dimensional condition using the list of growth factor showed in the published protocol (*96*). As in the paper, I was able to generate organoids although I found difficulties in the long-term maintenance of organoids which, after few passages *in vitro*, stop to grow. Moreover, a questionable aspect of the published protocol was the need to culture cells in 2D before their passage in 3D conditions taking in consideration the possible effect of the adherent culture on the genetic or epigenetic state of cells and the eventual selection of specific subpopulations (reviewed in *142*). Hence, in order to avoid the possible influence of the adherence culture condition and enable the optimized long-term expansion of FI organoids, I tried to improve the protocol starting to test different compounds already known to be useful to culture stem cells or other organoids systems or molecules that have an effect on fallopian tube *in vivo*. The inhibition of p38 MAPK, which normally stimulates cell differentiation, apoptosis and autophagy, seems to improve the self-renewal of different stem cells (*143*, *144*), so I tried to add SB202190 (p38 MAPK inhibitor) to the culture medium to ensure the long-term expansion of organoids also after several weeks. This compound, together with the addition of β-estradiol, T3 and BPE hormones allows the generation of organoids from cells directly embedded in 3D Matrigel, ensuring their long-term propagation.

Organoids could be generated with a high efficiency (~80%), showed a cystic sphere morphology, recapitulating an epithelium surrounding a cavity, and presented folds and invaginations of the epithelium after 10-12 days of growth as an hallmark of mature organoid culture (*Fig.17*). Moreover, the growth rate remained constant during the long-term culture (defined as at least 6 passages *in vitro*, approximately 3 months), with passaging at a 1:2-3 ratio required every 2-3 weeks

At this point, in order to understand if all compounds present in the culturing medium were really required for the growth, I started testing the removal of specific molecules. This allowed me to obtain organoids that were as less as possible influenced by exogenous factor and make the medium the most sustainable possible in terms of cost and ease of production. Comparing the generation efficiency and propagation ability of organoids at the removal of specific molecules, I observed that the N2 supplement was not needed, as well as the Wnt3A conditioned medium and FGF10. These results suggest that the activation of the Wnt pathway by R-Spondin1 was sufficient to ensure the survival of organoids with the EGF signal and the inhibition of BMPs representing the only pathways needed to ensure the generation and propagation of organoids. Furthermore, when these compounds were removed also SB202190, BPE and T3 hormones become unnecessary.

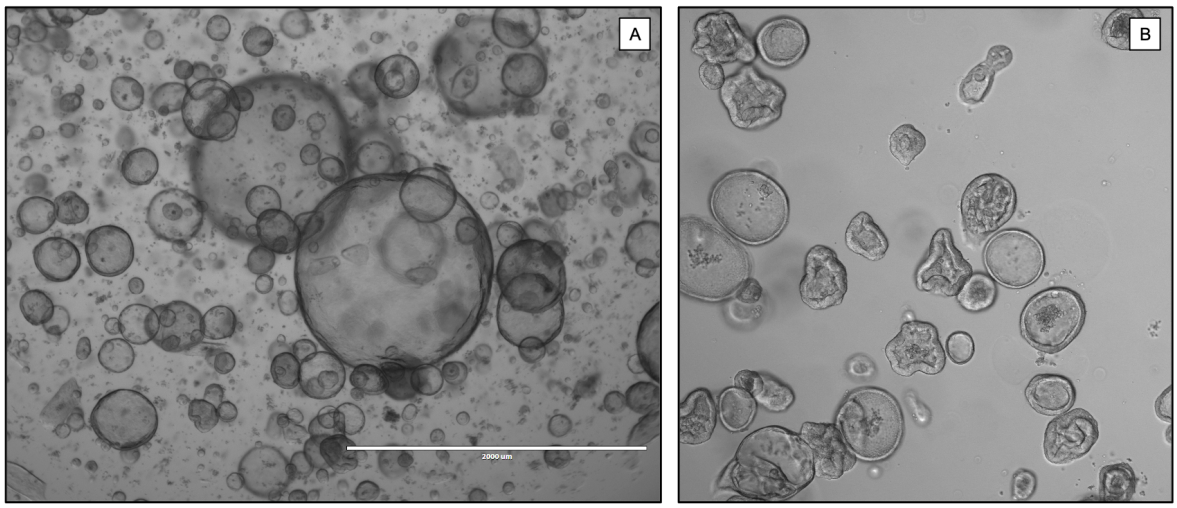

Figure 17. Brightfield (A) and confocal (B) pictures of fimbria-derived organoids.

Despite the success in derivation of organoids from FI, no protocols tested allowed me to achieve their biobanking. Indeed, although it was possible to freeze organoids for short periods, the long-term storage (several months) seems to affect the ability of organoids to recover after the thawing. This was true for organoids generated at any step described above, without observable differences also testing different freezing protocols.

The problem of freezing/thawing of organoids was not encountered in both the papers published by Kessler and colleagues first and Clevers' lab later (*10*). In this latter publication, the authors showed a modified protocol for the generation of FI organoids that allows the generation, long-term expansion and biobanking of FI organoids. I successfully reproduced the protocol in terms of generation and propagation of organoids, but I still not achieved a positive result in terms of long-term freezing.

1.2 Generation of OSE organoids

Conversely from fallopian tube, the generation of organoids from the OSE was not reported at the beginning of the project and only few cell lines were available to study this tissue. Moreover, the adherent culture of primary cells of OSE presents drawbacks that have hampered the possibility to use them for molecular biology experiments, first among all the poor propagability *in vitro*. For these reasons, the interest in generating an organoid model to study and manipulate this tissue was very high.

Given the frequent cycle of rupture and repair during the menstrual period, the presence of ASCs acting to ensure the homeostasis of the tissue was strongly supported (reviewed in *3*). However, few information about these stem cells, their niche and the molecular pathways orchestrating their functions were accessible in literature. Hence, no real starting point were available to initiate the organoids culture of OSE.

On the basis of what was done on fallopian tube and the similarities of the two tissues, I reasoned that culturing cells in the same way could be a valid initial approach aimed at generating a protocol. I started isolating and culturing epithelial cells with the protocol used in the lab for the 2D culture of OSE cells and, upon their growth, subsequently harvested cells and transferred them in a Matrigel matrix drop. The first culture medium used was the same of FI organoids. However, it was not possible to generate organoids in this way, probably for the lack of some essential factor in the medium.

For this reason, I tested several variation to the growth medium, such as the addition to the basal FI organoids medium (*96*) of inhibitors (SB202190, CHIR99021), hormones (progesterone, β-estradiol, T3 and BPE) and small molecules (N-Acetyl-L-Cysteine). Despite these trials, however, it was not possible to generate organoids from the OSE. During the long timespan of these trials (> 1 year), on the FI platform I was able, in the meanwhile, to avoid the need for the 2D culture step required to generate organoids. Hence, I reasoned that the step of 2D culture of OSE cells could somehow impact their subsequent growth as organoids, probably due to the induction of differentiation or the prevalent selection of terminally differentiated cells, with a limited proliferation potential. So, I decided to start the culture of isolated cells of OSE directly in 3D and this choice seemed to overcome the problem, allowing the achievement of the generation of OSE organoids. However, despite these organoids show the correct cystic sphere morphology recapitulating an epithelium (*Fig.18*), their proliferation rate was really low and achieve their propagation was not possible. Hence, I tested again several compounds and concentrations, in order to optimize the protocol and achieve at least a short-term

propagation albeit aiming the long-term one. In the meanwhile, Sachs and collaborators published a protocol for the generation of breast cancer organoids (*93*), showing that the key addition compared to previously established human organoid protocols was the mitogen Neuregulin-1 (or Heregulin-β), a ligand of the HER tyrosine kinases -3 and -4. Hence, I decided to test the addition of this compound to the factor cocktail, and I observed that combined with β-estradiol, T3 and BPE allow the propagation of organoids, although only for few passages (generally less than <4, with a couple of samples expanded till passage 9 and 7). The long-term passaging of OSE organoids and the possibility to freeze and thaw (and so to biobank) them was still not achieved. Moreover, both the propagation rate (1:1.5-2) and the derivation efficiency (~15%) were really low.

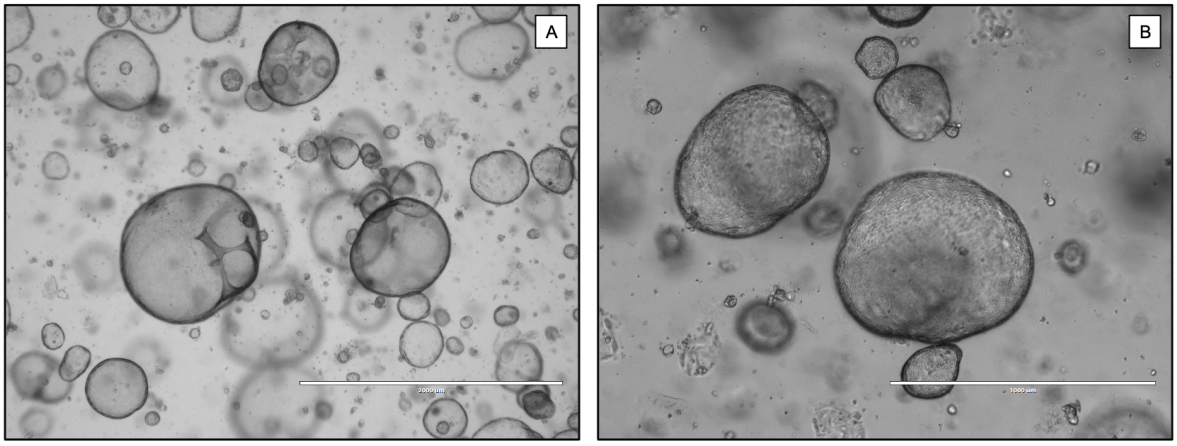

Figure 18. Brightfield pictures of OSE organoids at 2X (A) and 10X (B) magnification.

Recently, the Clevers' lab published a paper showing a protocol for the generation of organoids from the OSE. In the paper they were able to achieve the generation and long-term propagation, although with a slow rate, of organoids, using a medium that differs from the one I used for the high concentration of Wnt3a (50% of conditioned medium), a reduction in the percentage of R-Spondin1 conditioned medium and the addition of Forskolin and Hydrocortisone. I tried to replicate the protocol provided on 6 different OSE samples, although I did not have the availability of the Noggin conditioned medium indicated in the protocol that was also not available to purchase from the indicated source at the time of experiments Hence, I used the same concentration of Noggin used for all the other organoids systems, but I was not able to reproduce the result on all the 5 different tested samples, with organoids that after few weeks lose the proliferative potential and could not be expanded more.

The recap of all medium tested on OSE samples is showed in Fig. 19.

A

Token	Supplement	Pathway/ Function	
C	CHIR99021	Wnt/b-catenin signalling activator	
H	Heregulin-b	EGF signalling activator	
K	Forskolin	cyclic AMP (cAMP) activator	
S	SB202190	p38 MAPk inhibitor	
B	BPE	Hormone	
D	B-Estradiol	Hormone	
T	T3	Hormone	
P	Progesteron	Hormone	
W	Wnt3a	Wnt/b-catenin signalling activator	
A	A83-01	TGF-b signalling inhibitor	Complete Medium = Basic + EFNRA
R	R-Spondin 1	Wnt/b-catenin signalling activator	
E	EGF, human	EGF signalling activator	
F	FGF 10	FGFR2b signalling activator	
N	Noggin	BMP signalling inhibitor	
	N2 supplement	Nutrient, transferrin	
	Y-27632	ROCK signalling inhibitor	
	B27 supplement	insulin signalling, antioxidants	
	Nicotinamide	Co-enzyme precursor	
	GlutaMax	Nutrient	
	Primocin	Antibiotics	
	Hepes	Buffer	
	Pen/Strepto	Antibiotics	
	Adv. DMEM/F12	Base medium	

Basal medium

Basic medium

B

Media tested on OSE or OC primary samples for establishment of organoids					
Medium	# OC	# OSE	Medium	# OC	# OSE
Basal	2	2	Basic + EFN	2	/
Basic	2	/	Basic + EFNAS	2	2
Basal + R	3	2	Complete	4	2
Basal + RW	3	2	Complete + W	4	2
Basal + ER	2	/	Complete + S	3	2
Basal + ERW	2	/	Complete + P	3	2
Basal + EN	3	/	Complete + DTB	4	2
Basal + ENR	3	2	Complete + DTBW	4	2
Basal + ENRW	3	2	Complete + DTBP	3	3
Basal + EF	2	/	Complete + DTBPW	2	3
Basal + EFN	2	/	Complete + DTBS	3	2
Basal + EFNR	2	2	Complete + C	3	2
Basal + EFNRW	2	2	Complete + DTBSC	3	2
Basal + EFNA	3	/	Complete + H	4	3
Basal + EFNRA	3	2	Complete + HS	3	2
Basal + ENFRAW	3	2	Complete + HSDTB	4	2
Basal + EFNRAS	3	2	Hill et al.	5	/
Basal + EFNRWAS	3	2	Kopper et al.	9	5

Figure 19. Summary of molecules and media tested for the growth of HGSOC and OSE organoids.

A: *List of components tested for the growth of organoids and relative identifier token.* ***B:*** *Summary table of media tested on HGSOC and OSE samples. The numbers of samples are intended as biological replicates. Some different media were tested on same samples.*

1.3 Derivation of OC organoids

Similarly to what seen for the OSE, the potential of organoids to study OC was completely not exploited at the beginning of this PhD project, but there was an urgent need to develop a model that can recapitulate in vivo complexity and allow to study the disease, deconvoluting its heterogeneity and complexity.

Respect to the OSE, the biological knowledge of OC was wider and came from different cell lines, primary cultured cells, PDTX and molecular biology experiments performed directly on tissues. Moreover, the presence of cancer stem cells (CSCs) sustaining the progression of OC, and thus drive the tumor-derived organoid formation (tumuroidogenesis), was strongly supported (*57*, *145*).

Despite of these aspects, the starting points were again the protocol provided by Kessler and colleagues for FI organoids and the expertise acquired in the lab in culturing tumors' primary cells in adherent condition.

Initially, the derivation of primary cells from tumors and metastatic ascites was performed following the protocol already used in the lab for the isolation of cells to be plated in 2D culture. Like for normal healthy samples, first trials were done culturing cells in Matrigel after an initial passage in 2D. However, since other cancer organoids system were generated plating cells (or aggregate of cells) directly in Matrigel, the two essays were carried out in parallel. The initial medium used for the growth of tumor organoids was the one used for the generation of FI organoids, albeit with negative results in terms of obtaining organoids-resembling structures. Hence, to achieve the organoid generation I needed to optimize the medium used and I started testing several additives, looking for compounds and factors hypothesized or used to support OC growth but also needed to generate other kind of tumor organoids. This brought to the initial addition to the medium of SB202190, β-estradiol, T3 and BPE, making trials in parallel on cells plated directly in 3D or upon a 2D passage, in 3 replicates on at least 3 patients. With the implementation of these additives to the basal medium I was able to generate small clumps of cells that likely recapitulate an organoid but were far away to be considered organoids especially in terms of dimension (only around 50μm), pointing to the need to test the addition of other compounds to the mixture. However, since in the meanwhile the need to culture cells in 2D for normal organoids failed, I started plating tumor cells directly in tridimensional culture, also on the basis that all the other cancer organoids culture system did not present any step in adherence.

Furthermore, this was also theoretically support by the consideration that the bidimensional culture should drive the selection of specific cells subpopulations, reducing the heterogeneity and complexity of the primary tumors, an aspect important to avoid with organoids cultures.

The bypassing of the adherent culture step was promising also in this case, allowing to achieve organoids-like structure of higher dimension, although with a very limited propagability potential. Therefore, the next additives tested, were CHIR99021, progesterone and PGE2, without any particular improvement in the expansion of cultures. At this point, considering that cancers *in vivo* tend to sustain themselves modifying the surrounding environment and observing that other cancer organoids require few additives that normal healthy ones, I tried a reverse approach removing components in order to succeed in the propagation of organoids. Consequently, I started to culture OC organoids in the basal medium conditioned only with R-Spo1 and B27, and I observe an increase in the organoids' derivation efficiency and a propagation for a couple of passages. The addition of EGF, Noggin, A83-01 and FGF helps in achieve a short-term propagation of organoids, reaching 4 passages *in vitro*, although the proliferation rate clearly slow down during passaging, ending with cells that did not allow further expansion.

These organoids show a compact sphere morphology, recapitulating a disorganized tissue, with cells inside the organoids becoming necrotic after several days of culture (*Fig.20*).

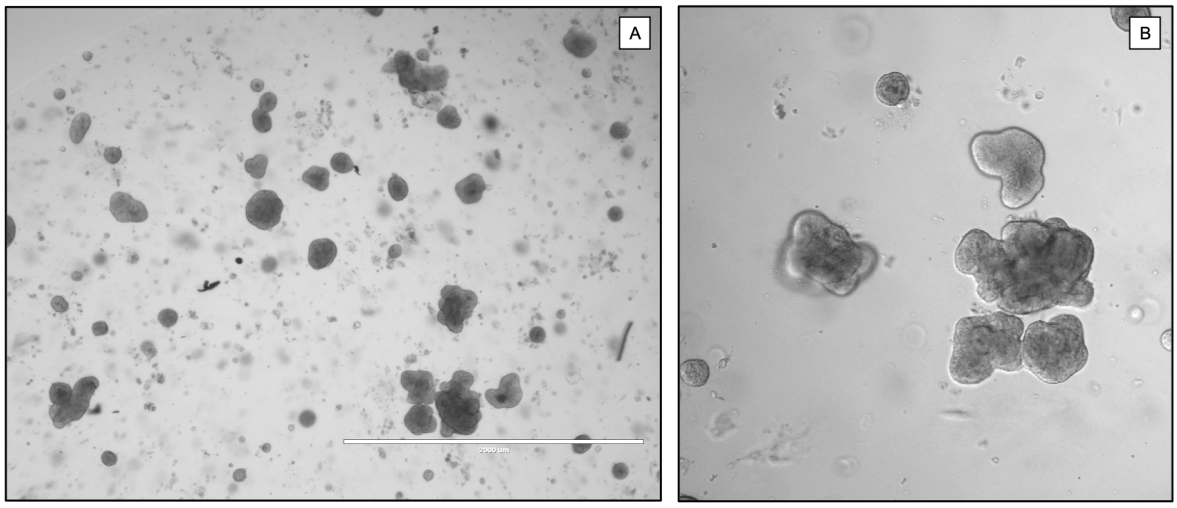

Figure 20. Brightfield (A) and confocal (B) pictures of OC-derived organoids.

Since a long-term propagation of organoids was not achieved despite the test of several culture media, made of various compounds or with different concentrations, I tried to focus the attention on other possible variables.

Among them, I hypothesized that the extracellular matrix used to culture organoids could not be adequate, probably for its stiffness or maybe for its composition, having a negative impact on the growth of tumor organoids. So, to assess this theory, the subsequent trial was to test different matrix, culturing the same sample in parallel in Matrigel or in another artificial extracellular matrix. ECM available were the Cultrex® Reduced Growth Factor Basement Membrane Extract (BME) Type R1, the BME Type II, the BME 3-D culture, the Rat Collagen and the Laminin. The test was carried out on 3 different samples in triplicates but, again, I failed in accomplishing a positive result.

Taken together, these results seem to suggest that it is not possible to generate organoids from OC at the current state of knowledge. The publication of the paper on Breast Cancer organoids has rekindled hopes, providing a new protocol to test and a key additive, the Neuregulin-1, which was crucial for the growth of that kind of organoids. Hereafter, I promptly tried the addition of Neuregulin-1 to the culture medium, testing it on four different samples in triplicates. However, neither the addition of this factor allowed to increase the expansion rate and realize a long-term propagation of OC organoids.

In 2018, D'Andrea and collaborators published a paper showing the genomic characterization of short-term organoids, using them to study the DNA repair inhibitor response, particularly relevant since 50% of HGSOC are predicted to have DNA repair defects. Although described as "short-term", in the text is reported the ability to propagate organoids from 6 passages up to 30, a timespan compatible with something that could be considered as "long-term". Despite this controversial aspect, in the paper they provided a protocol from which I drew information, noting that it was really similar to ones I already tested. Main differences between the two culture media were the increased concentration of EGF and the addition of FGF2 and PGE2. I decided to test the published protocol, both in terms of medium composition and passaging protocol, but it did not improve the propagation rate of organoids (*Fig.21*).

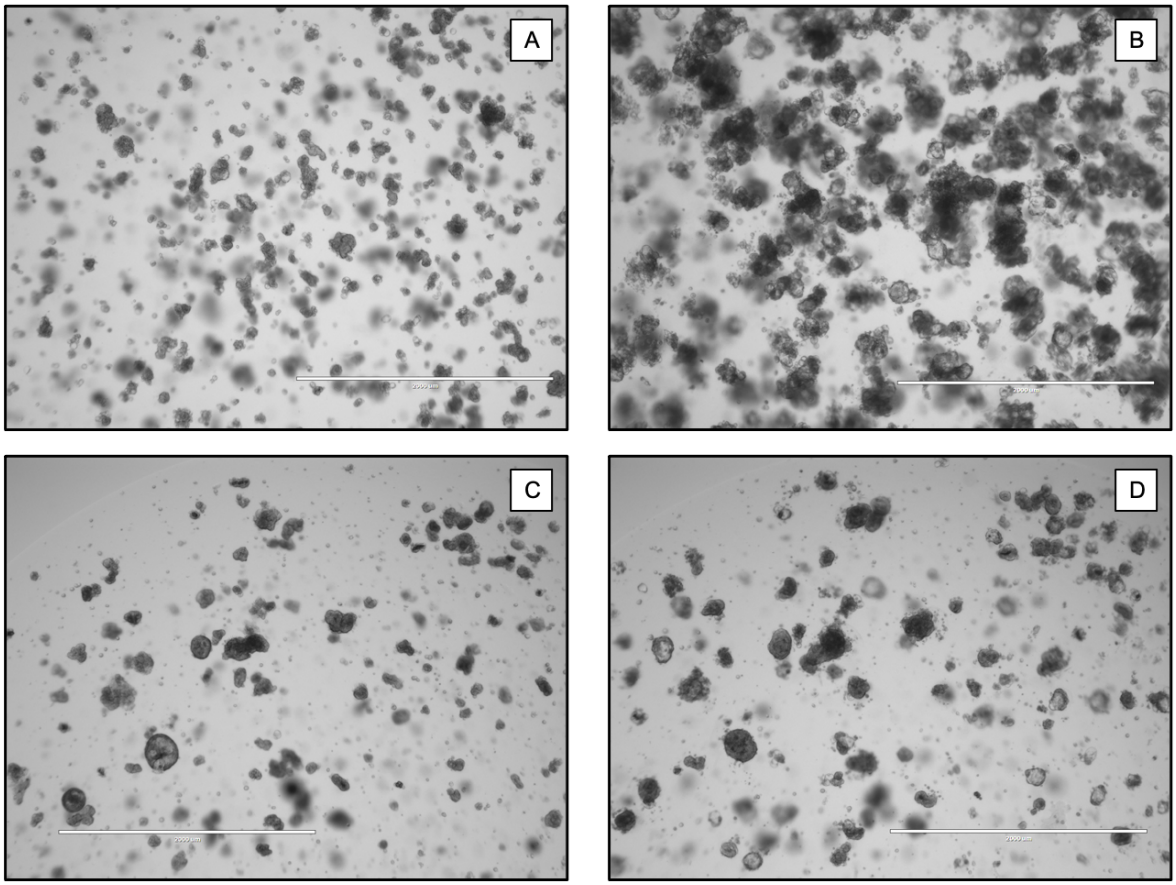

Figure 21. Brightfield pictures of OC organoids cultured with Hill et al. protocol (*9*)**.** *Organoids at P0 (first raw) and P2 (second raw) cultured after 1 day (A-C) and 12 days (B-D) of culture.*

The final achievement of long-term propagating organoids was reached by the Clevers' lab in late 2019, showing the generation and genetic characterization of an OC tumor organoids biobank. They derive organoids from different tumor histotypes, with differences in the derivation rate. For HGSOC the derivation efficiency was around 55%, underlying the difficulties in generate organoids from this kind of tumor. However, they provided protocols for generating and propagating organoids for more than 30 passages, showing the potential of this platform to capture the intra- and inter-tumor heterogeneity. The protocols provided where really similar to one combination already used, foreseeing the presence of Forskolin as unique missing additive, and halving the EGF concentration. In some specific cases they also need the addition of Wnt3a conditioned medium and HGF. Henceforth, I tried provided protocols, replicating the sample processing procedure, the culture media and also the splitting techniques with the only difference in the use of Noggin as recombinant protein instead of his conditioned medium used in the paper. The application of the protocol allowed me to generate organoids really efficiently, but, again,

it did not allow me to propagate organoids for more than 3-4 passages, with a decrease in the proliferative capacities upon passages (*Fig.22*).

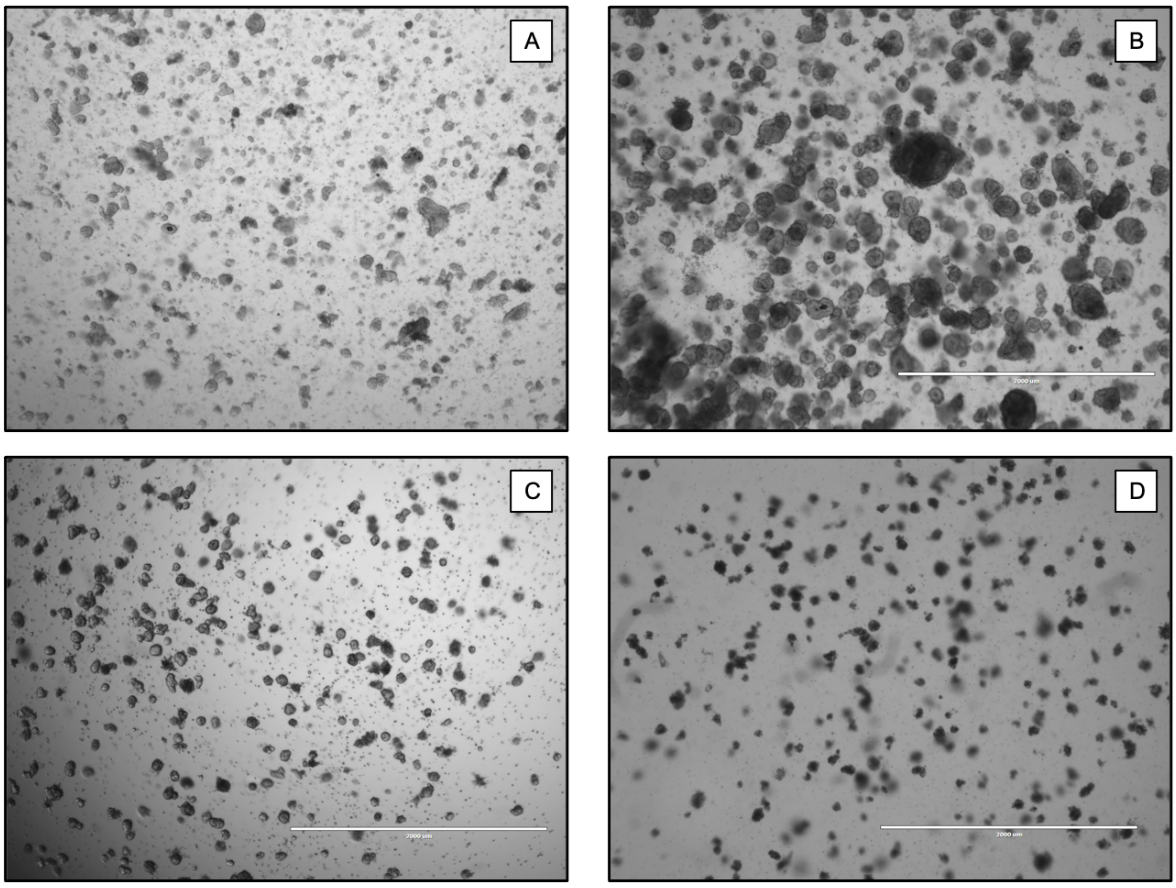

Figure 22. Brightfield pictures of OC organoids cultured with Clevers' lab protocol (*10*)**.** *Organoids at P0 (first raw) and P3 (second raw) cultured after 1 day (A-C) and 12 days (B-D) of culture.*

The recap of trials done on OC samples is showed in Fig. 19.

2. Histological characterization of OC organoids

Normal and tumor organoids recapitulate primary tissue at the morphological level. However, in order to assess if organoids recapitulate histological features of primary tissues, I performed an immunohistochemical characterization, evaluating the expression of tissue specific markers.

The immunofluorescence (IF) staining was performed on both normal healthy FI organoids and tumor organoids after two passages *in vitro*. OSE organoids were not characterized given their low expandability and the relatively large amount of cells needed for IF experiments in the used protocol.

Immunofluorescence staining of FI organoids reveal the presence of both secretory cells, given the expression of the specific marker PAX8, and ciliated cells, identified by the presence of cilia marked by the expression of the detyrosinated tubulin. Moreover, organoids express Cytokeratin 7 (CK7), confirming that they are composed of only epithelial cells *(Fig.23)*.

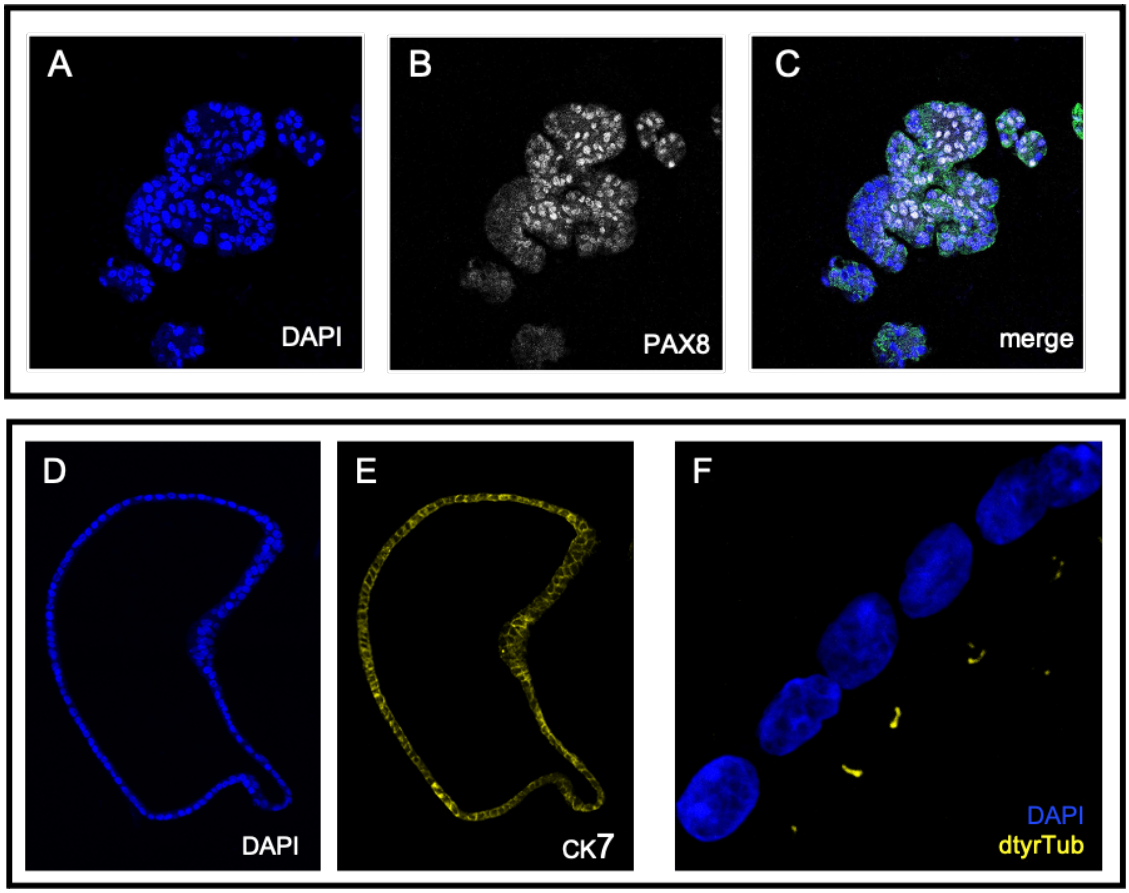

Figure 23. Immunofluorescence staining of FI-derived organoids.

Expression in FI organoids of tissue specific markers: ***A-D:*** *Nuclei stained with DAPI.* ***B:*** *Secretory cells are PAX8 positive.* ***C:*** *Merging of nuclei marked with DAPI and expressing Pax8.* ***E:*** *The expression of CK7 confirm that organoids are composed only of epithelial cells.* ***F:*** *The detyrosinated tubulin mark ciliated cells staining specifically the cilia.*

Another interesting aspect observed was the cellular polarization detectable in FI organoids, with nuclei localized to the opposite site of the organoids' lumen. This data provides a hint of the presence of differentiated cells into organoids that scale back the possibility that organoids resemble cystic spheroids generated by proliferating stem cells.

The ability of tumor organoids to recapitulate a primary tumor were analyzed assessing the expression of PAX8, a known marker of HGSOC and cytokeratin 7 (CK7), to confirm the epithelial nature of organoids. The existence of actively proliferating cells was assessed by the presence of Ki67 positive cells *(Fig.24)*.

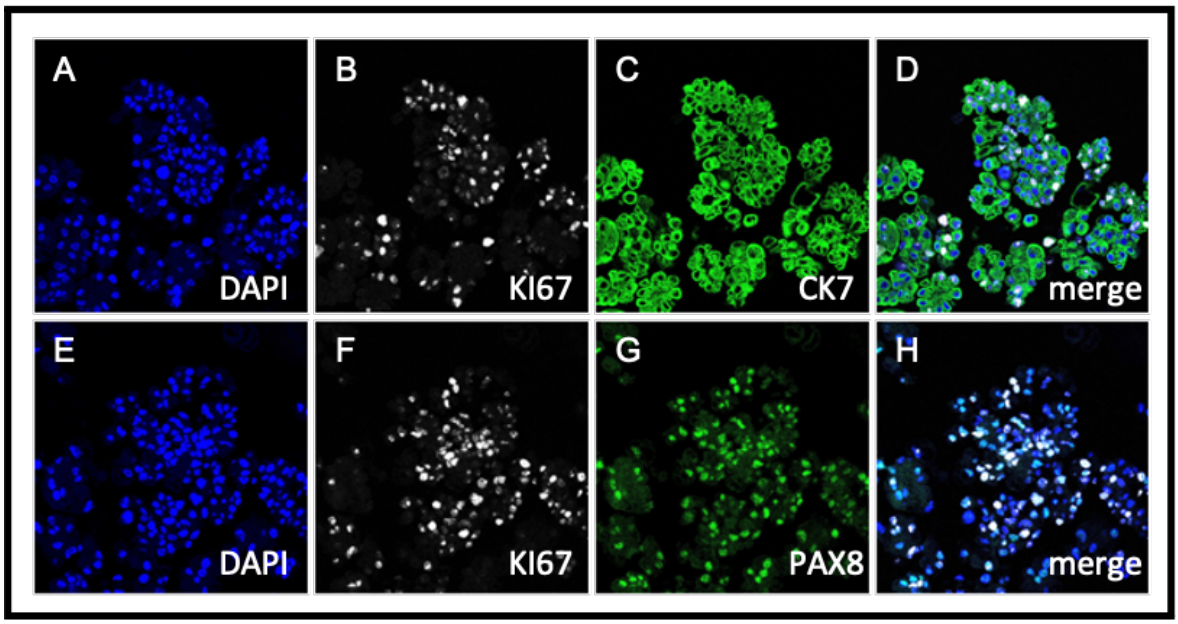

Figure 24. Immunofluorescence staining of tumor organoids.

Expression of tissue specific markers in AS organoids: ***A-E****: Nuclei stained with DAPI.* ***B-F****: Proliferative cells are stained with Ki67.* ***C:*** *Epithelial cells are marked by CK7.* ***D-H:*** *Merging of different staining.* ***G:*** *Organoids express PAX8, a common marker of OC.*

3. Single cell RNA sequencing confirm the ability of organoids to recapitulate primary tissues

To define the cellular composition of organoids and assess their ability to recapitulate primary tissues also at the transcriptomic landscape level, I decided to perform single-cell RNA sequencing (scRNAseq) comparing organoids with primary fresh tissues from which they are derived. scRNAseq has emerged in the last years as a powerful method able to simultaneously measure cell-to-cell expression variability of thousands of genes. Through the detection of genes expressed in each specific cell, this method allows to identify specific cell population within the tissue of interest. This is of particular relevance for those tissues whose knowledge of cellular composition is still unripe and need to be unraveled. Moreover, it is a perfect method to assess the ability of a technology to model the tissue of interest and study its features.

Given the propagability of only normal healthy organoids, the scRNAseq analyses were performed on a cohort of three lines of FI organoids and one line of OSE organoids, comparing them to cells directly isolated from fresh tissues and processed for the scRNAseq pipeline. The platform used for the single cell library preparation was the Chromium of the 10x Genomics and 5000 cells for samples were sequenced on an Illumina NovaSeq.

The data were analyzed by the bioinformatic unit of the lab and, in order to obtain a global representation of the dataset, was applied a non-linear dimensionality reduction visualization algorithm, the UMAP (Uniform Manifold Approximation and Projection for Dimension Reduction) (*136*) to visualize data. This algorithm has been shown to identify biologically meaningful cell clusters that retain consistency across a broad range of parameters variation, such as metric and number of neighbors.

Data plotted as UMAP on the visualization platform used to analyze data, CellxGene Vip (*138*), show that organoids and tissues are well related within each group but have differences that make them to be separated from each other. To find well-connected clusters in networks was used the Leiden algorithm, allowing the identification of 20 different clusters *(Fig.25)*.

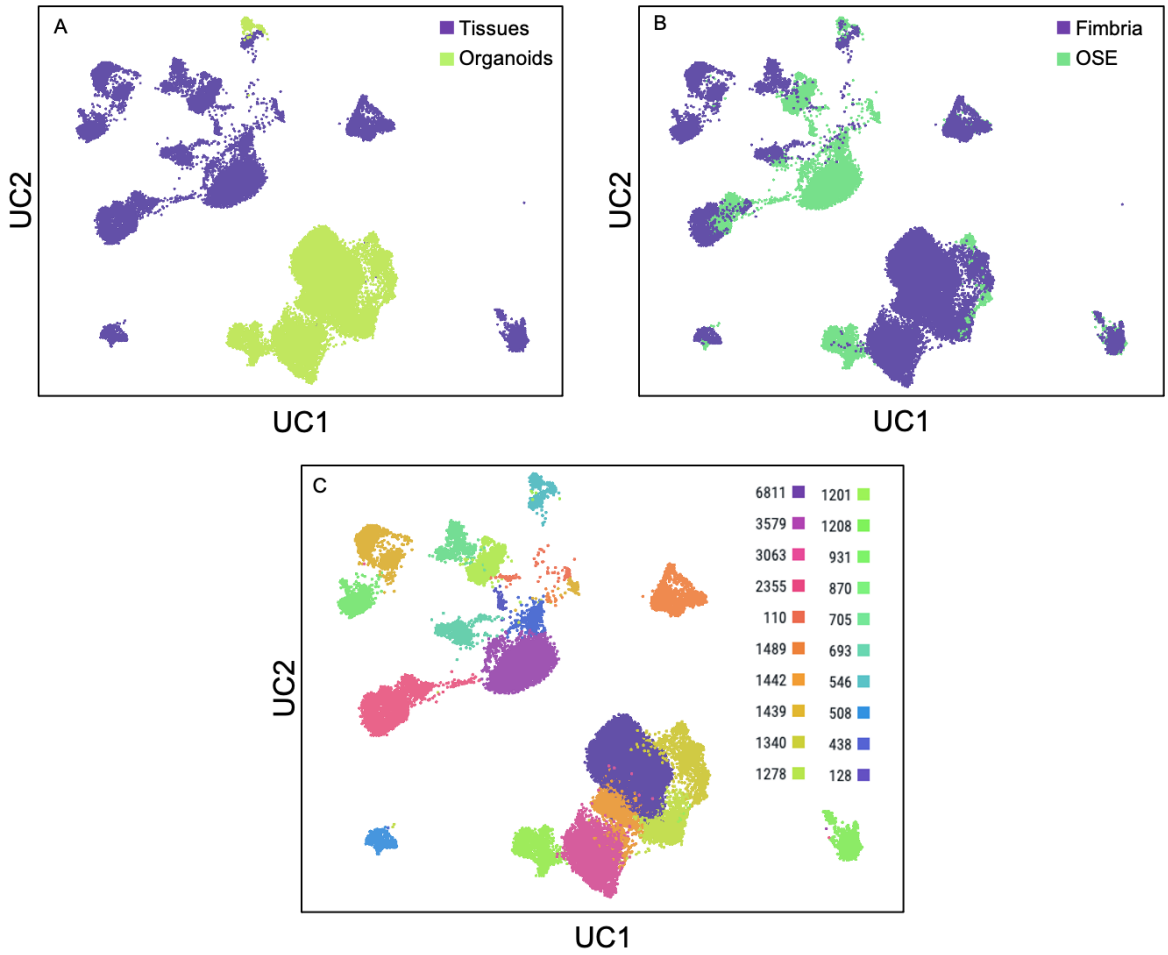

Figure 25. UMAP representation of single cell transcriptomes data.

Each cell is represented by a dot. ***A:*** *Plotting of data distinguished for sample type: violet: tissues cells; green: organoids cells.* ***B:*** *Plotting of data separated for tissue type: violet: fimbria; green: OSE.* ***C:*** *The Leiden clustering allow the identification of 20 different clusters.*

In order to investigate the cellular composition of analyzed tissues, I took advantage of described cell-type specific gene markers (*3*) to define transcriptional signatures to interrogate our dataset.

First of all, I started to look at data analyzing the composition of organoids and primary tissues. The expression levels of the epithelial marker KRT7 and the mesenchymal marker Vimentin show that, as expected, organoids are mainly composed of epithelial cells, while primary tissues present a mix of mesenchymal and epithelial cells *(Fig.26)*.

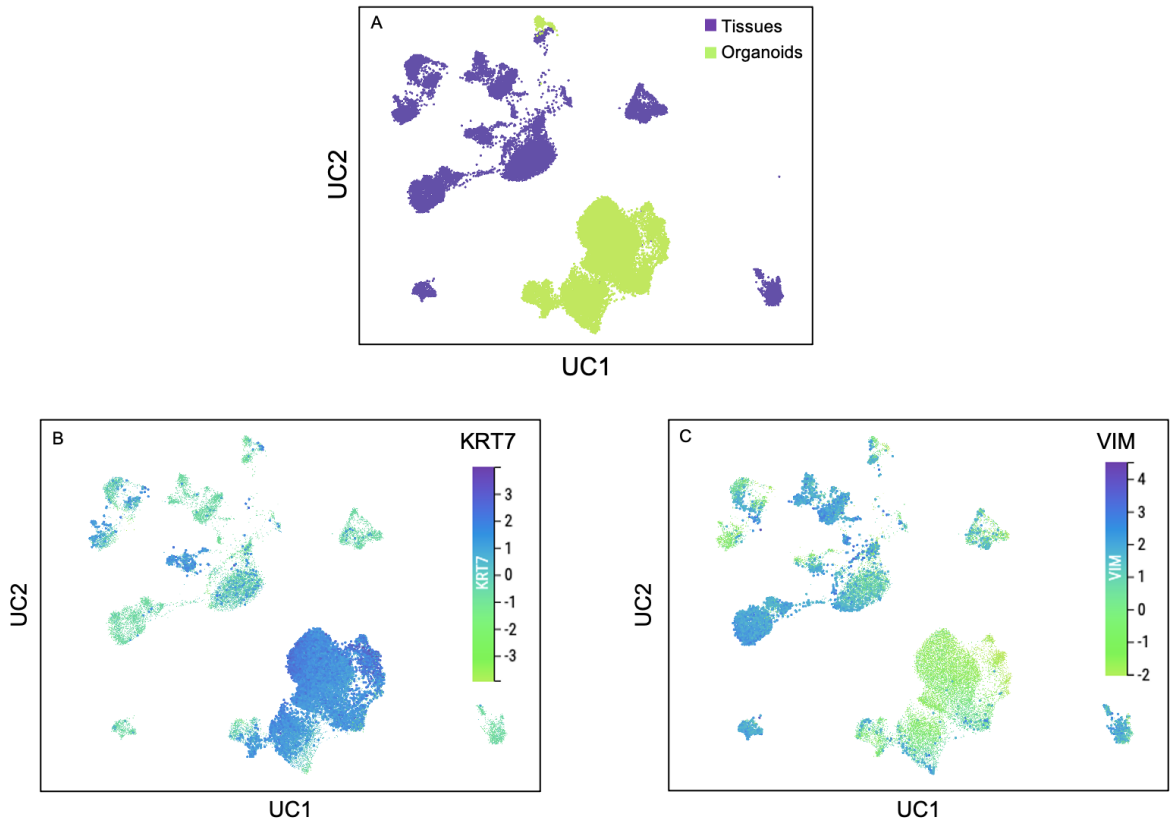

Figure 26. Organoids are mainly composed of epithelial cells

Analyses of epithelial and mesenchymal gene markers ***A:*** *Recap of sample types: violet: tissues cells; green: organoids cells.* ***B:*** *Expression of the epithelial marker cytokeratin 7 (KRT7) confirm the epithelial composition of organoids and highly present in primary tissues.* ***C:*** *The expression of the mesenchymal marker Vimentin (VIM) is mainly present in primary tissues respect to organoids.*

At this point, I started to investigate the presence of contaminating/infiltrating cells, looking for common markers of blood cells and endothelium. As expected, conversely from the primary tissue samples, organoids do not present contaminant hematopoietic, immune and endothelial cells, as shown by the lack ok expression of CD45, CD8A, CD14, TEK and VWF markers *(Fig.27)*.

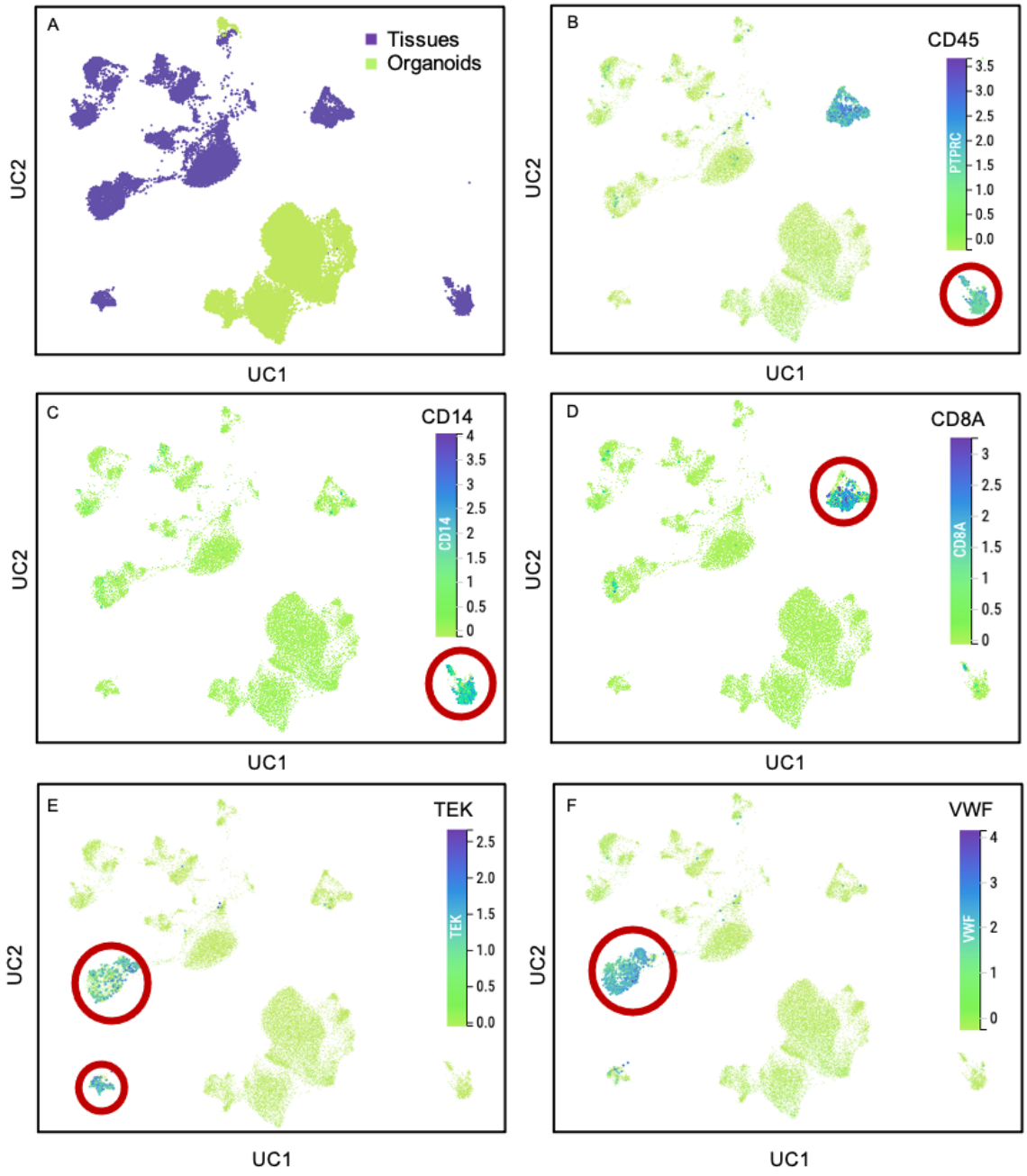

Figure 27. Organoid samples do not present contaminant hematopoietic, immune and endothelial cells.

Analyses of specific gene markers ***A:*** *Recap of sample types: violet: tissues cells; green: organoids cells.* ***B:*** *Expression of the hematopoietic cells' marker CD45.* ***C:*** *CD14 expression allow to identify macrophages.* ***D:*** *The CD8A expression is used to mark cytotoxic T-lymphocytes. Conversely from primary tissues, organoids lack of cells expressing these three markers.* ***E:*** *The expression of the Vascular Endothelial marker TEK and* ***F:*** *the endothelial cells megakariocytes marker VWF confirm the absence of endothelial cells in organoids.*

Large-scale single-cell transcriptomic datasets usually contains non-biological factors that can cause changes in the data produced by the experiment defined as batch effects. These batches could derive, for example, from the use of different technologies or by different run of sequencing and such effects can lead to inaccurate conclusions and so their removal is important for data integration.

In my dataset, the distinct nature of the two sample types, the sample processing procedures and the separate set of library preparation and sequencing, strongly support the presence of batch effects, whose correction could improve the quality of the output. For this reason, before I started analyzing data, with the bioinformatic unit of the lab we decided to apply an autoencoder strategy to batch correct and integrate data. Moreover, in order to obtain better integrated data, we decided to remove from the dataset, before the batch correction, all the contaminant subpopulations identified in primary tissues.

3.1 scRNAseq of FI organoids

Before the batch correction, single cells data show that there is a significant distance between organoids and primary tissues *(Fig.28-A)* with only few cells similar between the two sample types and close in the UMAP representation *(Fig.28-C)*. Conversely, after batch correction, the two cell populations data are correctly integrated, with a strong overlap between the two *(Fig.28-B)*.

In the overlapping cells was scored the subpopulation of ciliated cells, characterized by the expression of the two defining markers FOXJ1 and TUBB4 *(Fig.29-B)*. The presence of the ciliated cells subpopulation was a really relevant finding that points to the ability of organoids to recapitulate fimbrial epithelium cellular composition. Indeed, in normal 2D culture the ciliated cells are lost during passages or must be cultured specifically for their growth (*146*), pointing out the advantage of organoids in modelling the tissue. In order to check for eventual overcorrection of data due to the technique, I assessed the retention of the expression level of specific cell population gene markers, starting specifically from the analysis of the ciliated cells overlapping previously of data integration. The presence of ciliated cells also after the batch correction would be an initial hint indicating the good quality of the correction. The analysis of the data after the batch correction show that this cell population is still present and well-integrated between the sample types *(Fig.29-C)*, supporting that the batch correction has not hampered the preservation of cell type purity. However, the presence of a single cell type is not sufficient and only the preservation of several cell types should be considered as a good indicator of the correction' quality.

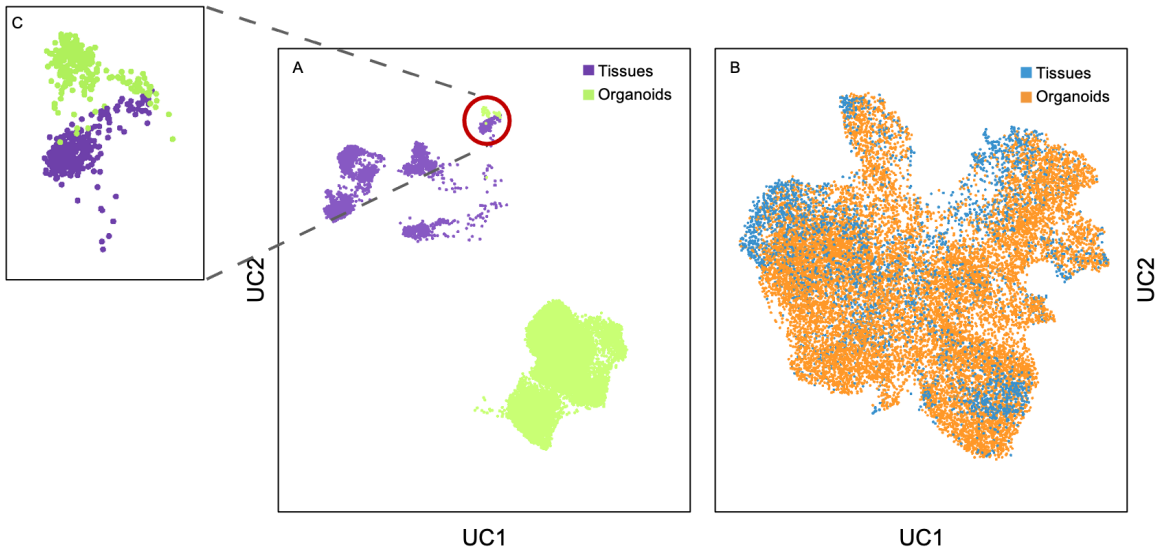

Figure 28. The batch effect correction allows a better integration of data.

UMAP of single cell transcriptomic data of fimbria samples. ***A:*** *Data before the batch correction. Sample types: violet: tissues cells; green: organoids cells.* ***B:*** *Data after the autoencoder batch correction are more integrated than before. Sample types: blue: tissues cells; orange: organoids cells.* ***C:*** *Magnification of the only integrated subpopulation before the batch correction.*

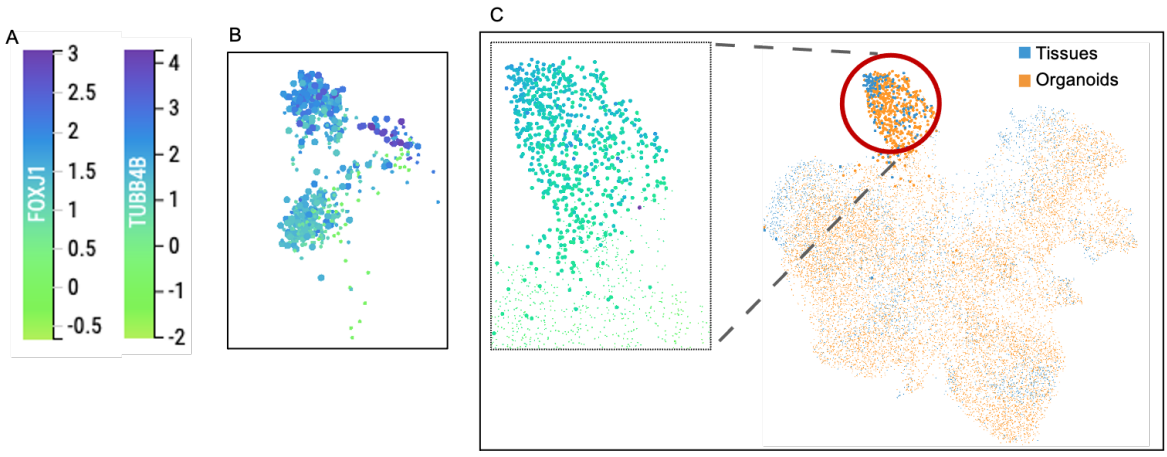

Figure 29. Ciliated cells of the fimbrial epithelium are preserved in organoids culture.

A: *Color scale indicator of FOXJ1 and TUBB4B genes' expression. Cells expressing these two genes simultaneously will be colored in tonality of blue.* ***B:*** *Magnification of the cell population of Fig. 27-C colored for the expression of FOXJ1 and TUBB4B.* ***C:*** *Cells expressing FOXJ1 and TUBB4B after the batch correction are marked in blue (tissue cells) and orange (organoids). In the magnification cells are colored in tonality of blue on the basis of the expression of genes in panel A.*

To confirm initial observation, I checked the presence of the other two well-known cell subpopulations of the fimbrial epithelium, the secretory cells, which are characterized by the expression of PAX8, and basal cells, considered as CD44 positive. Analyzed data showed that $PAX8^+$ cells represent the main population of both organoids and primary tissue *(Fig.30B)*, occupying a well-defined space in the UMAP. Likewise, the basal cells are present in both sample types, with a slight enrichment in organoids, and occupy a distinct area of the UMAP *(Fig.30C)*.

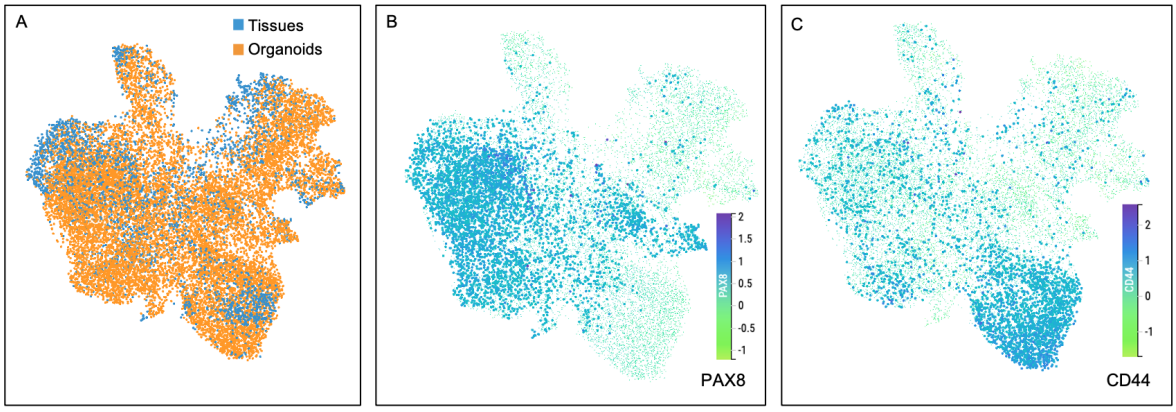

Figure 30. Organoids are composed of both secretory and basal cells.

***A**: Recap of integrated data separated for sample type: blue: tissues cells; orange: organoids cells.* ***B:** Secretory cells expressing PAX8 are marked in tonality of blue.* ***C:** $CD44^+$ basal cells are colored in tonality of blue.*

At this point, in order to identify other cell subpopulations, we decided to cluster cells applying the Leiden algorithm (*140*). The Leiden clustering identified 10 different clusters *(Fig.31)* in which it was possible to easily collocate the three already identified subpopulation. Indeed, cluster 6 is clearly represented by the subpopulation of ciliated cells, as well as cluster 0 and 1 comprise $PAX8^+$ secretory cells and basal cells (identified as $CD44^+$) respectively.

In order to shed light on the composition of the tissue, I performed a differential expression analysis (DEA) between unidentified clusters and the overall population, analyzing the top 100 differentially expressed genes (DEGs) and selecting only ones presenting a LogFC >1. Then, selected genes were subjected to EnrichR analysis in order to identify pathways and Gene Ontology (GO) enrichments.

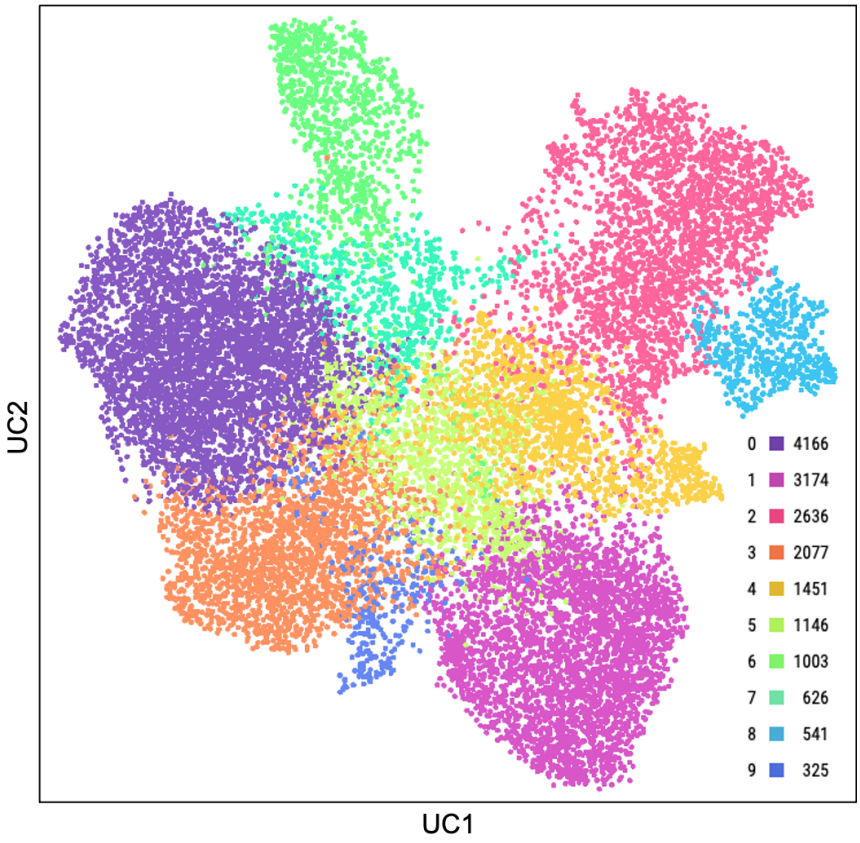

Figure 31. Leiden algorithm on batch corrected data of FI allowed to identify 10 cluster. *Leiden algorithm identified 10 clusters of which clusters 0,1 and 6 represent secretory, basal and ciliated cells respectively.*

I started analyzing the cluster 3 with a DEA that identified 89 DEGs, which relates with the TNF signaling pathways in KEGG and with the inflammatory response (GO:0006954) and the chemokine-mediated signaling pathway (GO:0070098) categories in the GO for biological processes. These results suggest that these cells are related with an immune response, although there is still the lack of particular features that allow their classification as a specific subpopulation.

Then, I performed the DEA of cluster 4 identifying 88 DEGs which correlate for the complement and the coagulation cascades in the KEGG database and for the regulation of pinocytosis (GO:0048548), the phospholipid scrambling (GO:0017121) and the regulation of coagulation (GO:0050818) for the GO biological function and the membrane raft (GO:0030673) for the GO of cellular component. The DEA suggested that this cluster include some kind of plasma cells, that, together with the cells of cluster 3, could be assumed to act as a local secretory immune system of the fallopian tube. Moreover, both cluster 3 and 4 present the expression of secretory markers, identifying their collocation in the secretory cells compartment.

The cluster 5 present 64 DEGs, with enriched estrogen signaling pathway in the KEGG database, but no significant GO enrichment. The involvement in the estrogen pathway could allude that this cell type represents a kind of progenitor cells that under the estrogen signaling could further differentiate in ciliated cells. Indeed, the relationship between the estrogen and the generation of ciliated cells was showed by a recent publication of Zhu and collaborators, in which they observe that the estrogen promoted the differentiation of multi-ciliated cells (MCCs) through estrogen receptor β, following the reduction of DLL1, a ligand of Notch (*147*).

Then, DEA revealed that cluster 7 is characterized by the expression of 67 DEGs (among which KLF2, KLF6, FOS, JUN, EGR1, IRF1, ecc) related with the stimulation of transcription (GO:0045944). This feature could suggest a proliferating progenitor role for these cells, that is also supported by the fact that this cluster is enriched (51%) in cells that are in the S or G2M phase of the cell cycle, similar to $CD44^{+}$ basal cells (47%) and three times more than the remaining population (16%).

Differently from all the others, the cluster 9 did not present any particular distinguishing features that could suggest a possible role for this subpopulation. These cells present a slight expression of hematopoietic genes such as CD45 and could probably be represented from cells that escape the selection and were not excluded before the batch correction.

Finally, cluster 2 and 8 show a similar result in the DEA, which collocates both clusters in the extracellular matrix organization (GO:0030198) GO classification for the biological processes. This particular collocation could lead to the assumption that this cell type is generated by a partial epithelial-mesenchymal transition (EMT). Moreover, cells of these clusters express EMT markers such as VIM, CD105, CD34, Snail, Slug, Fibronectin and Twist *(Fig.32)*.

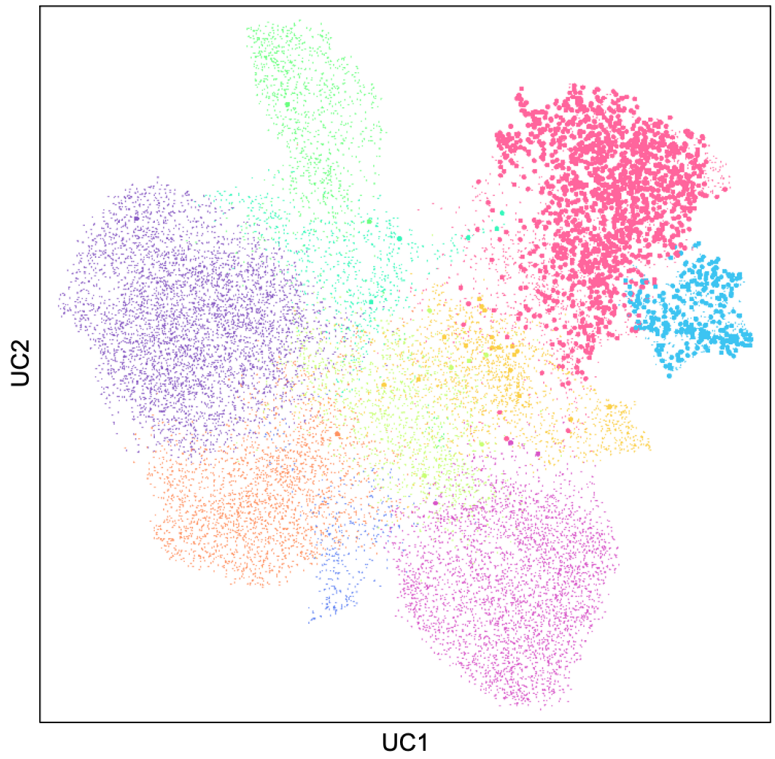

Figure 32. Cluster 2 and 8 present cells expressing EMT markers.

The UMAP shows that only cells of cluster 2 and 8 express the EMT markers VIM, ENG, CD34, SNAI1, SNAI2, FN1 and TWIST2, confirming their plausible EMT phenotype.

At this point, in order to validate the generated data, I took advantage of the recent published paper by Hu and colleague in which was performed a single cells transcriptomic characterization of primary samples of fallopian tube. In the paper the group identified new specific markers for the ciliated and secretory cells but also uncovered clusters of cells likely representing still unidentified subpopulations (*148*).

First of all, I addressed the ciliated cells of our dataset assessing the expression of ciliated markers identified in the paper such as CCDC17, CCDC78, CAPS and TEKT1 (*148*). The expression of these markers confirmed our result *(Fig.33A)*. Then, I did the same with the listed secretory markers, assessing the presence of genes like MSLN, CRISP3, CXCL2, MMP7, CLDN1 and TM4SF1 indicated in the paper. Again, our secretory cells express the indicated markers *(Fig.33B)*.

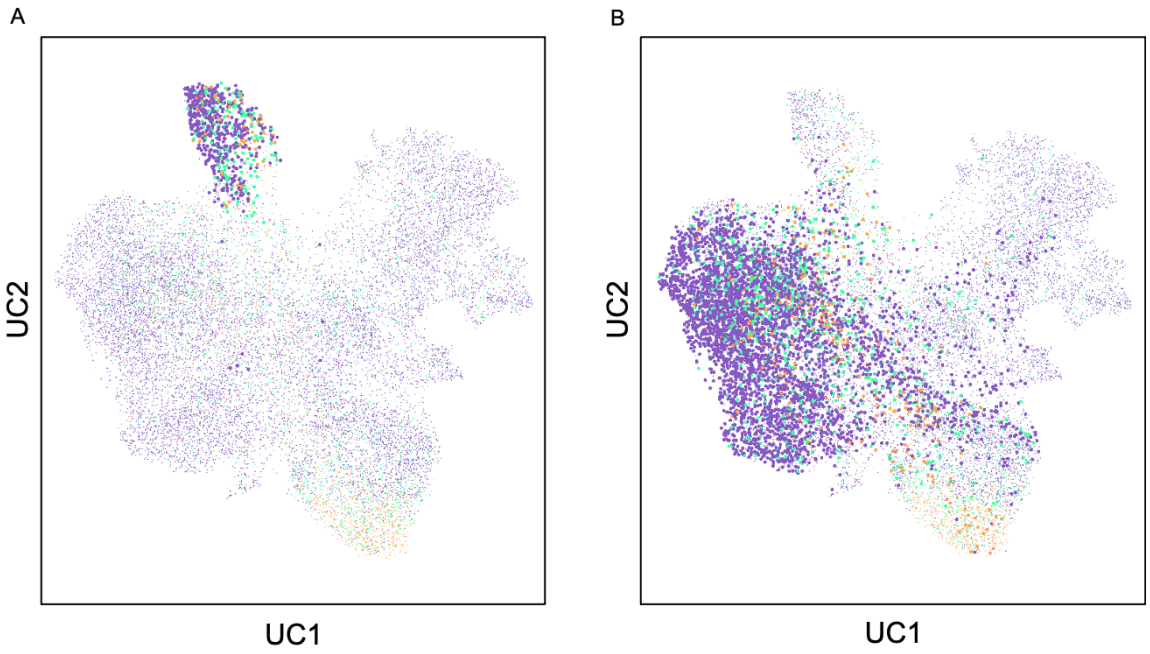

Figure 33. Expression of ciliated and secretory cells markers identified in Hu et al. dataset (*148*)**.**

A: *The UMAP shows cells expressing simultaneously CCDC17, CCDC78, CAPS and TEKT1 genes, defined as marker of ciliated cells. The expression is confirmed in the ciliated cell subpopulation.* ***B:*** *Cells simultaneously expressing secretory markers MSLN, CRISP3 and MMP7. The pattern of expression is confirmed to secretory cells.*

An important aspect of the publication was the identification of specific cell population that cluster together. They identified 9 different clusters of which 5 were discharged for lack of distinguishing features or low library complexity. The remaining 4 were identified as EMT, KRT17, cell cycle and differentiated clusters. Interestingly, the genes classifying the EMT cluster relate in our dataset with cells that we identified as EMT-like committed *(Fig34-A)*.

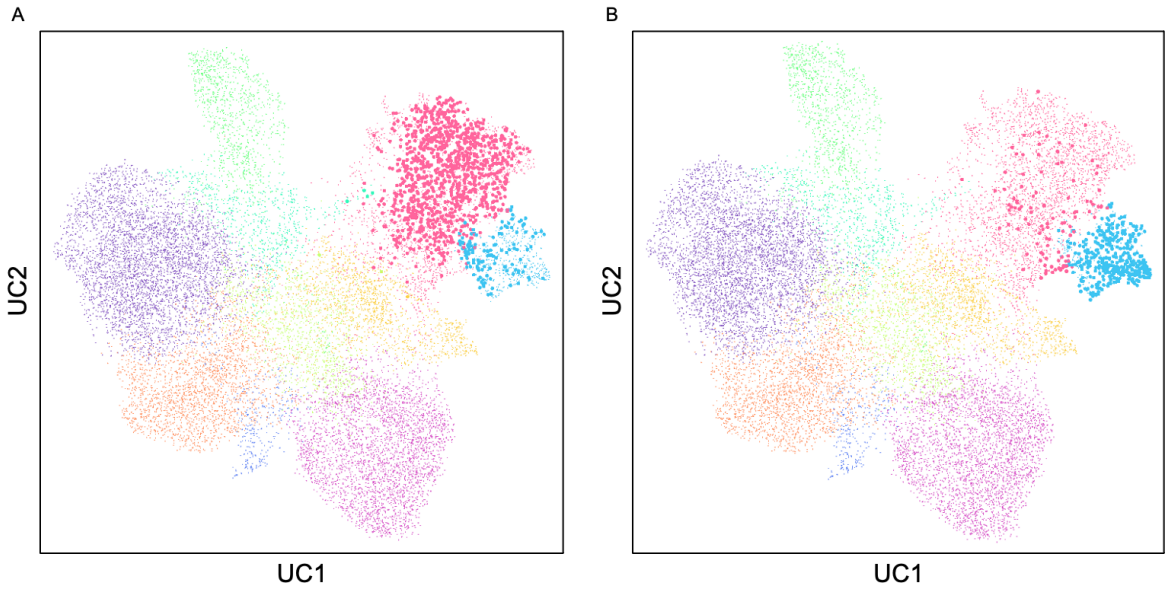

Figure 34. C7-EMT cluster genes from Hu dataset** (148) **are expresses in our data.
***A:** The UMAP shows cells expressing the top 7 genes of C7 clusters ranked for LogFC (ACTA2, TIMP3, TAGLN, TPM2, SPARC, DCN, MFAP4) and present also in our dataset.*
***B:** The expression of COL1A2 and COL3A1, related to stromal cells, is mainly present in cluster 8.*

The overlapping of the two population strongly supports the evidence that our dataset retains the *in vivo* features of the primary tissue and that organoids well recapitulate this tissue of origin. Moreover, in the paper they assessed the expression of the two stromal markers COL1A2 and COL3A1 to distinguish the stromal cells of the fimbria and the EMT subtype. When I performed the same analysis on my data, I observed that these two markers are mainly express in the cluster 8 rather than cluster 2, providing an additional classification of our dataset clusters *(Fig.34-B)*.

Then, I assessed the expression of genes of other clusters in my dataset and I observed that the C9 cell cycle cluster is totally absent in our dataset, since listed genes are not expressed neither from organoids nor from primary samples. Probably, differences in the sensitivity of the two sequencing methods (SMART-Seq vs Chromium 10X) hampers the detection of the same genes.

For the C3 cluster, which is defined as the differentiated cluster, I noticed that it does not fall in a specific cluster in our dataset but cells expressing those genes are spread around the UMAP, with genes detected in secretory cells, ciliated cells and in the EMT-like cluster. Interestingly, the $CD44^{+}$ cells did not express genes of the differentiated cluster, an important aspect supporting the hypothesized role of these cells to act as stem cells.

Moreover, the CD44^{+} are enriched for the expression of genes (we selected the top 6 genes ranked for LogFC and present in our dataset: JUN, FOS, TXNIP, GADD45B, SOCS3, SPRY1, MYC) of the C6 cluster, which in the paper is identified as the cell stress cluster and removed from the further analysis. This aspect is relevant because the cells expressing genes of the C6 cluster are also the one that show proliferation in our dataset, given the presence of cells in the G2M phase of the cell cycle *(Fig.35)*. This should suggest that probably the lack of the analysis of the CD44 gene in the published dataset hamper their detection of this important population.

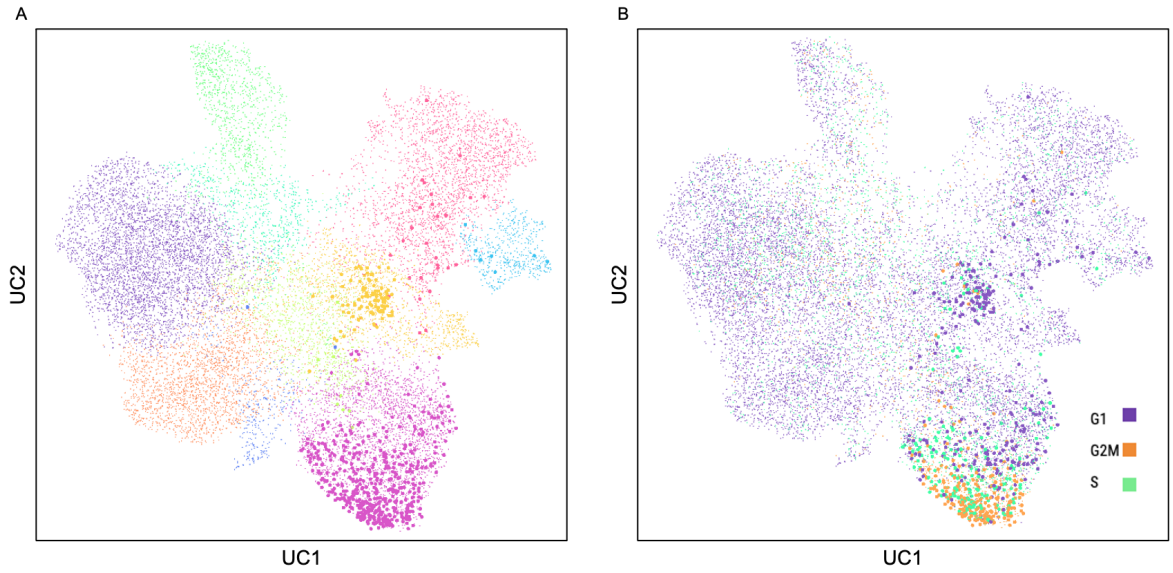

Figure 35. Proliferative basal cells are related to the C6 cluster (cell stress) of the Ahmed' lab dataset (*148*)**.**

A: *Cells expressing the C6 cluster genes of the published dataset relates with the basal cells of our dataset.* ***B:*** *Cells highlighted in panel A are mainly present in the G2M phase of the cell cycle.*

Furthermore, the C4-KRT17 cluster does not find a strict correlation with one of our clusters but some cells of cluster 0 and 1 express the analyzed genes.

Finally, an interesting finding was that genes enriched in the C8 clusters, that was excluded from the analysis in the paper since classified as patient specific inflammatory cluster, were also enriched in cluster 3 and 4 of our dataset, that I found to be related to the inflammatory response. The analysis was performed on the top 5 genes ranked for LogFC and present also in our dataset: CXCL1, CCL2, ICAM1, MT2A and TNFAIP3 *(Fig.36)*.

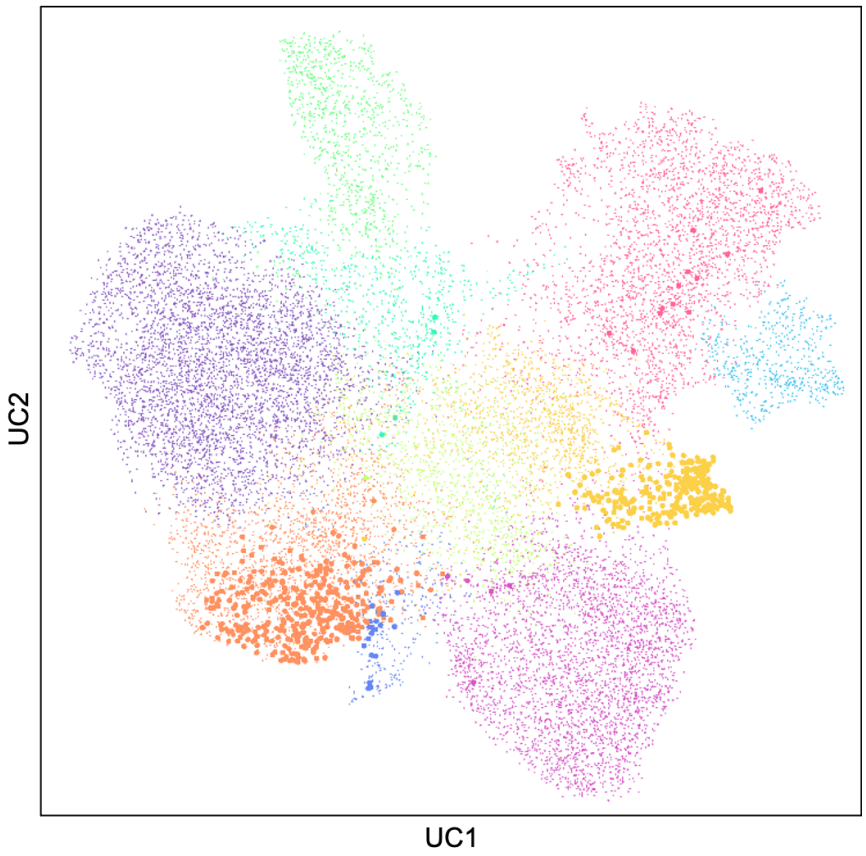

Figure 36. Expression of genes of C8 cluster from Hu et al. (*148*) ***in our dataset.***
Cells of cluster 3 and 4 are enriched for the expression of genes related to the C8 cluster of the published dataset defined as patient specific cluster enriched for inflammatory markers.

At this point, in order to look at data from a different viewpoint and analyze the features of our dataset in its entirety, with the bioinformatic unit we decided to apply another nonlinear dimensionality reduction method and generate a diffusion map. This method is based on a biologically relevant distance metric, the diffusion distance, that allows to preserve the underlying structure of the original dataset. Hence, enabling a meaningful measure of the distances and trajectories intervening across any two given cells, the diffusion map allow the analysis of continuous dynamic processes, such as the pseudotemporal ordering of cells along the differentiation paths, capturing the expected differentiation structure of cells (*137*).

When we plot our cells as a diffusion map, we could see that two different branches starts from a common point that is represented from the cluster 1, the $CD44^{+}$ basal cells, supporting their putative stem role. The two branches ended with the stromal cells and EMT-like cluster on one side and the $FOXJ1^{+}$ ciliated cells from the other side *(Fig.37)*.

This latter result also supports the evidence that ciliated cells are highly differentiated cells of the fimbrial epithelium. The secretory cells are present between the basal cells and the ciliated one and interestingly it seems that cluster 5 and 6 follow a path towards the cluster 6 of ciliated cells. A trajectory inferring analysis will provide further details on this aspect.

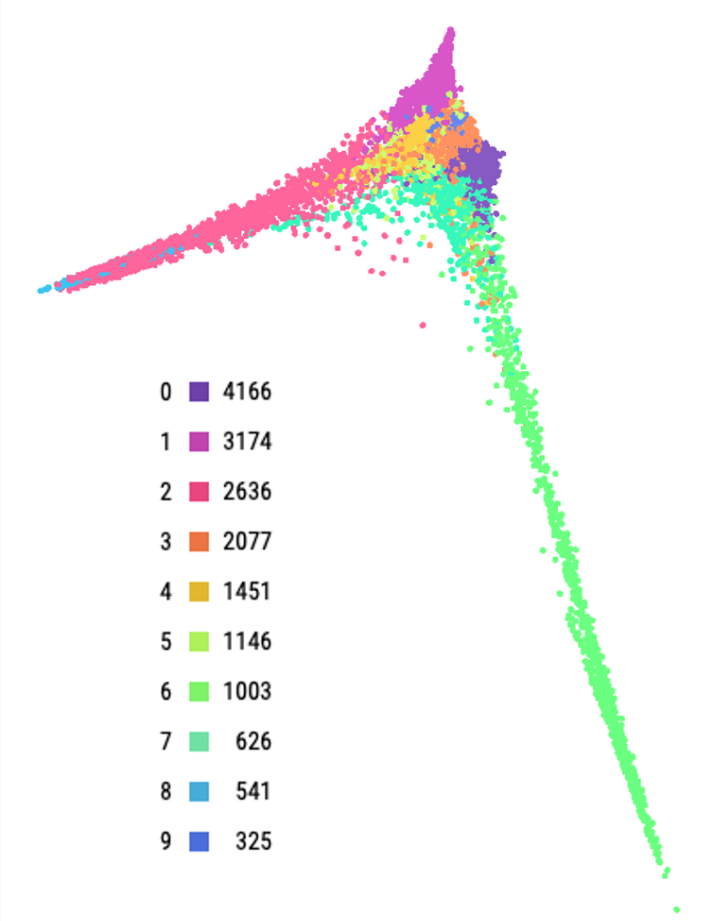

Figure 37. Diffusion map reveals the presence of two branches starting from a common point.

Each cell is a point colored on the basis of its cluster and the basal cells cluster 1, considered as the putative stem cluster, is the starting point of the two branches that ends with ciliated and EMT-like cells respectively.

Finally, I compared organoids and primary tissue in terms of cluster composition, analyzing both our cluster classification and the four clusters of the paper from Hu and colleagues identified in our dataset. The cellular composition of organoids and primary tissue show that the first are enriched in basal cells, an observation that found compliance in the stem nature of organoids, while primary tissue, as expected, present more EMT-like cells, for both cluster 2 and 8 of our dataset and C7 cluster of published datasets *(Fig.38)*.

Another population less represented in organoids is the secretory PAX8^{+} one (cluster 0) *(Fig.38-A)*.

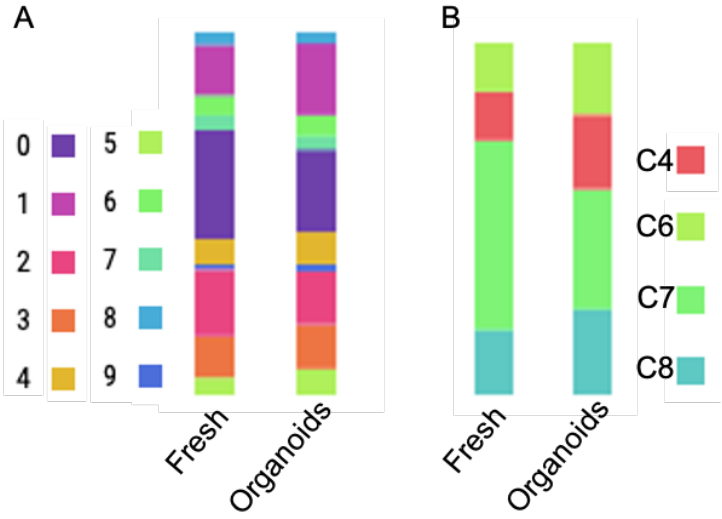

Figure 38. Histogram showing the retention of clusters between primary tissue and organoids.

A: *Retention of clusters in our dataset show that organoids are enriched in basal cells and slightly impoverished of EMT-like cells and secretory cells.* ***B:*** *Clusters derived from Hu and colleague's dataset identified in our data and compared between organoids and primary tissue show an enrichment in organoids of stressed-proliferative cells and KRT17 cluster and confirm a poor presence of EMT-like cells.*

3.2 scRNAseq of OSE organoids

Similarly for the fimbria samples, we performed the batch correction in order to achieve a better integration of the data. Albeit the batch correction, when we plotted data as a UMAP we could see that there is still the presence of two distinct populations that, however, now comprise both organoids and primary tissue cells *(Fig. 39)*.

Before proceeding with the analysis, I first started analyzing the expression of the main marker of OSE cells, the Calretinin Binding protein 2 (CALB2), which is well expressed in both primary tissue and organoids of two populations, confirming the retaining of this marker in organoid samples *(Fig.40)*.

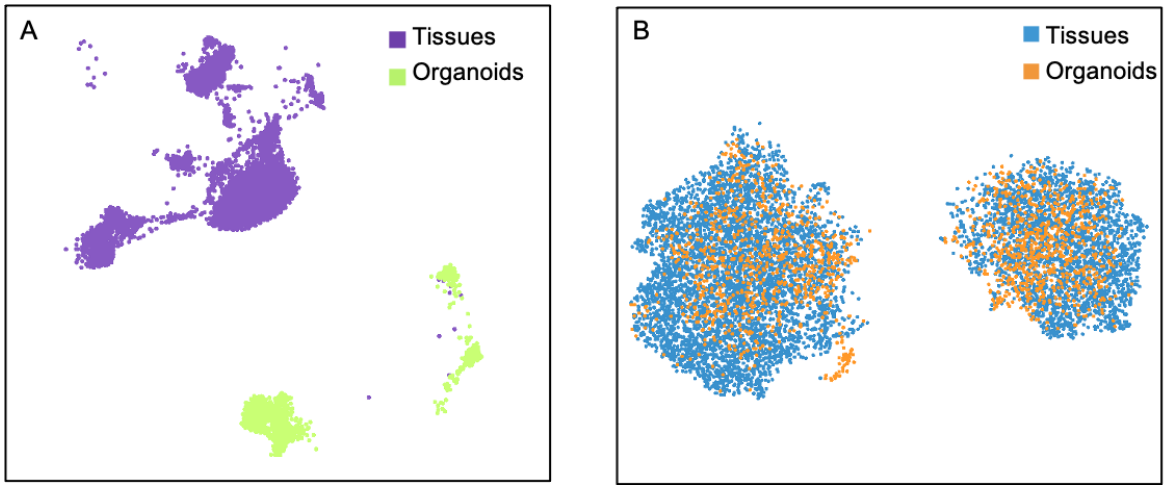

Figure 39. Batch correction integrates cells among sample type but leave the presence of two distinct subpopulations.

Single cell transcriptomic data of OSE samples are showed as UMAP. ***A:*** *Data before the batch correction. Sample types: violet: tissues cells; green: organoids cells.* ***B:*** *Data after the autoencoder batch correction are integrated between samples type but are segregated in two populations.*

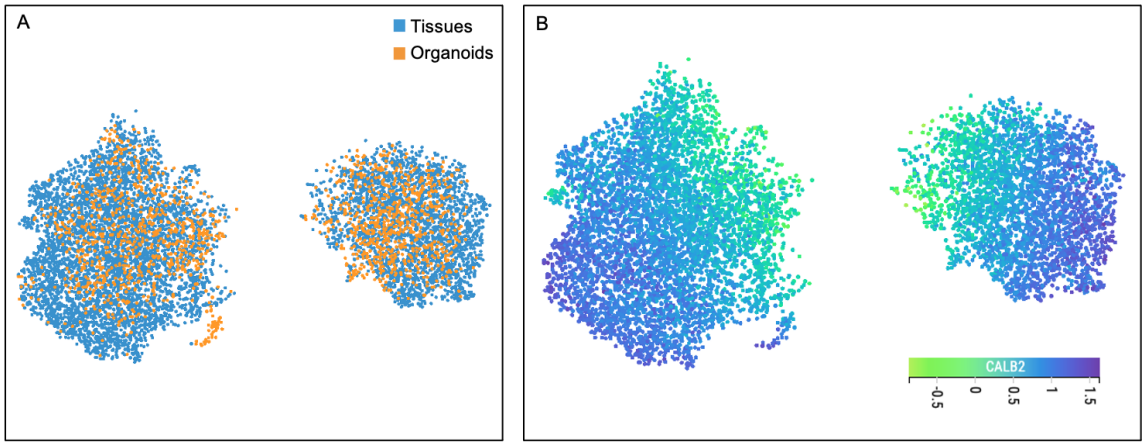

Figure 40. OSE organoids retain the expression of the OSE marker CALB2.

A: *Recap of integrated data separated for OSE sample type: blue: tissues cells; orange: organoids cells.* ***B:*** *The expression level of CALB2 is showed in tonality of blue.*

At this point, given the lack of other well-known markers of OSE, I started addressing the presence of putative stem cell markers. Among the recognized stem markers expressed by OSE cells, in our dataset I found the expression of only SFRP1, LHX9 and ALDH1A2.

These markers are well expressed in a portion of both organoids and primary samples of the two subpopulations, but they did not allow to shed light on the composition of the two distinct subpopulations *(Fig.41)*.

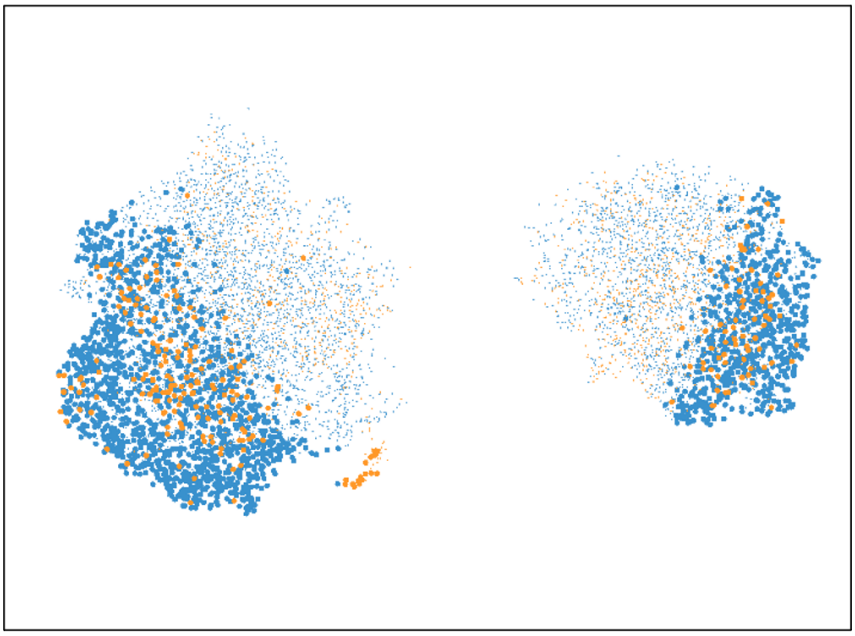

Figure 41. Stemness markers are expressed in organoids and primary tissue of both subpopulations identified in the UMAP.
Cell expressing marker of stemness are highlighted in violet (primary samples) and orange (organoids).

At this point to understand the differences among the two subpopulations I performed a DEA between the two, identifying 61 DEGs with a LogFC>1, that however did not present any particular distinguishing features. Indeed, when listed in EnrichR relates with the Apelin signaling pathway in the KEGG database and the glycerolipid biosynthetic process (GO:0045017) in the GO for biological processes. The DEA unfortunately did not provide any major insight into the data and composition of the two clusters and other samples will be sequenced to shed light on the aspect.

4. Genetic manipulation of FI organoids to induce in vitro tumorigenesis

The possibility to genetically manipulate organoids and use them as a novel *in vitro* model of tumorigenesis that can recapitulate both early stages and progression of the tumorigenic process was of great impact (*126*, *149*). The ability to generate healthy FI organoids recapitulating the primary tissue raised the possibility to manipulate this model and exploit it to study early step of the ovarian cancer tumorigenic process in a normal context, generating what we defined in the lab as induced Tumorigenic Organoids (iTOs). Moreover, the possibility to use this approach on normal FI organoids was showed by Kopper and colleagues, genetically manipulating organoids both through the use of CRISPR/Cas9 and lentiviral infection (*10*).

Taking in consideration the dual origin of the OC, the idea was to study the early stages of the tumorigenic process in a cell of origin-specific way. However, given the requirement for a long-term expandable model and the low efficiency in the generation of OSE organoids, all the efforts were put on the manipulation of FI organoids. The vector designed for the experiment foresees a Tet-On 3G system with the constitutive expression of a nuclear mRuby3, to mark in red the nuclei of cells, and an inducible expression of a farnesylated mNeonGreen upon the addition of doxycycline or tetracycline. The expression of mNeongreen could be coupled with the expression of a shRNA if it is cloned inside the miRE region of the vector.

Despite the experimental design is already decided, experiment plans were not completed, although the set up for the lentiviral infection of organoids was already done.

4.1 Lentiviral infection of HEK293T

The benchmarking of the vector was done on HEK293T cells. Cells were infected and after two days was assessed the expression of mRuby3. Once confirmed, 0.2µg/ml of doxycycline were added and the mNeongreen expression was evaluated after 48 hr of exposition. The Fig. 42 show HEK293T cells with red nuclei and green membrane, confirming the efficiency of the vector.

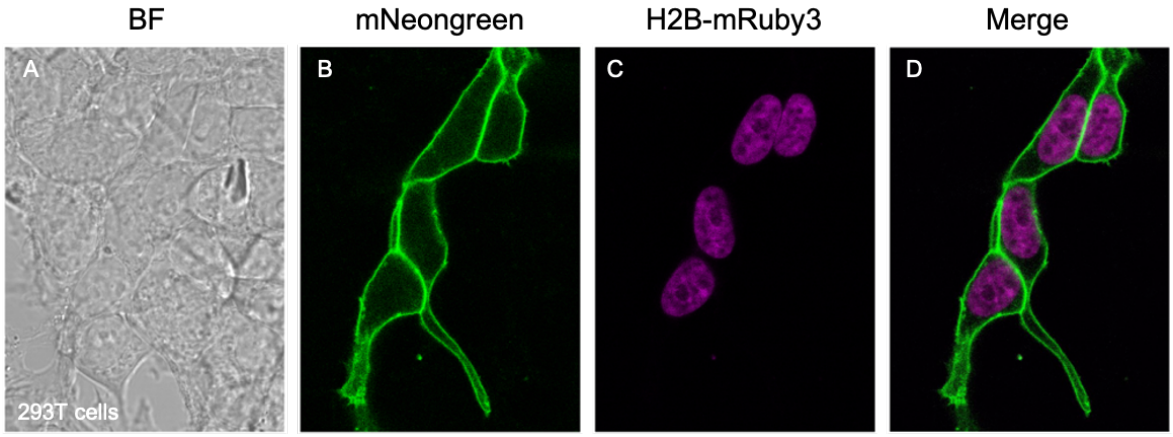

Figure 42. Benchmarking of VB1021msk vector on HEK293T cells.

A. *Brightfield picture of HEK293T cells.* ***B.*** *Induction of the mNeongreen expression after 48 hrs of Doxycycline exposition.* ***C.*** *293T nuclei expressing H2B-mRuby3.* ***D.*** *Merging of B-C.*

4.2 Lentiviral infection of organoids

Once confirmed the efficiency of the vector, we analyzed the possibility to infect and manipulate normal organoids. The idea is to obtain organoids with a mosaic infection, where only few cells in the whole organoids are infected, in order to recapitulate the transformation of a cell in a normal context and study how it could be able to drive the tumorigenesis. To obtain this kind of infection it is better to infect cells directly when organized as organoids and not when cultured in 2D. The tumoral progression of targeted cells is planned to be followed both by imaging and single cells sequencing *(Fig.43)*.

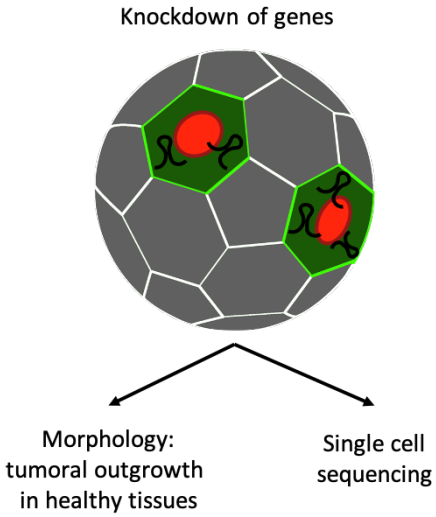

Figure 43. Schematical representation of the lentiviral infection of organoids.

Through imaging I will take advantage of the clear morphological differences already benchmarked between normal and tumor tissues to follow the tumoral outgrowth in the healthy tissue. Conversely, the introduction in the cells of an exogenous gene, the H2B-mRuby3, allows their identification by scRNAseq and the analysis of the transcriptional changes occurring. Moreover, the scRNAseq allows to inspect also the transcriptional alterations induced in normal cells as the result of the interaction of tumor cells with the surrounding normal environment.

The infection of normal FI organoids was carried out on 3D organoids after 3 passages *in vitro*. The lentiviral infection efficiency was low but allows to generate organoids with spot of targeted cells (with red nuclei) that, upon the addition of doxycycline, express also the green on the membrane and so could express specific shRNAs to induce the tumorigenesis *(Fig.44)*.

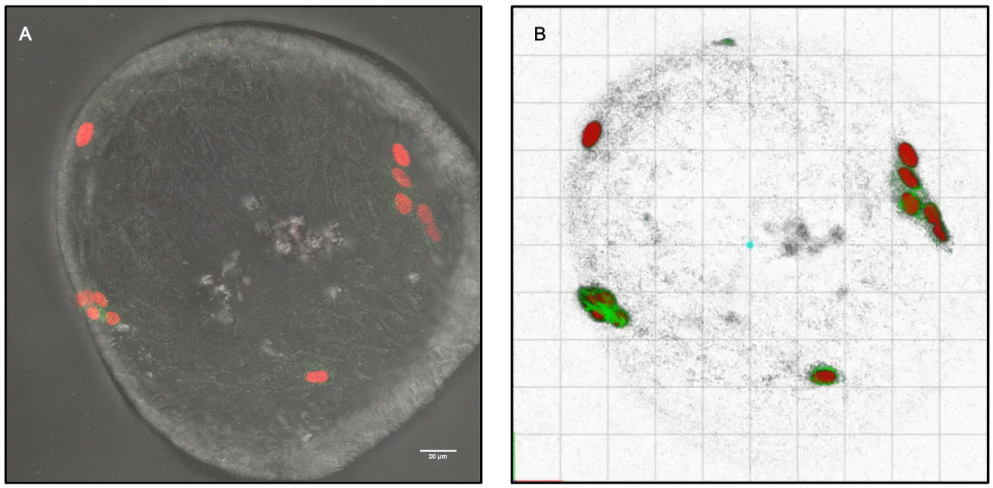

Figure 44. Organoids infected with the lentiviral vector VB1021msk.

A. *Brightfield picture of organoids show spot of infected cells.* ***B.*** *3D reconstruction of infected organoids after doxycycline induction to highlight the mNeongreen expression.*

In order to perform the complete experiment, we still need to improve the virus production efficiency and have a higher lentiviral titration. Moreover, we still need to refine the final list of genes and pathways to be targeted to induce the tumorigenesis.

5. PAX8 as a driver of OC tumorigenesis

Among all genes normally known to be of relevance for OC, *PAX8* plays a relevant role, given its historical record as a defining marker for HGSOC (reviewed in *150*). However, interestingly not all HGSOC samples express PAX8 and recently we addressed this aspect determining whether this could be related to the cell of origin of the disease (*12*) since its expression is shared with the fimbrial epithelium but not with the OSE. We found that PAX8 remains differentially expressed between FI-like and OSE-like tumors, thus recapitulating the expression pattern from the tissues of origin and, moreover, differentially methylated among FI and OSE samples and, also, between FI-like and OSE-like tumors, in an anti-correlative fashion with gene expression, confirming the findings (*12*).

Given these aspects and its putative relevance for OC tumorigenesis (although for the FI-like specific subtype), it becomes interesting to study *PAX8* and its interactomes, in order to detect pathways and identify possible molecules to be used in the culture medium of OC organoids to improve the propagation efficiency. Moreover, since PAX8 mostly binds at non-promoter sites and is enriched at super-enhancers, where it can globally regulate genes involved in tumorigenesis (*151*), and given its relationship with the FI-like subtype, it is also a suitable gene to be studied to identify targets to test thorough the genetic manipulation of FI organoids.

Despite its importance and multiple roles, nowadays commercially available antibodies for PAX8 are still not specific, recognizing also other homologous genes members of the PAX family (*152*). For this reason, in the lab we decided to use a different approach to study PAX8, in order to avoid the possible cross-reactivity of antibodies. We decided to use the Halo-Tag to specifically target the genes. HaloTag is a self-labeling protein tag of 297 residue peptide (33 kDa), designed to covalently bind to a synthetic ligand. This feature allow to perform numerous applications including protein purification, protein:protein or protein:DNA interactions, cellular imaging and more, without the use of antibodies. This system offers us an efficient alternative to the standard chromatin immunoprecipitation (ChIP) method, bypassing the antibodies limit described above. To isolate proten:DNA interactions, the HaloTag is fused to the protein of interest and then crosslinked to DNA with formaldehyde and captured on a specific resin, which forms a highly specific, covalent interaction with the HaloTag portion of the fusion protein. Then, upon the de-crosslinking is possible to purify the captured DNA fragment and perform the sequencing.

To perform this analysis, I choose to use OC cell lines, in order to avoid problems of cells number availability and use a simpler system than primary cells to be edited.

5.1 Selection of cell lines and PAX8 expression analyses

Among available cell lines, the choice fall on lines most likely recapitulating HGOSC, on the basis of the classification drown up by Domcke and colleagues (*34*) *(Fig.8)*.

I decided to select three cell lines expressing PAX8 and three not expressing it. Moreover, 1 FI and 1 OSE non tumorigenic lines were chosen as controls. Selected cell lines were:

- Kuramochi, OVSAHO and NIH-OVCAR3 as PAX8 positive ($PAX8^{+}$)
- TYK-Nu, OV90 and OV7 as PAX8 negative ($PAX8^{-}$)

The expression level of PAX8 was checked in the Broad Institute Cancer Cell Lines Encyclopedia (CCLE) comparing the RNA expression levels of PAX8 by two datasets, generated by Affymetrix and RNA sequencing *(Fig.45)*. Only OV7 were not analyzed in the paper but chosen given their level of PAX8 expression. Other low PAX8 expressing cell lines were discarded since classified as unlikely HGSOC.

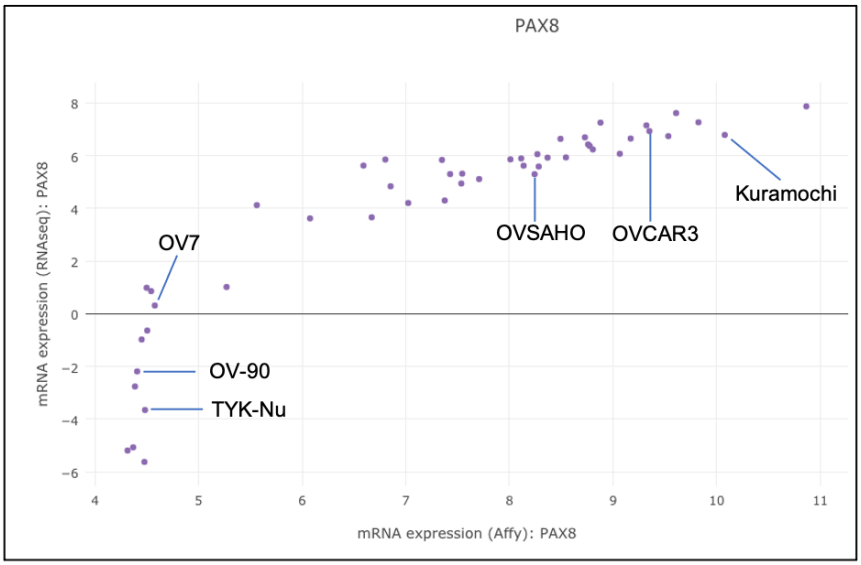

Figure 45. PAX8 RNA expression levels in different OC cell lines reported in the CCLE.

Once correctly identified, cell lines were cultured and the expression of PAX8 was analyzed at the protein level through both western blot analysis and immunofluorescence staining.

Western blot against PAX8 shows that the protein expression follows the mRNA expression levels, with Kuramochi, OVCAR3 and OVSAHO expressing PAX8 and OV-90, OV7 and Tyk-Nu lacking its expression *(Fig.46A)*. The immunofluorescence confirms the data seen by western blot *(Fig.46B)*.

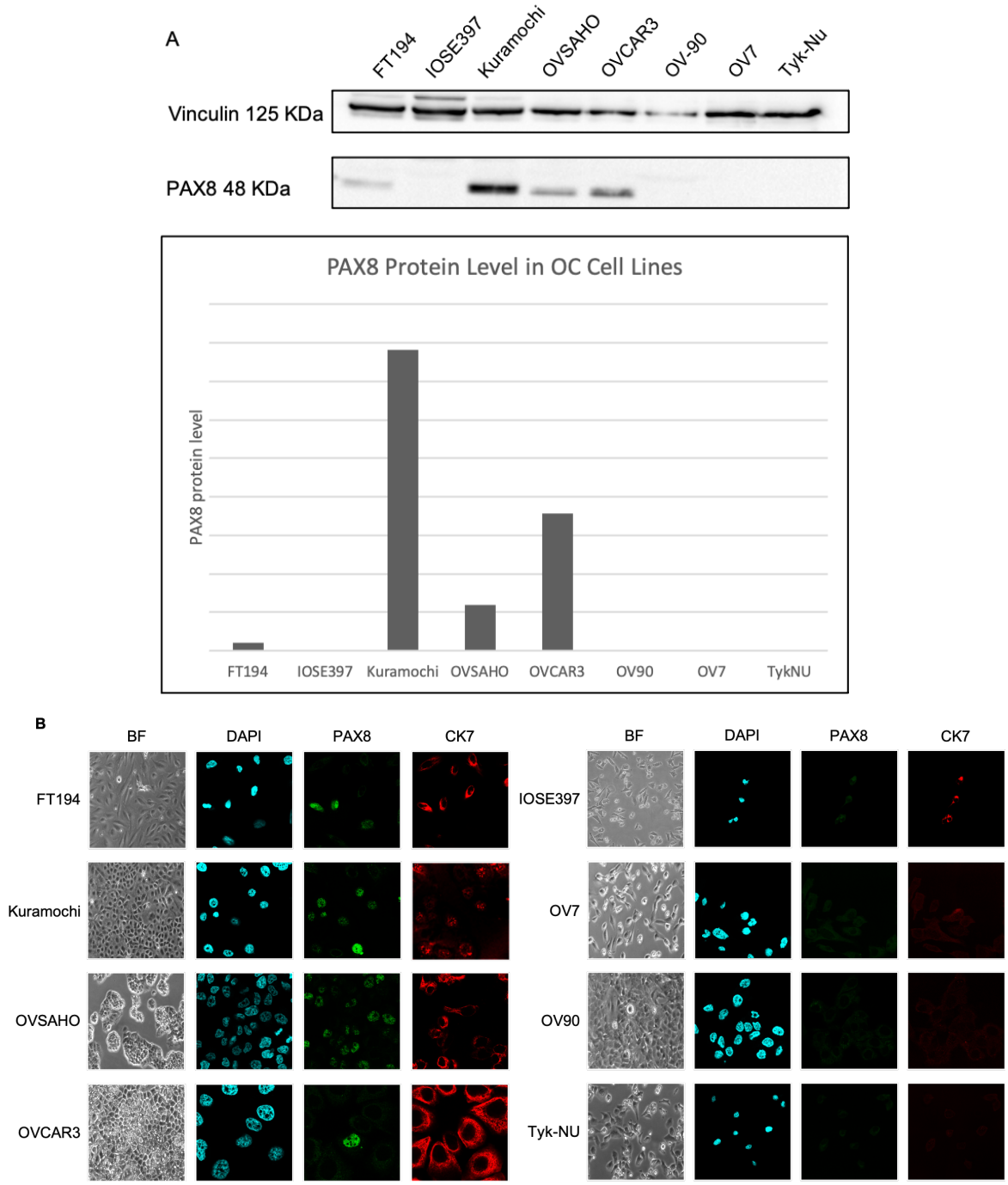

Figure 46. Analysis of the PAX8 protein expression levels in selected OC cell lines.

A: *In the upper panel is showed the western blot of PAX8 while in the lower panel the pixel intensity quantification is represented as histograms. Data show that only PAX8$^+$ cell lines express PAX8.* ***B:*** *Immunofluorescence staining against PAX8 and CK7. The staining confirms the PAX8 protein expression in PAX8$^+$ cell lines.*

Upon the confirmation of the PAX8 expression, PAX8$^+$ cell lines underwent CRISPR/Cas9 editing for the fusion of the HaloTag protein to PAX8.

5.2 HaloTagging of PAX8

The CRISPR/Cas9 gene editing system foresee the electroporation in cells of a synthetic Cas9 protein coupled with the gRNA and the donor plasmid vector. Before performing the experiment, PAX8$^+$ cell lines that must undergo CRISPR/Cas9 editing where tested to find optimal electroporation condition. To do so, cells were electroporated with a GFP expressing vector and after 48 hours inspected to assess the transfection efficiency. The chosen condition for each cell lines (*Table 6*) were the one with the right balance among GFP$^+$ cells and the cells viability *(Fig.47)*.

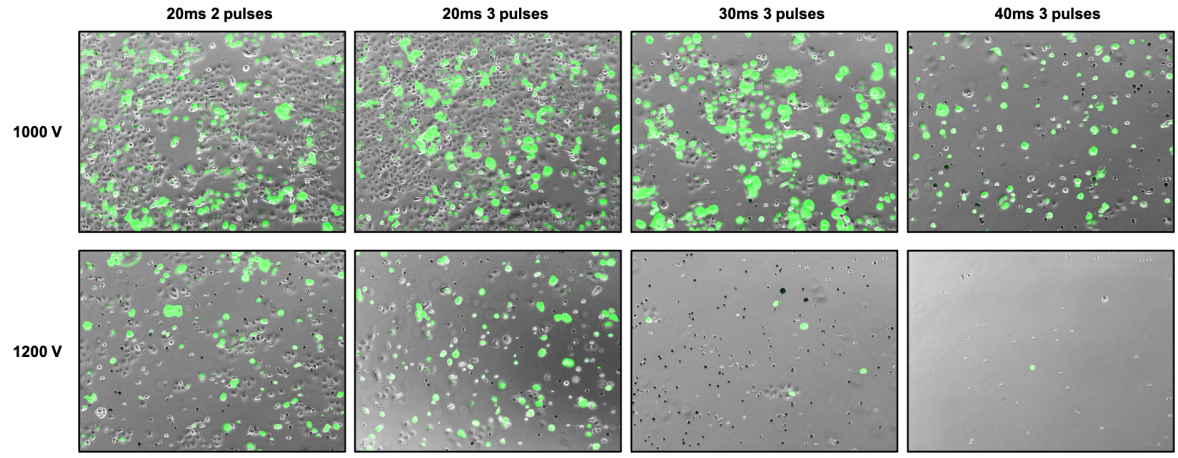

Figure 47. Pictures of NIH-OVCAR3 transfected with pCAG-GFP plasmid.

The GFP expression was evaluated by imaging and 8 different condition were tested. The chosen condition was the one with the higher number of GFP$^+$ cells in relation to the total number of viable cells (1000V, 30ms and 3 pulses).

Once best electroporation conditions were identified, I proceeded with the electroporation of the CRISPR/Cas9 system in all three PAX8$^+$ cell lines. The transfected cells were selected in Hygromycin for 7-10 days or, in case of NIH-OVCAR3 that were hypersensitive to Hygromycin, were selected by FACS sorting after the staining with the TMR fluorescent ligand *(Fig.48)*.

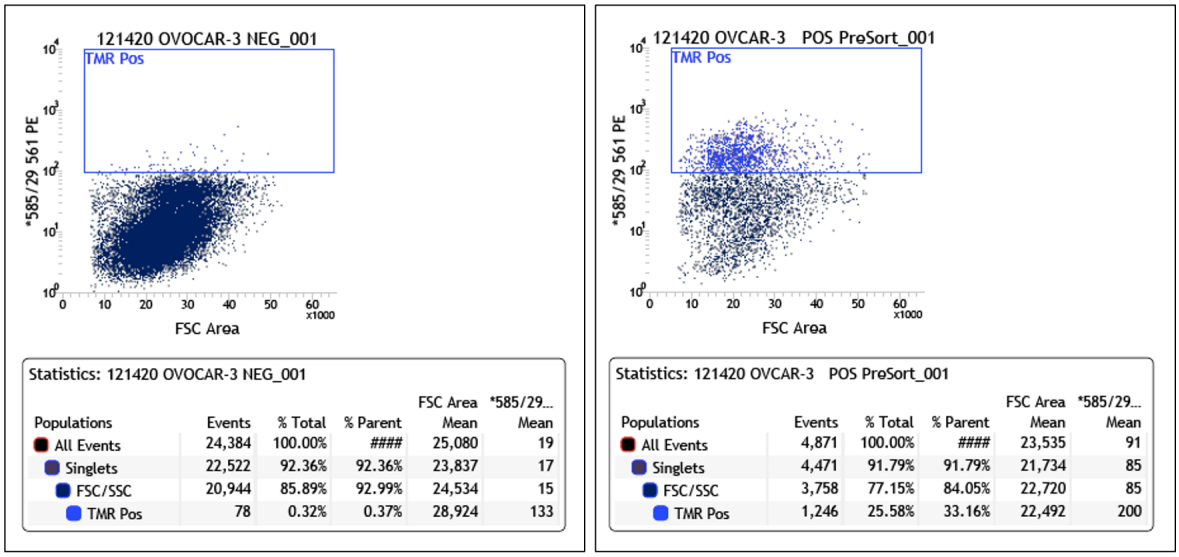

Figure 48. FACS cell sorting of NIH-OVCAR3.

Cells were stained with TMR ligand and then positive cells were sorted. ***Left panel:*** *NIH-OVCAR3 not transfected used as control.* ***Right Panel:*** *26% of CRISPR/Cas9 electroporated NIH-OVCAR3 were positive for TMR.*

The success of the genetic engineering of cells selected in hygromycin was assessed by staining cells with the TMR ligand and analyzing the fluorescence by imaging or FACS *(Fig.49).*

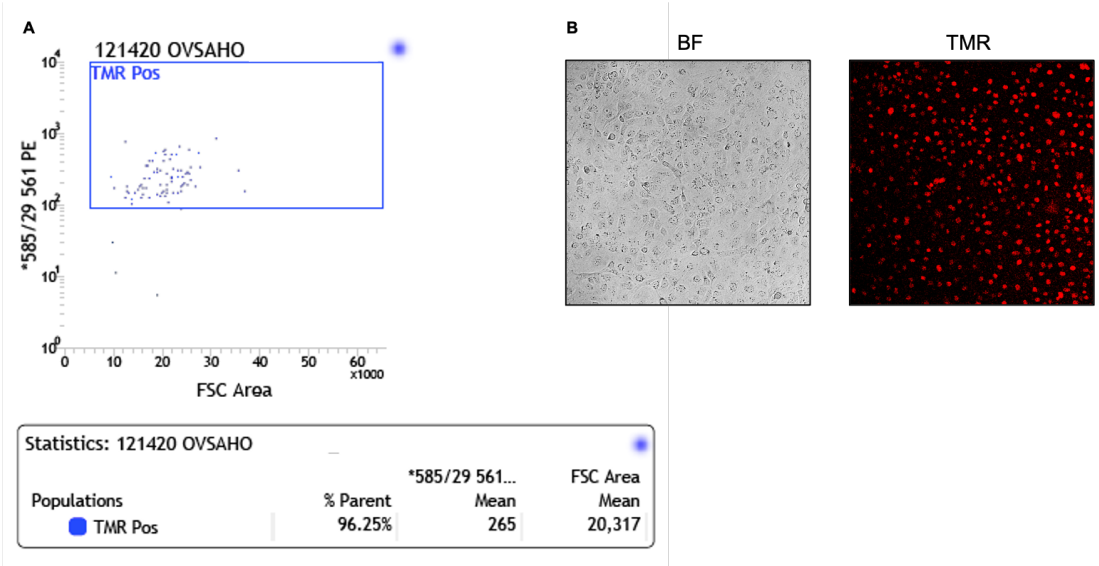

Figure 49. Validation of the positivity of cells selected with Hygromicin.

A: *FACS analysis of OVSAHO confirms the positivity of cells.* ***B:*** *Brightfield and fluorescent TMR staining pictures of Kuramochi cells. The staining confirm the positivity of Kuramochi.*

To validate again the fusion of the HaloTag to the PAX8 protein, I performed a western blot comparing transfected cells and non-transfected controls, using antibodies against both PAX8 and HaloTag. The result confirms the introduction of the HaloTag sequence to the gene *(Fig.50)*.

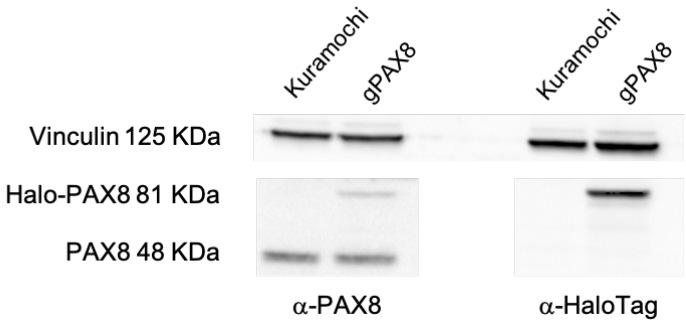

Figure 50. Western Blot validation of HaloTag insertion in the PAX8 gene locus of Kuramochi cells.

Western blot analysis showed that control cells did not present signal at the Halo-PAX8 molecular weight when using both an α-PAX8 and α-HaloTag antibodies. Moreover, in the control there is the lack of signal also at the PAX8 molecular weight when using the α-HaloTag antibody. Conversely, transfected cells react both at the PAX8 and the Halo-PAX8 molecular weight when using an α-PAX8 antibody and the Halo-PAX8 is detected alone when using an antibody α-HaloTag.

At this point, in order to assess the zygosity of the genetic engineering, Halo-tagged cell lines were plated clonally at single cells in 96 well plates and allowed to grow to generate single cell-derived clones. In this way, single cells representing single clones could be tested to assess the presence of the Halo-Tag sequence on one or both alleles. Once expanded enough, colonies were subjected to a PCR screen that detect the presence and the zygosity of the HaloTag.

The screen foresees the use of 3 different couple of primers to map the presence or absence of the HaloTag on alleles. The screen was performed only on Kuramochi cells, from which I derived 48 different colonies. Of 48 colonies, 3 presents absence of insertion or chromosomal rearrangement, 44 were heterozygous and 1 was homozygous. The presence of a signal in 5' and 3' sites indicate the insertion of the HaloTag in at least one allele. The presence in these sites coupled with the absence of signal from the Locus site indicate the homozygosity. The PCR screen displaying the presence of homo- and heterozygous colonies is showed in Fig. 51.

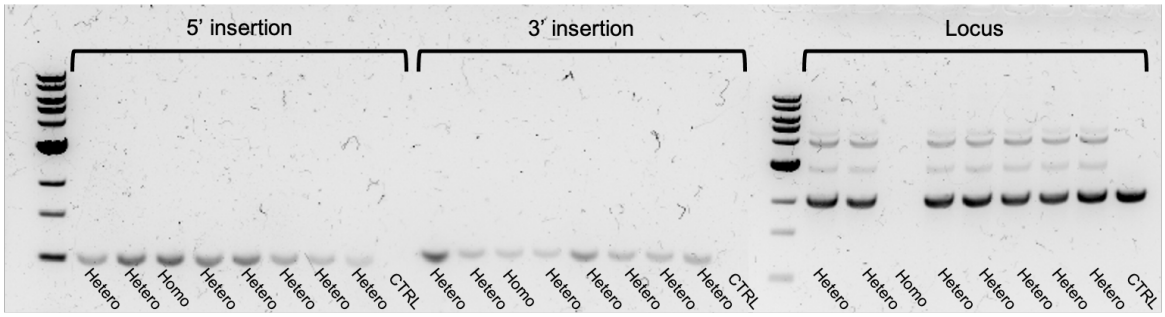

Figure 51. PCR screen of genetically engineered Kuramochi cells.

The presence of HaloTag is indicated by the signal from the 5' and 3' primers. The locus signal indicates the lack of insertion. Signal from all three couples of primer specify a heterozygous clone while the absence of the signal only from the locus indicate an homozygouse clone. The indicated control is represented by non-transfected Kuramochi cells that, as expected, lack of signals from the 5' and 3' insertions while retaining the locus signal.

5.3 HaloChip of Kuramochi

Once the zygosity of clones was identified, I selected both one homo- and heterozygous clone and subjected them to the HaloCHIP system to identify the PAX8 interactome and shed light on pathways and target genes of relevance in the regulation of OC tumorigenesis.

The two selected clones were cultured and once expanded enough the protein:DNA interactions were crosslinked through the exposition of cells to formaldehyde. Then cells were lysed, and the chromatin was sonicated in order to obtain DNA fragments of 500–1,500bp in size. The chromatin smear obtained after the sonication is showed in Fig. 52.

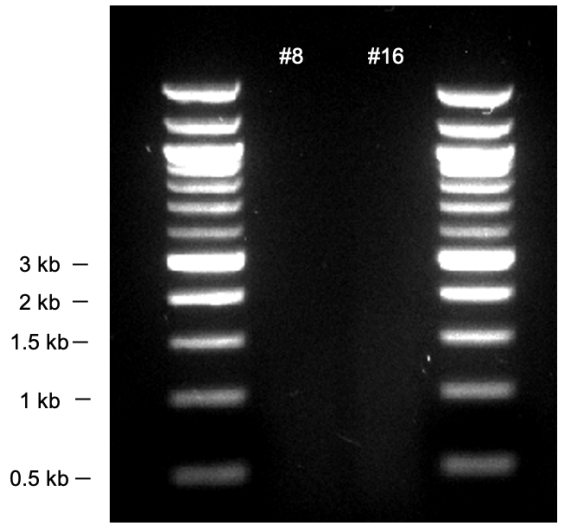

Figure 52. The agarose gel electrophoresis shows the chromatin smear.
A blurred smear is present between 500 and 1500 bp of the two samples.

At this point, the sheared chromatin is incubated with the HaloLink resin and the reacted chromatin is saved, de-crosslinked and purified for the library preparation and subsequent sequencing *(Fig.53)*. Although the HaloChIP was already performed, the bioinformatic analysis of sequencing data are still ongoing.

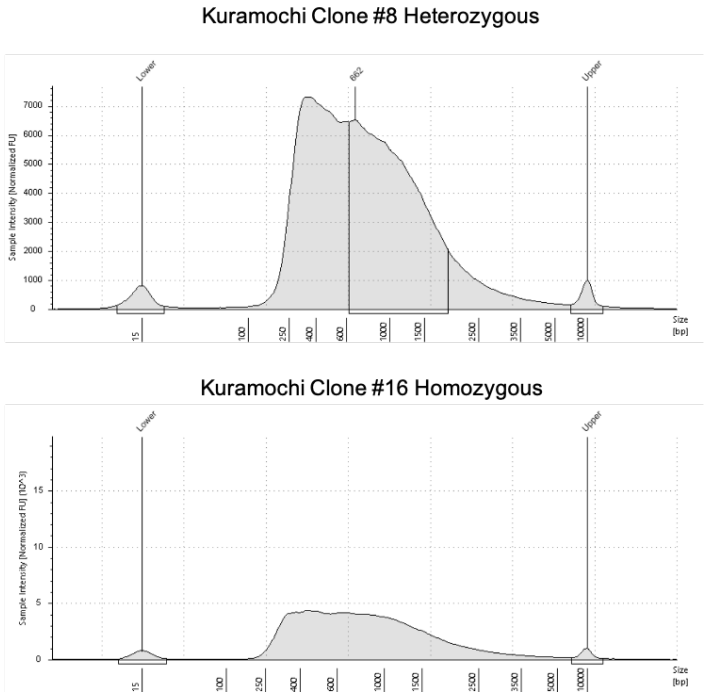

Figure 53. Bioanalyzer data of library prepared from Halo-tagged Kuramochi cells.

DISCUSSION

DISCUSSION

Ovarian Cancer is a leading cause of cancer-related death, with high incidence and mortality due to the late diagnosis and the failure of surgery and chemotherapy to eradicate the disease. Among all different subtypes, high-grade serous ovarian cancer (HGSOC) is the main responsible for malignant cases and death, representing a major unmet need in oncology (*16*). The lack of suitable experimental model that recapitulate the tumor heterogeneity, the histopathology and the pathogenesis of the disease together with the persistent uncertainty regarding the tissue of origin have hampered the development of new targets and therapies (*2*, *19*). These aspects are reflected in the negligible progress achieved over the last decades in terms of patients' outcome since the introduction of platin-derived compounds as first-line treatment in the 1980s. For this reason, the development of reliable experimental models able to address salient clinical challenges, such as early detection, tumor recurrence and acquired chemotherapy resistance, as well as the investigation of the disease in light of its cellular origin, are of high priority in OC research.

The cell of origin of the disease was heavily debated in the last years, with two tissues strongly supported as responsible for the tumor development, the ovarian surface epithelium (OSE) first the fimbrial epithelium (FI), the distal tract of the fallopian tube, later (*3*, *4*). Indeed, in contrast to the previously accepted "incessant ovulation" theory, according to which the tumor could arise in ovaries because of mutations accumulated throughout the continuous break/repair cycle of the OSE during menstrual cycle, more recent evidence has increasingly emphasized the role of FI as the most likely tissue of origin of HGSOC, with the identification of STIC carrying a core subset of mutations present in both primary and metastatic tumors from the same patient as major driver of the hypothesis. This evidence led to new theories that contributed to a lasting uncertainty about the relative involvement of either epithelium, fueling the debate about it.

In our lab, we recently addressed this issue using an approach based on the use of DNA methylation as a retained marker from normal tissues in tumors. The power of this kind of approach was already shown for the assignment of the origin to the so defined "tumors of unknown primary" (*33*), that drove the development of an epigenetic profiling test named EPICUP. Through the derivation of the DNA methylation profiles of normal healthy FI and OSE, the identification of differentially methylated sites (DMS) between the two (OriPrint) and the analysis of their presence in tumors, we were able to distinguish tumors

originated from the OSE from the ones arisen from the FI. Through OriPrint we were able to segregate tumors when analyzing both cultured cells and whole frozen tissues, assigning to the cell of origin an important role in the determination of the heterogeneity among different tumors. Moreover, translating this approach to transcriptomics made us able to assign also an origin to tumors of a FFPE retrospective cohort and to published dataset, validating the robustness of the method. By this approach we not only identified that HGSOC can derive from both candidate tissues but also that OSE-derived tumors have a negative impact on patients' prognosis (*12*), highlighting the clinical importance of the cell of origin and the prospective relevance of our approach in improving the clinical setting of patients with HGSOC.

Conversely from the cell-of-origin issue, that have been deeply explored and for what we provide new important insights, the lack of clinical suitable human models is still an important limit for the understanding of molecular mechanisms driving the pathogenesis of the disease, and more reliable technological advancements to study HGSOC have been exploited only recently. Indeed, the more common systems used to model HGSOC, such as common cancer cell lines (CCL), laborious and expensive mouse models and patient-derived primary cell cultures, although are useful for specific applications present drawbacks that hamper their ability to resemble the human disease and, moreover, they do not take into account the cell of origin of the tumor. For these reasons, the need to establish other models that better allow to study the pathology and bring effective advancements in the clinical setting was strongly supported.

Among technological progresses, organoids emerged as a powerful system able to phenotypically and genotypically recapitulate the human malignancy. Organoids are defined as "structure containing several cell types that develop from stem cells or organ progenitors and self-organize through cell sorting and spatially restricted lineage commitment, similar to the process in vivo" (*41*). They can be derived both from healthy and diseased tissues of each individuals and propagated *in vitro*, allowing their comparison to highlight biologically-relevant differences. Moreover, tumor-derived organoids are able to integrate the genetic, epigenetic and cellular heterogeneity of their parental tissue, capturing the essential uniqueness of each individual tumor (*5*). OC has started to exploit the organoids potential only recently, with several papers showing their use to study different aspect of the pathology (*9–11*, *130–132*, *134*).

In the work presented in this thesis I approached the problem of the inadequacy of HGSOC models trying to generate organoids of both normal healthy samples (FI and OSE) and

tumor samples (in the form of primary tumors and metastatic ascites), in order to obtain a long-term propagable platform to study the disease, its onset and its progression.

The aim of the work was to characterize organoids at the immunophenotypic and single cell transcriptomic levels, comparing them to primary tissues and assessing whether they were able to retain *in vitro* some specific features of *in vivo* primary tissues.

The methodological starting point of the project was the work of 2015 by Kessler and colleagues that showed the derivation of organoids from the fallopian tube (*96*). At the time of the beginning of this PhD, it was the only organoid system already generated for the type of samples relevant for the project.

Over the course of years, I was able to generate of organoids from the entire spectrum of samples, although with different efficiency and propagability rates. Indeed, the generation and propagation rate of organoids derived from healthy tissues was sensibly higher than the one achieved for tumors organoids. Moreover, a consistent difference was present also between the two normal samples, with fimbria-derived organoids that show the highest derivation efficiency among all tissues (~80%) and a long-term propagability that, making exception for two OSE samples, was not achieved with other organoids system treated. Conversely from my results, during years other works from two different labs showed the derivation of propagable organoids even from those tissues on which I have failed, providing new information and protocols to test.

The first report of organoids derived from OC samples was provided by Hill and colleagues in 2018 (*9*), showing the use of short-term OC organoids to study the DNA repair inhibitor response. A curiosity of this work was that although defined as short-term, the authors tested that they were able to propagate organoids for ~30 passages. This makes interesting to assess how different lab' consider as "short-term" or "long-term" the propagability of organoids, suggesting to the need to find a common consensus about this definition. The subsequent year, the work by Kopper and colleagues (*10*) showed the achievement of the long-term propagation of organoids derived from all the four tissues I was studying, highlighting also their genetic characterization and biobanking. Their cohort comprise tumor organoids as well as fallopian tube and OSE organoids.

After these two works, very recently other groups published papers showing protocols for the generation of OC-derived organoids and their use to study the disease (*11*, *130–132*), but, interestingly, OSE-derived organoids were grown only from the Clevers' lab, highlighting the difficulties to generate organoids derived from this tissue.

Unfortunately, conversely from other research groups, despite several trials I was not able to reproduce any protocol tested, failing mainly in the long-term propagation of organoids which, after few passages *in vitro*, stop their growth acquiring a quiescent-like phenotype.
Recently, Kessler and collaborators published another interesting work that, conversely from the others, show the need of a low Wnt environment to generate HGSOC derived organoids. They show that the lack of exogenous Wnt signal activation is indeed a requirement for maintaining stemness and preventing differentiation in HGSOC organoids and not only related to the presence of Wnt in the serum, which is normally avoided from the growth medium. They also confirmed the functional relationship between low-Wnt signal and maintenance of HGSOC growth potential *in vitro* observing that the activation of the Wnt pathway through the GSK3-β inhibitor CHIR also inhibits organoid growth. The efficiency of this protocol, strongly different from the others, will be tested in future.
Notwithstanding not all published protocols were tested (papers published in 2020), the impossibility to reproduce the published results suggests that, probably, there are still unclear factors, that could be dissimilar among different laboratories, contributing to the effective generation of organoids. If for OSE organoids, whose generation have not been reproduced by any research group, it could be conceivable the presence of unknown factors regulating the stemness of OSE cells or the occurrence of some kind of stochastic factors, our inability to derive organoids from tumor samples is harder to explain. Indeed, differences could be found at any level of the protocol, from the surgery of patients to the biobanking of biopsies, their storage, the time elapsed before their processing, the generation of conditioned medium, the resuspension and storage of growth medium molecules, the splitting procedures and so on. Probably, an higher level of standardization in the procedures could help in overcome problems regarding the establishment of organoid cultures. Another possibility considered was the lack of detailed information in the protocol that hamper its correct replication. However, from the in-depth discussion I had with Dr. Oded Kopper of the Clevers' lab, no differences emerged from what was written in the text and what was done by them and by me.
Despite the difficulties encountered in organoids generation, when characterized at the immunophenotypic level, FI-derived organoids retain the expression of tissue specific biomarkers, such as CK7, indicating their epithelial nature, and PAX8 and the de-tyrosinated tubulin, demonstrating the presence of the secretory and ciliated subpopulations, providing a first input of their ability in recapitulate the tissue from which they are derived. The same was true also for HGSOC organoids at low passages, that

express PAX8, a common marker of HGSOC, are epithelial, given the expression of CK7, and present proliferative $KI67^+$ cells.

To further understand how normal organoids recapitulated primary tissues' features, we analyzed the transcriptome of single cells of normal FI and OSE organoids, comparing them with cells directly isolated from primary tissues. The better efficiency achieved with FI-derived organoids was also reflected in the better results obtained from the analysis of single cells' transcriptomics data. Indeed, scRNAseq data of FI samples showed that organoids are mainly composed of the same tissue types present in primary tissues, expressing the three major cellular subtypes of the fimbria: secretory, ciliated and basal stem-like cells.

Then, the application of the Leiden algorithm allowed to identify 10 different clusters of which some of them, potentially, could represent new subpopulations, each one characterized by specific features. Among them, cluster 0, 1 and 6 are respectively representative of secretory, basal and ciliated cells. Cluster 3 and 4 were characterized by cells with a transcriptional landscape related with the inflammatory response, the chemokine signaling and that acts like plasma cells. These data retrieve an old theory proposed in the far 1990 by Kutteh and collaborators (*153*) that suggests the presence of a local secretory immune system in the fallopian tube, a hypothesis that will be interesting to address by further transcriptomic and immunophenotypic analyses of the tissue, in order to shed more light on the composition and the localization of this subpopulations.

Another interesting cluster, the number 5, was characterized by cells with DEGs enriched in the estrogen signaling pathway and could be represented by a subpopulation specifically reacting to the estrogen signal. An interesting work published recently by Zhu and collaborators showed the relationship between estrogen and the generation of ciliated cells, demonstrating that estrogen promote the differentiation of multi-ciliated cells (MCCs) through the estrogen receptor β, following the reduction of DLL1, a ligand of Notch (*147*). The results of this work could suggest the existence of a specific cell type representing some kind of progenitor cells that, controlled by the estrogen signaling, could further differentiate in ciliated cells and the identified cluster could represent specifically this population. Another putative progenitor subpopulation is represented by cluster 7, featured by the expression of genes with a GO related to the stimulation of the transcription. The observation that this cluster is also enriched in cells that are in the S or G2M phase of the cell cycle support the proliferating progenitor role of these cells.

Moreover, other two identified clusters, numbers 2 and 8, showed a EMT-like phenotype, that could indicate cells committed towards a mesenchymal fate by the chronic exposure to the oxidative stress generated by the follicular fluid during oocyte capture (*29*) and probably involved in cancer development.

Finally, cluster 9 does not showed any distinguishing feature and the slight expression of blood cells markers could indicate the presence of contaminant blood cells.

To further address the observations made regarding various clusters and to investigate the dataset to a higher level, it will be interesting to perform an Ingenuity Pathway Analysis (IPA) on DEGs of each cluster, in order to gain more insight on the cellular composition of the tissue. Indeed, IPA enables analysis, integration, and understanding of data from gene expression with a higher specificity respect to EnrichR.

To further validate identified clusters, I decided to compare them with the ones described in the work by Hu and colleagues in which they investigated by Smart-Seq the transcriptome of primary fallopian tube single cells (*148*). By this analysis, I observed the overlapping of the cluster defined by them as "C7-EMT" with clusters 2 and 8 that I identified as EMT-like, and that the expression of genes of the C3 cluster, that they defined as the "differentiated cluster", were not univocally localized in one of our identified clusters but, instead, scattered among secretory, ciliated and EMT-like cells. Probably the difference in the sequencing method used (Smart-seq2 vs 10X genomics) make this latter population to being more spread between the several differentiated populations of our dataset. Indeed, Smart-seq2 is more sensitive for gene detection while 10X could detect rare cell populations due to high cell throughput (*154*). Moreover, I also detected that DEGs of cluster C6, which was discarded from their analysis being characterized by an association to cell stress, are mainly expressed in CD44 basal stem like cells of our dataset. This observation suggests a possible misattribution of such phenotype in the publication.

In addition to this, when we plot our dataset as a diffusion map it is possible to observe a putative starting point from which two branches starts, directed towards two different directions. The observation that CD44 basal cells are present in the starting point of the diffusion map support their putative stem role, with highly differentiated ciliated cells and cells of the EMT-like cluster present at the end of the two branches. Between basal and ciliated cells, it is possible to identify the presence of cluster 5 and 6, in a sort of directional path that support the hypothesis of a progenitor role for these cells, especially in the differentiation commitment towards the ciliated subpopulation. However, to further address this possibility, a pseudotime analysis or other system of trajectory inference based

on the combination of transcriptomics and the ratio of spliced/unspliced reads (*155*) are more recommended and will be performed soon by the bioinformatic unit of the lab.

Taken together, the data indicate that our dataset is a *bona-fide* representation of the *in vivo* cells and that FI-derived organoids recapitulate the primary tissue in terms of gene expression.

For the OSE the situation is quite different, since organoids and primary tissue, despite being similar between each other, are present as two different populations for which it was compelling to identify specific features. The only remarkable preliminary result is the expression of the Calretinin binding protein 2 (CALB2) a bona fide marker of the tissue, although additional profiling of samples and analysis are required to shed light on the composition of the tissue and ability of organoids to model it.

Given the failure in the generation of HGSOC derived organoids, I decided to employ an additional experimental platform that foresees the genetical manipulation of organoids for the generation of an *in vitro* model of tumorigenesis able to recapitulate both early stages and progression of the tumorigenic process. This system was initially described to model colorectal cancer development (*126*, *127*, *149*), through the introduction of CRISPR-mediated mutation of tumor driver genes in normal organoids, and the feasibility of such approach in OC was demonstrated recently by Kopper and colleagues applying it on normal FT organoids (*10*). Taking in consideration the dual origin of HGSOC, the possibility to study the early stages of the tumorigenic process in a cell of origin-specific way is potentially transforming. However, given the ability to generate only healthy FI organoids capable of recapitulate the primary tissue and being expanded for long period, at the moment I decided to start to exploit this approach only on them. The overall idea is to generate a mixed organoid composed of normal cells and cells with a tumor prone background, that in the lab we defined as induced Tumor Organoids (iTOs), generated introducing specific mutations in genes known to be frequently mutated in HGSOC (such as TP53). Then, the tumor-prone organoids are pushed towards a tumorigenic fate by the introduction of subsequent specific individual or combined mutations already predicted to be relevant to pathology by the transcriptomic data already generated in the lab for the study on HGSOC cell of origin (*12*) or genes expected to drive the tumorigenic process. The induction of tumorigenesis in cells growing in a normal tissue context will be assessed by imaging and high-throughput sequencing at single cell resolution to identify alterations that are fundamental in driving tumorigenesis. Another interesting aspect that could be addressed is that the tumorigenic background of iTOs will allow also an unconventional

discovery approach, in which study the effect of random mutations induced by radiomimetics (e.g., neocarzinostatin, bleomycin), and identify the ones able to drive tumorigenic onset and progression.

For the targeted approach, a first experimental system was ideated foreseeing the use of a lentiviral vector specifically designed to induce the knockdown of selected genes in organoids. The lentiviral vector was benchmarked on FI organoids, although the complete set of experiments inducing the knockdown of genes still need to be performed, since the infection of organoids founds several challenges ranging from the virus production efficiency and the consequent low viral titer, to the direct infection of 3D structures to obtain a mosaic structure.

As alternative, in case I will fail with the lentivirus-based approach, the design of a CRISPR/Cas9 experiment to perform the knockout of same genes was taken in consideration.

Another potential aspect impacting the success of the genetic engineering approach is the choice of genes to be altered for the induction of tumorigenesis. From data available in the lab derived from previous analysis, we observed that PAX8 is expressed in the fimbrial epithelium but not in the OSE and we showed that it remains differentially expressed and methylated between FI-like and OSE-like tumors (*12*), providing an explanation to why it is not expressed in all HGSOCS cases. Given its historical record as defining marker for HGSOC (reviewed in *150*), it could play a pivotal role in the tumorigenic process, especially for tumors arisen from the FI. Indeed, PAX8 mostly binds at non-promoter sites and is enriched at super-enhancers, where it can globally regulate genes involved in tumorigenesis (*151*) and evidence shows that the knockdown of PAX8 in HGSOC results in increased apoptosis and reduced proliferation and migration in cancer cell lines (*156*). Hence, studying this gene and its interactome by ChIP-Seq could provide relevant target to test in the genetic manipulation platform and identify factor that could be tested in the culture media of tumor organoids to allow their growth. However, despite its importance, commercially available antibodies for PAX8 are still not specific, recognizing also other homologous genes members of the PAX family (*152*). To solve this problem, we decided to use an antibodies-free approach to avoid the eventual cross-reactivity in the immunoprecipitation. Thus, the experimental design as based on the use of the Halo-Tag system, that offers an efficient alternative to the standard chromatin immunoprecipitation (ChIP) to study protein:DNA interaction. The system foresees the fusion of the Halo-Tag to the protein of interest to perform then the immunoprecipitation using a resin that bound

the Halo-Tag and allow to identify the targets. Given the lack of tumor organoids and the challenge of perform genome editing on primary cells, the experimental pipeline was performed on three different cell lines classified as likely HGSOC, although only one (Kuramochi cells) underwent the Halo-ChIP and the analysis of targets is still ongoing. Once I will have results from the explorative experiment on Kuramochi confirming the efficiency of the system, I will proceed with the Halo-ChIP also on OVSAHO and NIH-OVCAR3, that were already engineered with the Halo-Tag.

In summary, despite the recent demonstration that both fimbrial and ovarian surface epithelium originate HGSOC in humans, clinically relevant model to study the pathology taking in consideration also the cell-of-origin still lack and are emerging only recently. In this PhD work I tried to generate an organoids platform to study onset, progression and molecular features of HGSOC. However, it was challenging to generate organoids from the entire cohort of samples and only organoids derived from the fimbrial epithelium support an efficient derivation and a long-term *in vitro* expansion, faithfully recapitulating the primary tissue. Despite of this, further efforts on the completion of the system will allow to generate a platform that will enable to refine the identification of relevant dysregulated pathways in HGSOC according to the tumor-specific cell of origin, hopefully leading to a better understanding of the pathology and the discovery of clinically relevant targets to improve the care of patients with HGSOC.

BIBLIOGRAPHY

BIBLIOGRAPHY

1. J. Prat, FIGO Committee on Gynecologic Oncology, FIGO's staging classification for cancer of the ovary, fallopian tube, and peritoneum: abridged republication. *J Gynecol Oncol*. **26**, 87–89 (2015).
2. S. Vaughan *et al.*, Rethinking ovarian cancer: recommendations for improving outcomes. *Nat. Rev. Cancer*. **11**, 719–725 (2011).
3. A. Ng, N. Barker, Ovary and fimbrial stem cells: biology, niche and cancer origins. *Nat. Rev. Mol. Cell Biol.* **16**, 625–638 (2015).
4. A. N. Karnezis, K. R. Cho, C. B. Gilks, C. L. Pearce, D. G. Huntsman, The disparate origins of ovarian cancers: pathogenesis and prevention strategies. *Nat. Rev. Cancer*. **17**, 65–74 (2017).
5. J. Drost, H. Clevers, Organoids in cancer research. *Nat. Rev. Cancer*. **18**, 407–418 (2018).
6. H. Clevers, Modeling Development and Disease with Organoids. *Cell*. **165**, 1586–1597 (2016).
7. C. S. Verissimo *et al.*, Targeting mutant RAS in patient-derived colorectal cancer organoids by combinatorial drug screening. *Elife*. **5** (2016), doi:10.7554/eLife.18489.
8. E. Driehuis *et al.*, Pancreatic cancer organoids recapitulate disease and allow personalized drug screening. *Proc. Natl. Acad. Sci. USA* (2019), doi:10.1073/pnas.1911273116.
9. S. J. Hill *et al.*, Prediction of DNA Repair Inhibitor Response in Short-Term Patient-Derived Ovarian Cancer Organoids. *Cancer Discov.* **8**, 1404–1421 (2018).
10. O. Kopper *et al.*, An organoid platform for ovarian cancer captures intra- and interpatient heterogeneity. *Nat. Med.* **25**, 838–849 (2019).
11. K. Hoffmann *et al.*, Stable expansion of high-grade serous ovarian cancer organoids requires a low-Wnt environment. *EMBO J.* **39**, e104013 (2020).
12. P. Lo Riso *et al.*, A cell-of-origin epigenetic tracer reveals clinically distinct subtypes of high-grade serous ovarian cancer. *Genome Med.* **12**, 94 (2020).
13. Howlader N, Noone AM, Krapcho M, Miller D, Brest A, Yu M, Ruhl J, Tatalovich Z, Mariotto A, Lewis DR, Chen HS, Feuer EJ, Cronin KA (eds). SEER Cancer Statistics Review, 1975-2017, National Cancer Institute. Bethesda, MD, https://seer.cancer.gov/csr/1975_2017/, based on November 2019 SEER data submission, posted to the SEER web site, April 2020.

14. V. W. Chen *et al.*, Pathology and classification of ovarian tumors. *Cancer*. **97**, 2631–2642 (2003).
15. B. M. Reid, J. B. Permuth, T. A. Sellers, Epidemiology of ovarian cancer: a review. *Cancer Biol. Med.* **14**, 9–32 (2017).
16. WHO Classification of Tumours Editorial Board, *WHO Classification of Tumours of the Female Reproductive Organs (Medicine)* (World Health Organization, Lyon, ed. 4, 2014).
17. I.-M. Shih, R. J. Kurman, Ovarian tumorigenesis: a proposed model based on morphological and molecular genetic analysis. *Am. J. Pathol.* **164**, 1511–1518 (2004).
18. R. J. Kurman, I.-M. Shih, The dualistic model of ovarian carcinogenesis: revisited, revised, and expanded. *Am. J. Pathol.* **186**, 733–747 (2016).
19. D. D. Bowtell *et al.*, Rethinking ovarian cancer II: reducing mortality from high-grade serous ovarian cancer. *Nat. Rev. Cancer*. **15**, 668–679 (2015).
20. M.-A. Lisio, L. Fu, A. Goyeneche, Z.-H. Gao, C. Telleria, High-Grade Serous Ovarian Cancer: Basic Sciences, Clinical and Therapeutic Standpoints. *Int. J. Mol. Sci.* **20** (2019), doi:10.3390/ijms20040952.
21. Cancer Genome Atlas Research Network, Integrated genomic analyses of ovarian carcinoma. *Nature*. **474**, 609–615 (2011).
22. D. D. L. Bowtell, The genesis and evolution of high-grade serous ovarian cancer. *Nat. Rev. Cancer*. **10**, 803–808 (2010).
23. R. W. Tothill *et al.*, Novel molecular subtypes of serous and endometrioid ovarian cancer linked to clinical outcome. *Clin. Cancer Res.* **14**, 5198–5208 (2008).
24. M. F. Fathalla, Incessant ovulation--a factor in ovarian neoplasia? *Lancet*. **2**, 163 (1971).
25. N. Auersperg, Ovarian surface epithelium as a source of ovarian cancers: unwarranted speculation or evidence-based hypothesis? *Gynecol. Oncol.* **130**, 246–251 (2013).
26. E. Kuhn *et al.*, TP53 mutations in serous tubal intraepithelial carcinoma and concurrent pelvic high-grade serous carcinoma--evidence supporting the clonal relationship of the two lesions. *J. Pathol.* **226**, 421–426 (2012).
27. S. I. Labidi-Galy *et al.*, High grade serous ovarian carcinomas originate in the fallopian tube. *Nat. Commun.* **8**, 1093 (2017).

28. R. H. Young, From Krukenberg to today: the ever present problems posed by metastatic tumors in the ovary. Part II. *Adv Anat Pathol*. **14**, 149–177 (2007).
29. M. F. Fathalla, Incessant ovulation and ovarian cancer - a hypothesis re-visited. *Facts Views Vis Obgyn*. **5**, 292–297 (2013).
30. M. A. Eckert *et al.*, Genomics of ovarian cancer progression reveals diverse metastatic trajectories including intraepithelial metastasis to the fallopian tube. *Cancer Discov.* **6**, 1342–1351 (2016).
31. S. Zhang *et al.*, Both fallopian tube and ovarian surface epithelium are cells-of-origin for high-grade serous ovarian carcinoma. *Nat. Commun.* **10**, 5367 (2019).
32. R. F. Lowdon, H. S. Jang, T. Wang, Evolution of epigenetic regulation in vertebrate genomes. *Trends Genet.* **32**, 269–283 (2016).
33. S. Moran *et al.*, Epigenetic profiling to classify cancer of unknown primary: a multicentre, retrospective analysis. *Lancet Oncol.* **17**, 1386–1395 (2016).
34. S. Domcke, R. Sinha, D. A. Levine, C. Sander, N. Schultz, Evaluating cell lines as tumour models by comparison of genomic profiles. *Nat. Commun.* **4**, 2126 (2013).
35. R. Perets *et al.*, Transformation of the fallopian tube secretory epithelium leads to high-grade serous ovarian cancer in Brca;Tp53;Pten models. *Cancer Cell*. **24**, 751–765 (2013).
36. J. Kim, D. M. Coffey, L. Ma, M. M. Matzuk, The ovary is an alternative site of origin for high-grade serous ovarian cancer in mice. *Endocrinology*. **156**, 1975–1981 (2015).
37. Y. Lai *et al.*, Current status and perspectives of patient-derived xenograft models in cancer research. *J Hematol Oncol*. **10**, 106 (2017).
38. T. G. Shepherd, B. L. Thériault, E. J. Campbell, M. W. Nachtigal, Primary culture of ovarian surface epithelial cells and ascites-derived ovarian cancer cells from patients. *Nat. Protoc.* **1**, 2643–2649 (2006).
39. R. L. O Donnell *et al.*, The use of ovarian cancer cells from patients undergoing surgery to generate primary cultures capable of undergoing functional analysis. *PLoS One*. **9**, e90604 (2014).
40. C. Francavilla *et al.*, Phosphoproteomics of primary cells reveals druggable kinase signatures in ovarian cancer. *Cell Rep.* **18**, 3242–3256 (2017).
41. M. A. Lancaster, J. A. Knoblich, Organogenesis in a dish: modeling development and disease using organoid technologies. *Science*. **345**, 1247125 (2014).

42. P. Weiss, A. C. Taylor, Reconstitution of complete organs from single-cell suspensions of chick embryos in advanced stages of differentiation. *Proc. Natl. Acad. Sci. USA*. **46**, 1177–1185 (1960).
43. E. Smith, W. J. Cochrane, CYSTIC ORGANOID TERATOMA: (report of a case). *Can. Med. Assoc. J.* **55**, 151–152 (1946).
44. J. G. Rheinwald, H. Green, Serial cultivation of strains of human epidermal keratinocytes: the formation of keratinizing colonies from single cells. *Cell*. **6**, 331–343 (1975).
45. Grafting of burns with cultured epithelium prepared from autologous epidermal cells. *Lancet*. **1**, 75–78 (1981).
46. G. Pellegrini *et al.*, Long-term restoration of damaged corneal surfaces with autologous cultivated corneal epithelium. *Lancet*. **349**, 990–993 (1997).
47. K. Takahashi, S. Yamanaka, Induction of pluripotent stem cells from mouse embryonic and adult fibroblast cultures by defined factors. *Cell*. **126**, 663–676 (2006).
48. K. Takahashi *et al.*, Induction of pluripotent stem cells from adult human fibroblasts by defined factors. *Cell*. **131**, 861–872 (2007).
49. G. Cotsarelis, T. T. Sun, R. M. Lavker, Label-retaining cells reside in the bulge area of pilosebaceous unit: implications for follicular stem cells, hair cycle, and skin carcinogenesis. *Cell*. **61**, 1329–1337 (1990).
50. F. Arai *et al.*, Tie2/angiopoietin-1 signaling regulates hematopoietic stem cell quiescence in the bone marrow niche. *Cell*. **118**, 149–161 (2004).
51. D. T. Scadden, The stem-cell niche as an entity of action. *Nature*. **441**, 1075–1079 (2006).
52. F. M. Watt, B. L. Hogan, Out of Eden: stem cells and their niches. *Science*. **287**, 1427–1430 (2000).
53. R. R. Stine, E. L. Matunis, Stem cell competition: finding balance in the niche. *Trends Cell Biol.* **23**, 357–364 (2013).
54. L. Li, H. Clevers, Coexistence of quiescent and active adult stem cells in mammals. *Science*. **327**, 542–545 (2010).
55. A. Wilson *et al.*, Hematopoietic stem cells reversibly switch from dormancy to self-renewal during homeostasis and repair. *Cell*. **135**, 1118–1129 (2008).
56. A. Z. Ayob, T. S. Ramasamy, Cancer stem cells as key drivers of tumour progression. *J Biomed Sci*. **25**, 20 (2018).

57. M. Lupia, U. Cavallaro, Ovarian cancer stem cells: still an elusive entity? *Mol. Cancer*. **16**, 64 (2017).
58. M. B. Rookmaaker, F. Schutgens, M. C. Verhaar, H. Clevers, Development and application of human adult stem or progenitor cell organoids. *Nat. Rev. Nephrol.* **11**, 546–554 (2015).
59. M. Eiraku *et al.*, Self-organized formation of polarized cortical tissues from ESCs and its active manipulation by extrinsic signals. *Cell Stem Cell*. **3**, 519–532 (2008).
60. T. Sato *et al.*, Single Lgr5 stem cells build crypt-villus structures in vitro without a mesenchymal niche. *Nature*. **459**, 262–265 (2009).
61. N. Barker *et al.*, Identification of stem cells in small intestine and colon by marker gene Lgr5. *Nature*. **449**, 1003–1007 (2007).
62. G. Schwank *et al.*, Functional repair of CFTR by CRISPR/Cas9 in intestinal stem cell organoids of cystic fibrosis patients. *Cell Stem Cell*. **13**, 653–658 (2013).
63. M. A. Lancaster *et al.*, Cerebral organoids model human brain development and microcephaly. *Nature*. **501**, 373–379 (2013).
64. A. Fatehullah, S. H. Tan, N. Barker, Organoids as an in vitro model of human development and disease. *Nat. Cell Biol.* **18**, 246–254 (2016).
65. B. Artegiani, H. Clevers, Use and application of 3D-organoid technology. *Hum. Mol. Genet.* **27**, R99–R107 (2018).
66. M. Eiraku *et al.*, Self-organizing optic-cup morphogenesis in three-dimensional culture. *Nature*. **472**, 51–56 (2011).
67. H. Suga *et al.*, Self-formation of functional adenohypophysis in three-dimensional culture. *Nature*. **480**, 57–62 (2011).
68. K. W. McCracken *et al.*, Modelling human development and disease in pluripotent stem-cell-derived gastric organoids. *Nature*. **516**, 400–404 (2014).
69. J. R. Spence *et al.*, Directed differentiation of human pluripotent stem cells into intestinal tissue in vitro. *Nature*. **470**, 105–109 (2011).
70. T. Takebe *et al.*, Vascularized and functional human liver from an iPSC-derived organ bud transplant. *Nature*. **499**, 481–484 (2013).
71. F. Sampaziotis *et al.*, Cholangiocytes derived from human induced pluripotent stem cells for disease modeling and drug validation. *Nat. Biotechnol.* **33**, 845–852 (2015).

72. A. P. Wong *et al.*, Directed differentiation of human pluripotent stem cells into mature airway epithelia expressing functional CFTR protein. *Nat. Biotechnol.* **30**, 876–882 (2012).
73. S. X. L. Huang *et al.*, Efficient generation of lung and airway epithelial cells from human pluripotent stem cells. *Nat. Biotechnol.* **32**, 84–91 (2014).
74. B. R. Dye *et al.*, In vitro generation of human pluripotent stem cell derived lung organoids. *Elife*. **4** (2015), doi:10.7554/eLife.05098.
75. A. J. Miller *et al.*, Generation of lung organoids from human pluripotent stem cells in vitro. *Nat. Protoc.* **14**, 518–540 (2019).
76. M. Takasato *et al.*, Kidney organoids from human iPS cells contain multiple lineages and model human nephrogenesis. *Nature*. **526**, 564–568 (2015).
77. H. Clevers, K. M. Loh, R. Nusse, Stem cell signaling. An integral program for tissue renewal and regeneration: Wnt signaling and stem cell control. *Science*. **346**, 1248012 (2014).
78. H. Clevers, STEM CELLS. What is an adult stem cell? *Science*. **350**, 1319–1320 (2015).
79. H. Clevers, The intestinal crypt, a prototype stem cell compartment. *Cell*. **154**, 274–284 (2013).
80. T. Sato *et al.*, Long-term expansion of epithelial organoids from human colon, adenoma, adenocarcinoma, and Barrett's epithelium. *Gastroenterology*. **141**, 1762–1772 (2011).
81. N. Barker *et al.*, Lgr5(+ve) stem cells drive self-renewal in the stomach and build long-lived gastric units in vitro. *Cell Stem Cell*. **6**, 25–36 (2010).
82. S. Bartfeld *et al.*, In vitro expansion of human gastric epithelial stem cells and their responses to bacterial infection. *Gastroenterology*. **148**, 126–136.e6 (2015).
83. M. Huch *et al.*, Unlimited in vitro expansion of adult bi-potent pancreas progenitors through the Lgr5/R-spondin axis. *EMBO J.* **32**, 2708–2721 (2013).
84. S. F. Boj *et al.*, Organoid models of human and mouse ductal pancreatic cancer. *Cell*. **160**, 324–338 (2015).
85. M. Huch *et al.*, In vitro expansion of single Lgr5+ liver stem cells induced by Wnt-driven regeneration. *Nature*. **494**, 247–250 (2013).
86. M. Huch *et al.*, Long-term culture of genome-stable bipotent stem cells from adult human liver. *Cell*. **160**, 299–312 (2015).

87. A. D. DeWard, J. Cramer, E. Lagasse, Cellular heterogeneity in the mouse esophagus implicates the presence of a nonquiescent epithelial stem cell population. *Cell Rep.* **9**, 701–711 (2014).

88. C. E. Barkauskas *et al.*, Type 2 alveolar cells are stem cells in adult lung. *J. Clin. Invest.* (2013).

89. R. Jain *et al.*, Plasticity of Hopx(+) type I alveolar cells to regenerate type II cells in the lung. *Nat. Commun.* **6**, 6727 (2015).

90. W. R. Karthaus *et al.*, Identification of multipotent luminal progenitor cells in human prostate organoid cultures. *Cell*. **159**, 163–175 (2014).

91. C. W. Chua *et al.*, Single luminal epithelial progenitors can generate prostate organoids in culture. *Nat. Cell Biol.* **16**, 951–61, 1 (2014).

92. J. M. Rosenbluth *et al.*, Organoid cultures from normal and cancer-prone human breast tissues preserve complex epithelial lineages. *Nat. Commun.* **11**, 1711 (2020).

93. N. Sachs *et al.*, A living biobank of breast cancer organoids captures disease heterogeneity. *Cell*. **172**, 373–386.e10 (2018).

94. L. Alzamil, K. Nikolakopoulou, M. Y. Turco, Organoid systems to study the human female reproductive tract and pregnancy. *Cell Death Differ.* **28**, 35–51 (2021).

95. D. Y. Paik *et al.*, Stem-like epithelial cells are concentrated in the distal end of the fallopian tube: a site for injury and serous cancer initiation. *Stem Cells*. **30**, 2487–2497 (2012).

96. M. Kessler *et al.*, The Notch and Wnt pathways regulate stemness and differentiation in human fallopian tube organoids. *Nat. Commun.* **6**, 8989 (2015).

97. M. Y. Turco *et al.*, Long-term, hormone-responsive organoid cultures of human endometrium in a chemically defined medium. *Nat. Cell Biol.* **19**, 568–577 (2017).

98. M. Boretto *et al.*, Development of organoids from mouse and human endometrium showing endometrial epithelium physiology and long-term expandability. *Development*. **144**, 1775–1786 (2017).

99. S. Haider *et al.*, Estrogen signaling drives ciliogenesis in human endometrial organoids. *Endocrinology*. **160**, 2282–2297 (2019).

100. H. Li, L. Saucedo-Cuevas, S. Shresta, J. G. Gleeson, The neurobiology of zika virus. *Neuron*. **92**, 949–958 (2016).

101. F. R. Cugola *et al.*, The Brazilian Zika virus strain causes birth defects in experimental models. *Nature*. **534**, 267–271 (2016).

102. P. P. Garcez *et al.*, Zika virus impairs growth in human neurospheres and brain organoids. *Science*. **352**, 816–818 (2016).
103. M. Xu *et al.*, Identification of small-molecule inhibitors of Zika virus infection and induced neural cell death via a drug repurposing screen. *Nat. Med.* **22**, 1101–1107 (2016).
104. T. Zhou *et al.*, High-Content Screening in hPSC-Neural Progenitors Identifies Drug Candidates that Inhibit Zika Virus Infection in Fetal-like Organoids and Adult Brain. *Cell Stem Cell*. **21**, 274–283.e5 (2017).
105. D. Dutta, I. Heo, H. Clevers, Disease Modeling in Stem Cell-Derived 3D Organoid Systems. *Trends Mol. Med.* **23**, 393–410 (2017).
106. J. Mariani *et al.*, FOXG1-Dependent Dysregulation of GABA/Glutamate Neuron Differentiation in Autism Spectrum Disorders. *Cell*. **162**, 375–390 (2015).
107. J. F. Dekkers *et al.*, A functional CFTR assay using primary cystic fibrosis intestinal organoids. *Nat. Med.* **19**, 939–945 (2013).
108. P. D. Hsu, E. S. Lander, F. Zhang, Development and applications of CRISPR-Cas9 for genome engineering. *Cell*. **157**, 1262–1278 (2014).
109. J. Nie, E. Hashino, Organoid technologies meet genome engineering. *EMBO Rep.* **18**, 367–376 (2017).
110. Y. K. Kim *et al.*, Gene-Edited Human Kidney Organoids Reveal Mechanisms of Disease in Podocyte Development. *Stem Cells*. **35**, 2366–2378 (2017).
111. B. S. Freedman *et al.*, Modelling kidney disease with CRISPR-mutant kidney organoids derived from human pluripotent epiblast spheroids. *Nat. Commun.* **6**, 8715 (2015).
112. Y. Guan *et al.*, Human hepatic organoids for the analysis of human genetic diseases. *JCI Insight* (2017).
113. C. A. Thomas *et al.*, Modeling of TREX1-Dependent Autoimmune Disease using Human Stem Cells Highlights L1 Accumulation as a Source of Neuroinflammation. *Cell Stem Cell*. **21**, 319–331.e8 (2017).
114. D. Tuveson, H. Clevers, Cancer modeling meets human organoid technology. *Science*. **364**, 952–955 (2019).
115. M. van de Wetering *et al.*, Prospective derivation of a living organoid biobank of colorectal cancer patients. *Cell*. **161**, 933–945 (2015).
116. D. Gao *et al.*, Organoid cultures derived from patients with advanced prostate cancer. *Cell*. **159**, 176–187 (2014).

117. L. Broutier *et al.*, Human primary liver cancer-derived organoid cultures for disease modeling and drug screening. *Nat. Med.* **23**, 1424–1435 (2017).
118. K. Nanki *et al.*, Divergent Routes toward Wnt and R-spondin Niche Independency during Human Gastric Carcinogenesis. *Cell*. **174**, 856–869.e17 (2018).
119. H. H. N. Yan *et al.*, A comprehensive human gastric cancer organoid biobank captures tumor subtype heterogeneity and enables therapeutic screening. *Cell Stem Cell*. **23**, 882–897.e11 (2018).
120. S. H. Lee *et al.*, Tumor Evolution and Drug Response in Patient-Derived Organoid Models of Bladder Cancer. *Cell*. **173**, 515–528.e17 (2018).
121. F. Schutgens *et al.*, Tubuloids derived from human adult kidney and urine for personalized disease modeling. *Nat. Biotechnol.* **37**, 303–313 (2019).
122. X. Li *et al.*, Organoid cultures recapitulate esophageal adenocarcinoma heterogeneity providing a model for clonality studies and precision therapeutics. *Nat. Commun.* **9**, 2983 (2018).
123. N. Sachs *et al.*, Long-term expanding human airway organoids for disease modeling. *EMBO J.* **38** (2019), doi:10.15252/embj.2018100300.
124. F. Weeber, S. N. Ooft, K. K. Dijkstra, E. E. Voest, Tumor Organoids as a Pre-clinical Cancer Model for Drug Discovery. *Cell Chem. Biol.* **24**, 1092–1100 (2017).
125. S. F. Roerink *et al.*, Intra-tumour diversification in colorectal cancer at the single-cell level. *Nature*. **556**, 457–462 (2018).
126. M. Matano *et al.*, Modeling colorectal cancer using CRISPR-Cas9-mediated engineering of human intestinal organoids. *Nat. Med.* **21**, 256–262 (2015).
127. J. Drost *et al.*, Sequential cancer mutations in cultured human intestinal stem cells. *Nature*. **521**, 43–47 (2015).
128. N. Gjorevski *et al.*, Designer matrices for intestinal stem cell and organoid culture. *Nature*. **539**, 560–564 (2016).
129. C. G. Hubert *et al.*, A Three-Dimensional Organoid Culture System Derived from Human Glioblastomas Recapitulates the Hypoxic Gradients and Cancer Stem Cell Heterogeneity of Tumors Found In Vivo. *Cancer Res.* **76**, 2465–2477 (2016).
130. Y. Nanki *et al.*, Patient-derived ovarian cancer organoids capture the genomic profiles of primary tumours applicable for drug sensitivity and resistance testing. *Sci. Rep.* **10**, 12581 (2020).
131. N. Maenhoudt *et al.*, Developing Organoids from Ovarian Cancer as Experimental and Preclinical Models. *Stem Cell Rep.* **14**, 717–729 (2020).

132. C. J. de Witte *et al.*, Patient-Derived Ovarian Cancer Organoids Mimic Clinical Response and Exhibit Heterogeneous Inter- and Intrapatient Drug Responses. *Cell Rep.* **31**, 107762 (2020).

133. Y. Maru, N. Tanaka, M. Itami, Y. Hippo, Efficient use of patient-derived organoids as a preclinical model for gynecologic tumors. *Gynecol. Oncol.* **154**, 189–198 (2019).

134. T. Velletri *et al.*, Single cell derived organoids capture the self-renewing subpopulations of metastatic ovarian cancer: *BioRxiv* (2018), doi:10.1101/484121.

135. A. Butler, P. Hoffman, P. Smibert, E. Papalexi, R. Satija, Integrating single-cell transcriptomic data across different conditions, technologies, and species. *Nat. Biotechnol.* **36**, 411–420 (2018).

136. L. McInnes, J. Healy, J. Melville, UMAP: Uniform Manifold Approximation and Projection for Dimension Reduction. *arXiv* (2018).

137. L. Haghverdi, F. Buettner, F. J. Theis, Diffusion maps for high-dimensional single-cell analysis of differentiation data. *Bioinformatics*. **31**, 2989–2998 (2015).

138. K. Li *et al.*, cellxgene VIP unleashes full power of interactive visualization, plotting and analysis of scRNA-seq data in the scale of millions of cells. *BioRxiv* (2020), doi:10.1101/2020.08.28.270652.

139. T. Daouda, R. Chhaibi, P. Tossou, A.-C. Villani, Geodesics in fibered latent spaces: A geometric approach to learning correspondences between conditions. *arXiv* (2020).

140. V. A. Traag, L. Waltman, N. J. van Eck, From Louvain to Leiden: guaranteeing well-connected communities. *Sci. Rep.* **9**, 5233 (2019).

141. D. S. D'Astolfo *et al.*, Efficient intracellular delivery of native proteins. *Cell*. **161**, 674–690 (2015).

142. B. M. Baker, C. S. Chen, Deconstructing the third dimension: how 3D culture microenvironments alter cellular cues. *J. Cell Sci.* **125**, 3015–3024 (2012).

143. B. D. Cosgrove *et al.*, Rejuvenation of the muscle stem cell population restores strength to injured aged muscles. *Nat. Med.* **20**, 255–264 (2014).

144. S.-R. Yang *et al.*, NPC1 gene deficiency leads to lack of neural stem cell self-renewal and abnormal differentiation through activation of p38 mitogen-activated protein kinase signaling. *Stem Cells*. **24**, 292–298 (2006).

145. P. B. Ottevanger, Ovarian cancer stem cells more questions than answers. *Semin. Cancer Biol.* **44**, 67–71 (2017).

146. M. T. Comer, H. J. Leese, J. Southgate, Induction of a differentiated ciliated cell phenotype in primary cultures of Fallopian tube epithelium. *Hum. Reprod.* **13**, 3114–3120 (1998).

147. M. Zhu, T. Iwano, S. Takeda, Estrogen and EGFR Pathways Regulate Notch Signaling in Opposing Directions for Multi-Ciliogenesis in the Fallopian Tube. *Cells*. **8** (2019), doi:10.3390/cells8080933.

148. Z. Hu *et al.*, The Repertoire of Serous Ovarian Cancer Non-genetic Heterogeneity Revealed by Single-Cell Sequencing of Normal Fallopian Tube Epithelial Cells. *Cancer Cell*. **37**, 226–242.e7 (2020).

149. J. Drost *et al.*, Use of CRISPR-modified human stem cell organoids to study the origin of mutational signatures in cancer. *Science*. **358**, 234–238 (2017).

150. L. R. Hardy, A. Salvi, J. E. Burdette, UnPAXing the Divergent Roles of PAX2 and PAX8 in High-Grade Serous Ovarian Cancer. *Cancers (Basel)*. **10** (2018), doi:10.3390/cancers10080262.

151. E. K. Adler *et al.*, The PAX8 cistrome in epithelial ovarian cancer. *Oncotarget*. **8**, 108316–108332 (2017).

152. N. G. Ordóñez, Value of PAX 8 immunostaining in tumor diagnosis: a review and update. *Adv Anat Pathol*. **19**, 140–151 (2012).

153. W. H. Kutteh *et al.*, Secretory immune system of the female reproductive tract. II. Local immune system in normal and infected fallopian tube. *Fertil. Steril.* **54**, 51–55 (1990).

154. X. Wang, Y. He, Q. Zhang, X. Ren, Z. Zhang, Direct Comparative Analysis of 10X Genomics Chromium and Smart-seq2. *BioRxiv*, 615013 (2019).

155. M. Lange *et al.*, CellRank for directed single-cell fate mapping. *BioRxiv* (2020), doi:10.1101/2020.10.19.345983.

156. L. H. Rodgers, E. Ó hAinmhire, A. N. Young, J. E. Burdette, Loss of PAX8 in high-grade serous ovarian cancer reduces cell survival despite unique modes of action in the fallopian tube and ovarian surface epithelium. *Oncotarget*. **7**, 32785–32795 (2016).